Environmental change in western equatorial South America and the role of the Andes during the warm Pliocene (4.7 to 2.7 Ma): A palynological study

---

Dissertation for the Doctoral Degree in Natural Sciences
(Dr. rer. nat.)
in the Faculty of Geosciences
at the University of Bremen

submitted by

Friederike Grimmer

Bremen, August 2022

Versicherung an Eides Statt / *Affirmation in lieu of an oath*

gem. § 5 Abs. 5 der Promotionsordnung vom 18.06.2018 /
according to § 5 (5) of the Doctoral Degree Rules and Regulations of 18 June, 2018

Ich / I, **Friederike Grimmer**

versichere an Eides Statt durch meine Unterschrift, dass ich die vorliegende Dissertation selbständig und ohne fremde Hilfe angefertigt und alle Stellen, die ich wörtlich dem Sinne nach aus Veröffentlichungen entnommen habe, als solche kenntlich gemacht habe, mich auch keiner anderen als der angegebenen Literatur oder sonstiger Hilfsmittel bedient habe und die zu Prüfungszwecken beigelegte elektronische Version (PDF) der Dissertation mit der abgegebenen gedruckten Version identisch ist. / *With my signature I affirm in lieu of an oath that I prepared the submitted dissertation independently and without illicit assistance from third parties, that I appropriately referenced any text or content from other sources, that I used only literature and resources listed in the dissertation, and that the electronic (PDF) and printed versions of the dissertation are identical.*

Ich versichere an Eides Statt, dass ich die vorgenannten Angaben nach bestem Wissen und Gewissen gemacht habe und dass die Angaben der Wahrheit entsprechen und ich nichts verschwiegen habe. / *I affirm in lieu of an oath that the information provided herein to the best of my knowledge is true and complete.*

Die Strafbarkeit einer falschen eidesstattlichen Versicherung ist mir bekannt, namentlich die Strafandrohung gemäß § 156 StGB bis zu drei Jahren Freiheitsstrafe oder Geldstrafe bei vorsätzlicher Begehung der Tat bzw. gemäß § 161 Abs. 1 StGB bis zu einem Jahr Freiheitsstrafe oder Geldstrafe bei fahrlässiger Begehung. / *I am aware that a false affidavit is a criminal offence which is punishable by law in accordance with § 156 of the German Criminal Code (StGB) with up to three years imprisonment or a fine in case of intention, or in accordance with § 161 (1) of the German Criminal Code with up to one year imprisonment or a fine in case of negligence.*

Bremen, den 23. August 2022

_____

Gutachter:

Prof. Dr. Gerold Wefer

Prof. Dr. Hermann Behling

Datum des Promotionskolloquiums:

25.11.2022

„Im Grunde kehrt alles Große in der Welt auch im Kleinen wieder,
wenn man es nur erkennen will."
Alexander von Humboldt

Table of Contents

List of abbreviations

AMOC	Atlantic meridional overturning circulation
CAS	Central American Seaway
CONISS	constrained incremental sum-of-squares cluster analysis
DD	Decimal degrees
EEP	Eastern Equatorial Pacific
EEP CT	Eastern Equatorial Pacific cold tongue
EF	equatorial front
ENSO	El Niño-Southern Oscillation
EUC	Equatorial Undercurrent
GCR	Gulf Coast Repository
iNHG	intensification of the Northern Hemisphere glaciations
IODP	International Ocean Discovery Program
ITCZ	Intertropical Convergence Zone
LMF	lower montane forest
LR	lowland rainforest
MPWP	mid-Pliocene warm period
NECC	North Equatorial Countercurrent
ODP	Ocean Drilling Program
PUC	Peru Undercurrent
RCP	Representative Concentration Pathway
SALLJ	South American low-level jet
SEC	South Equatorial Current
SST	sea surface temperature
SSTA	sea surface temperature anomalies
UFL	upper forest line
UMF	upper montane forest
WC	Walker circulation
WPWP	Western Pacific Warm Pool
XRF	X-ray fluorescence

List of figures

List of tables

Abstract

The Pliocene is often used as an analogue for near-future climates as most boundary conditions and atmospheric CO_2 concentrations were similar to present-days and the global climate state resembled that projected for the mid-21st century. Therefore, studying the characteristics and mechanisms of this past warm period can help to constrain the impacts of current global warming. This study presents the opportunity to study vegetation and climate change in western equatorial South America in the context of major topographic changes (closure of the Central American Seaway, uplift of the Northern Andes) which have been associated with changes of atmospheric circulation patterns. In particular, the position of the Intertropical Convergence Zone (ITCZ) and the strength of the Walker Circulation during the Pliocene are still a matter of debate. As these climatic features are responsible for the precipitation patterns over western equatorial South America, a vegetation record from this area is suitable to infer when conditions became more humid or more arid. Furthermore, the uplift history of the Western Cordillera is not well resolved. The presence of high montane páramo vegetation can indicate when the Western Cordillera of the Northern Andes reached certain elevations for this vegetation to develop.

To elucidate these issues of debate, the pollen and spore assemblage of marine Ocean Drilling Program Site 1239 in the Eastern Equatorial Pacific is studied. The record comprises 150 samples mainly from the Pliocene, and therein two time windows (4.7 to 4.2 Ma and 3.6 to 2.7 Ma) at a higher resolution of ~10 ka.

The first part (Chapter 3) provides the basis for the interpretation of the pollen record, because it is necessary to understand the effects of Andean uplift on climate and biodiversity as well as to constrain as much as possible the timing of Andean uplift. Concerning climatic effects, the Andes block atmospheric flow and cause higher convective precipitation in the Andean lowlands. Modelling experiments show that the Andes cause a northern position of the ITCZ over the eastern Pacific by generating shifts in the sea surface temperature gradient. With Andean uplift, new high montane environments were created, providing opportunities for taxa from different floristic realms to immigrate to these areas and for in situ evolution of new páramo species.

Concerning the timing of Andean uplift, there is evidence for final topographic growth of the Northern Andean Eastern Cordillera during the late Miocene to Pliocene, while the timing of uplift of the Western Cordillera remains unclear due to missing paleoaltimetry estimates. Paleoelevations for the Central Andean Western Cordillera differ strongly.

The second part (Chapter 4) focuses on humidity changes in an early Pliocene interval (4.7 Ma to 4.2 Ma). These changes are discussed in relation to a possible southward shift of the ITCZ in response to the restriction of the surface water exchange across the Central American Seaway. Hydrological changes were recorded by two complementary proxies: the pollen group "humid indicators" and the elemental ratio of Fe/K in the sediment. Between 4.55 and 4.42 Ma, humidity increases, pointing towards a southward shift of the ITCZ. Despite a short less humid phase, the record shows overall humid conditions and a closed forest cover. Furthermore, the presence of high montane páramo vegetation since 6 Ma suggests that the Western Andean Cordillera had already reached elevations above the upper forest line by the late Miocene.

In the third part (Chapter 5), the pollen record from the Piacenzian (3.9 Ma to 2.7 Ma) is presented. After 3.75 Ma, new taxa from more distant floristic realms appear in the páramo (e.g. *Sisyrinchium, Orthrosanthus*). From 3.5 Ma on, shifts of the upper forest line suggest temperature fluctuations towards cooler conditions. This cooling occurred contemporaneously with the onset of cooling in other Northern Hemisphere records and might be a precursor of Northern Hemisphere Glaciations. Between 3.3 and 3.05 Ma, the palynomorph concentration doubled. This was potentially caused by shifts of the pollen transport as an effect of tectonic processes and/or climate change, and of the pollen production. An increase of Amaranthaceae pollen after 3.1 Ma implies an enlargement of the coastal desert and thus drier conditions in the lowlands. This shift might be related to a strengthening of the Pacific Walker circulation, which would be in agreement with other paleoceanographic reconstructions.

Zusammenfassung

Das Pliozän wird oft als Analog für das Klima der nahen Zukunft genutzt, da die meisten Rahmenbedingungen und atmosphärische CO_2 Konzentrationen den heutigen ähnelten und das globale Klima das widerspiegelte, welches für die Mitte des 21. Jahrhunderts vorhergesagt wird. Daher kann die Untersuchung der Merkmale und Mechanismen dieser vergangenen Warmzeit helfen, die Auswirkungen der aktuellen Erderwärmung einzugrenzen.

Diese Studie macht es möglich, Vegetations- und Klimaveränderungen im west-äquatorialen Südamerika im Kontext bedeutender topographischer Veränderungen (Schließung des Isthmus von Panama, Erhebung der nördlichen Anden) zu untersuchen, die mit der Veränderung atmosphärischer Zirkulationsmuster in Zusammenhang gebracht wurden. Insbesondere sind die Position der Innertropischen Konvergenzzone (ITCZ) und die Stärke der Walker Zirkulation im Pliozän noch umstritten. Da diese klimatischen Besonderheiten für die Niederschlagsmuster über dem west-äquatorialen Südamerika verantwortlich sind, ist eine Vegetationsrekonstruktion aus diesem Gebiet sinnvoll, um abzuleiten, wann die Bedingungen feuchter oder trockener wurden. Darüber hinaus ist die Geschichte der Gebirgsbildung der Westkordillere nicht gut erforscht. Die Präsenz von hochmontaner Páramo-Vegetation kann anzeigen, wann die Westkordillere der nördlichen Anden die nötige Höhe zur Entwicklung dieses Vegetationstyps erreichte.

Um diese Diskussionsgegenstände näher zu beleuchten, wird der Inhalt an Pollen und Sporen eines marinen Bohrkerns der Ocean Drilling Program Site 1239 im östlichen äquatorialen Pazifik untersucht. Der Datensatz umfasst 150 Proben überwiegend aus dem Pliozän, wovon zwei Zeitfenster (4,7 bis 4,2 Ma und 3,6 bis 2,7 Ma) eine höhere Auflösung von ~10 ka haben.

Der erste Teil (Kapitel 3) stellt die Basis für die Interpretation der Pollen und Sporen Daten dar, da es notwendig ist, die Auswirkungen der Erhebung der Anden auf das Klima und die Biodiversität zu verstehen und die Anden-Erhebung zeitlich so gut wie möglich einzugrenzen. Was klimatische Auswirkungen betrifft, blockieren die Anden die atmosphärische Strömung und verursachen höhere konvektive Niederschläge im andinen Tiefland. Modellexperimente zeigen, dass die Anden eine nördliche Position der ITCZ über dem östlichen Pazifik verursachen, indem sie Veränderungen des Meeresoberflächentemperaturgradienten bewirken. Mit der Erhebung der Anden wurden neue hochmontane Lebensräume geschaffen, die das Einwandern von Taxa aus anderen Florenreichen in diese Gebiete und die in situ Evolution neuer Páramo Arten ermöglichten. Was die zeitliche Eingrenzung der Anden Heraushebung betrifft, gibt es Hinweise auf finales topografisches Wachstum der Ostkordillere der nördlichen Anden im späten Miozän bis Pliozän, während die zeitliche Eingrenzung der Heraushebung der Westkordillere aufgrund

fehlender Daten unklar bleibt. Zeitliche Schätzungen der Heraushebung der Westkordillere der zentralen Anden unterscheiden sich stark.

Der zweite Teil (Kapitel 4) konzentriert sich auf Feuchtigkeitsveränderungen in einem Intervall des frühen Pliozäns (4,7 Ma bis 4,2 Ma). Diese Veränderungen werden im Bezug zu einer möglichen Südwärts-Verlagerung der ITCZ als Antwort auf die Verengung des Oberflächenwasser-Austausches durch den Mittelamerikanischen Seeweg diskutiert. Hydrologische Veränderungen wurden von zwei komplementären Proxies erfasst: der Pollengruppe „Feuchte-Indikatoren" und dem elementaren Verhältnis von Fe/K im Sediment. Zwischen 4,55 und 4,42 Ma wird es feuchter, was auf eine Südwärts-Verlagerung der ITCZ hindeutet. Trotz einer kurzen weniger feuchten Phase zeigen die Daten insgesamt feuchte Bedingungen und eine geschlossene Bewaldung an. Darüber hinaus weist die Anwesenheit von hochmontaner Páramo-Vegetation seit 6 Ma darauf hin, dass die Westkordillere der Anden bereits im späten Miozän Höhen oberhalb der Waldgrenze erreicht hatte.

Im dritten Teil (Kapitel 5) wird der Probensatz aus dem Piacenzium (3,9 Ma bis 2,7 Ma) vorgestellt. Nach 3,75 Ma kommen neue Taxa aus entfernteren Florenreichen im Páramo an (z. B. *Sisyrinchium, Orthrosanthus*). Von 3,5 Ma an deuten Verlagerungen der Waldgrenze auf Temperaturschwankungen hin zu kühleren Bedingungen hin. Diese Abkühlung fand zeitgleich mit dem Einsetzen von Abkühlen in anderen nordhemisphärischen Datensätzen statt und könnte ein Vorläufer der nordhemisphärischen Vereisungen sein.
Zwischen 3,3 und 3,05 Ma verdoppelte sich die Palynomorph-Konzentration. Dies wurde möglicherweise durch Veränderungen des Pollentransports als Auswirkung tektonischer und/oder klimatischer Veränderungen und der Pollenproduktion verursacht. Eine Zunahme der Amaranthaceae Pollen nach 3,1 Ma deutet eine Vergrößerung der Küstenwüste und somit trockenere Bedingungen im Tiefland an. Diese Veränderung hängt möglicherweise mit einer Verstärkung der pazifischen Walker Zirkulation zusammen, was mit anderen paleozeanografischen Rekonstruktionen übereinstimmend wäre.

1 Introduction

The Pliocene (5.33 million years ago (Ma) to 2.58 Ma) is an epoch in earth's history when atmospheric CO_2 concentrations were similar to today's and around 30% higher than pre-industrial levels (Pagani et al. 2010; Seki et al. 2010). Mean annual temperatures were 4°C warmer during the early Pliocene (4.2-4.0 Ma) and 2.5°C warmer during the mid-Pliocene warm period (MPWP, ~3.3-3.0 Ma), compared to preindustrial conditions (Haywood et al. 2009; Haywood and Valdes 2004; Brierley et al. 2009). The physical geography, ocean circulation patterns and floral and faunal distributions were essentially similar to modern (Robinson, Dowsett, and Chandler 2008). Due to these similarities, the Pliocene has been proposed as an analogue for future climates (Zubakov and Borzenkova 1988; Burke et al. 2018). Burke et al. (2018) found that future climate after 2030 is likely to be similar to the mid-Pliocene warm period under the Representative Concentration Pathway 8.5 (RCP8.5) emission scenario. The RCP8.5 scenario is based on a CO_2 concentration of 1370 ppm in 2100. Under the rather moderate RCP4.5 scenario (650 ppm CO_2 in 2100), climate would be sustained at Pliocene-like conditions from 2040 on (Burke et al. 2018). Either scenario is alarming and stresses the need to improve both paleodata from the Pliocene and models in order to understand the mechanisms of climate change and to be able to react accordingly.

The MPWP is a target period for modelling studies within the Pliocene (Prescott et al. 2014; Haywood et al. 2009). In the MPWP, the atmospheric CO_2 concentration was between 300 and 450 ppm and the warm greenhouse state of the earth lasted long enough to approach equilibrium conditions. The ice sheets in Greenland and Antarctica existed, but were probably much smaller since a reconstructed sea level rise of > 6 m implies a large reduction of the global ice volume (Fischer et al. 2018). Concerning the vegetation, temperate and boreal vegetation shifted poleward. Deserts retreated, while tropical savannas and forests expanded (Dowsett et al. 2016). Global temperatures were distributed differently, with the high latitudes above 70°N being 10°-20°C warmer than today, while the tropics were nearly the same (Robinson, Dowsett, and Chandler 2008). Although most of the Pliocene is characterized by sustained warmth, from the Piacenzian (3.60 – 2.58 Ma) onwards, increasing indications for the onset of Northern Hemisphere glaciations can be observed. The first major occurrence of ice-rafted debris was recorded during the M2 glaciation (~3.3 Ma), indicating Northern Hemisphere ice sheet development (Flesche Kleiven et al. 2002).

Tropical sea surface temperatures (SSTs) in the Pliocene were similar to modern, except for the Eastern Equatorial Pacific (EEP) where SSTs were warmer than today and resembled El Niño conditions (Robinson, Dowsett, and Chandler 2008). The SSTs of the EEP direct movements of the Intertropical Convergence Zone (ITCZ) and modulate the zonal SST gradient. The zonal

gradient is important for the atmospheric Walker and Hadley circulation and the El Niño-Southern Oscillation (ENSO) (Fiedler and Talley 2006). ENSO describes a coupled ocean-atmosphere circulation system of the equatorial Pacific, involving interannual fluctuations of SSTs and sea-level pressure. The two extremes of the phenomenon are the warm phase (El Niño) and the cold phase (La Niña) (Bonham et al. 2009). Even small SST changes in the EEP have considerable impact on the atmosphere and global climate. The EEP has cooled by around 3-4°C since 4-5 Ma (Chaisson and Ravelo 2000; Groeneveld et al. 2006; Lawrence, Liu, and Herbert 2006; Wara, Ravelo, and Delaney 2005). At the same time, the Western Pacific Warm Pool (WPWP) seems to have remained constantly warmer (White and Ravelo 2020). Due to the enlarging zonal temperature difference, the easterly trade winds and the Walker circulation strengthened. This in turn caused the thermocline to shoal in the EEP since 4 Ma (Cannariato and Ravelo 1997; Ford et al. 2015). The gradual cooling of the EEP SSTs has changed the Pacific mean state from an El Niño-like mean state (also called "El Padre") to a more La Niña-like state (Ravelo et al. 2014; White and Ravelo 2020; Fedorov et al. 2006).

Besides ENSO, two major tectonic events had large impacts on the oceanography, climate, and biodiversity of western equatorial South America and the Eastern Equatorial Pacific: the closure of the Central American Seaway (CAS) and the uplift of the Northern Andes. The rise of the Isthmus of Panama caused major biogeographic, paleoceanographic and climatic changes and has therefore been of interest to researchers for many years. The formation of the Isthmus was caused by subduction of the Farallon Plate beneath the Caribbean and South American plates. This caused the development of the volcanic Panama Arc (O'Dea et al. 2016). The establishment of a coherent chronology of Isthmus formation has been challenging and is still disputed. Whereas Bacon et al. (2015), Jaramillo et al. (2017), Molnar (2017), and Montes et al. (2015) argue for an early closure of the CAS around 10 Ma, O'Dea et al. (2016) favor a late closure at 2.8 Ma. One issue in this debate seems to be the application of different definitions of the "Central American Seaway". While O'Dea et al. (2016) do not provide a definition, Bacon et al. (2015), Jaramillo (2018), Montes et al. (2015) and Sepulchre et al. (2014) define the CAS as the "oceanic seaway along the tectonic boundary of the South American plate and the Panamanian microplate". However, both sides agree that deepwater flow from the Pacific to the Caribbean was blocked at around 10 Ma and that the flow of shallow seawater was still possible until around 4 Ma (Montes et al. 2015; Jaramillo 2018; O'Dea et al. 2016).

Jaramillo (2018) summarizes the chronology of Isthmus formation as follows: A first major phase of terrestrial landscape development occurred during the early Miocene (~21 Ma), when a connection between central Panama and North America emerged. At this time, the width of the CAS has been estimated at around 200 km (Montes, Cardona, et al. 2012). The second major phase

occurred during the late Miocene, when a terrestrial connection of the Panama arc with Colombia was established. The CAS was fully closed by 10 Ma (Montes, Bayona, et al. 2012; Montes et al. 2015), blocking the flow of deep and intermediate water from the Pacific Ocean to the Caribbean. Between 10 and 3.5 Ma, surface water exchange between the Pacific Ocean and the Caribbean Sea was still possible through small passages other than the CAS (Coates et al. 2004). The progressive restriction of surface water exchange between the Pacific and the Caribbean has been recorded through salinity changes in the Caribbean. These salinity changes reached a critical phase between 4.7 and 4.2 Ma, when Pacific and Caribbean $\delta^{18}O$ records diverge (Steph, Tiedemann, Prange, et al. 2006). The remaining connections were finally capped between 4.2 and 3.5 Ma, when a continuous land bridge was established (Haug and Tiedemann 1998). Besides salinity changes, the closure of the CAS led to the shoaling of the eastern Pacific thermocline between 5.3 and 4 Ma (Tiedemann and Mix 2007; Steph et al. 2010; Song et al. 2017). In contrast, it is not clear how the closure of the CAS affected the position of the Intertropical Convergence Zone (ITCZ). The ITCZ is usually defined as the region of trade wind convergence close to the equator, characterized by ascending air, low atmospheric pressure, deep convective clouds and heavy precipitation (Poveda, Waylen, and Pulwarty 2006). The meridional shifts of the ITCZ respond to the seasonal insolation cycle. The rainbelt is located on average at around 6° N and oscillates over the Pacific Ocean between 9°-10° N in boreal summer and 2°-3° N in boreal winter (Schneider, Bischoff, and Haug 2014; Waylen and Poveda 2002). Also on longer timescales, the mean position of the ITCZ is displaced towards the warmer hemisphere, as indicated by paleorecords (e.g. Haug, Hughen, et al. 2001). Furthermore, Chiessi et al. (2021) showed that the ITCZ was not only subject to latitudinal shifts in the past, but also to contraction as shown for Northeastern South America during the Holocene. However, the mean position of the ITCZ in the Northern Hemisphere makes it clear that the ITCZ does not simply follow the insolation maximum (Schneider, Bischoff, and Haug 2014). It is one part of the meridional overturning Hadley circulation and the zonal overturning Walker circulation. The ascending air masses from the ITCZ flow away in the upper troposphere, descend in the subtropics, and flow back towards the ITCZ at the surface. This circulation forms the Hadley cell (Schneider, Bischoff, and Haug 2014). Coming back to the question how the closure of the CAS might have affected the position of the ITCZ, Schneider, Bischoff, and Haug (2014) suggest a northward shift of the ITCZ due to a strong Atlantic meridional overturning circulation (AMOC). AMOC strength in turn has been shown to be related to the closure of the CAS by several modelling experiments (summarized in Sepulchre et al. 2014). They showed that the interruption of the flow of deep and intermediate waters from the Pacific into the Caribbean leads to a strengthened AMOC (Sepulchre et al. 2014). This points towards a northward shift of the ITCZ in response to CAS closure, and is in agreement with another numerical modelling

experiment which also indicates an ITCZ northward shift in response to CAS closure (Steph, Tiedemann, Prange, et al. 2006). In contrast, changes of the inner Caribbean salinity gradient and aeolian grain size and flux data from the Eastern Pacific rather point towards a southward shift of the ITCZ (Steph, Tiedemann, Prange, et al. 2006; Hovan 1995). Investigating past latitudinal migrations of the ITCZ is important because the ITCZ controls tropical climate and vegetation. Tropical rainforest for instance needs at least 1500-1800mm annual precipitation without dry season (Hooghiemstra and van der Hammen 1998).

Reconstructions of the ITCZ over South America during the mid-Pliocene would be particularly interesting because they could elucidate the interplay of competing effects influencing the position of the ITCZ, i.e. the warmer and ice-free Northern Hemisphere would have favored a more northern ITCZ, while at the same time the EEP cold tongue was weaker, implying reduced ocean energy uptake and a southern position of the ITCZ (Schneider et al. 2014). While sea surface temperature reconstructions can be applied to study past shifts of the ITCZ over the ocean, vegetation change can give implications for ITCZ shifts over land.

The other tectonic process which had major impacts on the vegetation and climate of northwestern South America is the uplift of Andes. It is known from the Eastern Cordillera of Colombia, that this part of the Andes first reached elevations above the upper forest line in the late Pliocene. Only then, habitats suitable for the high Andean páramo vegetation emerged. In the early Pleistocene, a protopáramo vegetation was found in large areas between 2000 and 3000 m (Van der Hammen 1974a; Hooghiemstra and Van der Hammen 2004). Speciation in the páramo started only recently during the Pleistocene and is still ongoing (Madriñán, Cortes, and Richardson 2013).

For the reconstruction of past vegetation, pollen analysis is an effective tool. It is applied globally from the tropics to the poles to determine the climatic drivers of changes in the vegetation and to address biogeographical questions (Webb 1980; Bush 2001; Dupont 1999). The data obtained from pollen records can in turn be used to feed numerical climate models, which help us to understand the mechanisms of past climate change. Finally, both paleoclimate data and models help us to assess the effects of the current anthropogenic impact on global climate and biodiversity (Abels and Ziegler 2018). To mention only a few, global warming has led to upslope migration of species and increased local species richness (IPCC 2019). The three most extreme El Niño events (1982-1983, 1997-1998, 2015-2016) and the two strongest La Niña events (1988-1989, 1998-1999) since pre-industrialization have occurred within the last fifty years. Furthermore, the occurrence of extreme El Niño and La Niña events is projected to double in frequency during the 21st century when compared to the 20th century (IPCC 2019). The equatorial Pacific trade wind strengthening during the past two decades and Pacific SST cooling have been linked to an exceptionally warm

tropical Atlantic. In the tropical Andes, melting of glaciers and snow cover changes have led to local declines in agricultural harvest (IPCC 2019).

The Pliocene offers the possibility to investigate climate variability at orbital and sub-orbital timescales and also the climate response to longer-term processes such as ocean gateway changes and mountain uplift. Up to date, fairly little is known about Pliocene vegetation and climate changes in western equatorial South America, but an improved land surface reconstruction is necessary in order to provide a basis for climate models and validate model outputs. Due to a lack of long vegetation records from the Northern Andean Western Cordillera, the understanding of the development of the high Andean biota and the adaptation of the vegetation in relation to Andean uplift is sparse. The research questions related to these points, which are aimed to be answered in this study, are:

- How did the flora and vegetation of the study area change during the Pliocene, in particular between 4.7 and 2.7 Ma?
- How did uplift of the Northern Andes influence the vegetation in the study area? When and how did the páramo develop?
- What does the reconstructed vegetation development imply for the regional climate at that time?
- How is the onset of global cooling around 3.3 Ma manifested in the study area?

Investigation of these research questions will provide the basis for tackling the three hypotheses which are central to this thesis:

1) The ITCZ shifted southwards after the surface water exchange between the Pacific and Atlantic Ocean through the Central American Seaway became restricted between 4.7 and 4.2 Ma, resulting in increased precipitation in Ecuador. This hypothesis is addressed in the first paper (Chapter 4).

2) The Walker circulation strengthened before the intensification of the Northern Hemisphere glaciations (iNHG), between 3.6 and 3.1 Ma, resulting in further changes in vegetation and hydrology of Ecuador. This hypothesis is addressed in the second paper (Chapter 5).

3) Assuming a similar uplift history of both, the Eastern and Western Cordillera of the Northern Andes, the páramos of both Cordilleras also developed under temporally similar conditions, after ~3 Ma. This hypothesis is dealt with in both papers and in Chapter 3.

1.1 Modern vegetation in western equatorial South America

The altitudinal zonation of the present-day northern Andean vegetation is principally caused by the effect of declining temperature with increasing elevation (Hooghiemstra, Wijninga, and Cleef 2006). Furthermore, vegetation at a given elevation is influenced by moisture availability, topographic position, regional wind patterns, and land use (Hansen et al. 2003). The composition of the neotropical montane forest has been thoroughly investigated (e.g. Cuatrecasas 1934; Grubb et al. 1963; Jørgensen and León-Yánez 1999; Van der Hammen 1974a; Moscol Olivera and Cleef 2009).

Alexander von Humboldt was the first one who published an altitudinal zonation of the northern Andean vegetation (Humboldt and Bonpland 1807). The Colombian vegetation was later described in great detail by Cuatrecasas (1958). The lowland rainforest extends from sea level to 1000m altitude. The subandean forest extends from 1000m to 2400m, followed by the Andean forest from 2400m to 3800m. In contrast to the subandean forest, night frost occurs in the Andean forest (Pérez-Escobar et al. 2022). Páramos are found between 3800m (locally from 3200m) and 4700m (Cuatrecasas 1958).

Some characteristic plant species and genera in the Reserva Biologica San Francisco, Eastern Cordillera of the South Ecuadorean Andes, are listed in the following paragraph (Homeier et al. 2008). The lowland rainforest vegetation consists of different Arecaceae, *Terminalia amazonia* and *T. oblonga* (Combretaceae), *Piper* (Piperaceae), and *Psychotria* (Rubiaceae). In the lower montane forest, *Vismia tomentosa* (Clusiaceae), *Cyathea caracasana* (Cyatheaceae), *Inga* (Fabaceae), and *Miconia* (Melastomataceae) are found.

The upper montane forest, which is potentially the species richest area of all Andean floras (Pérez-Escobar et al. 2022) is made up of *Ilex rimbachii* (Aquifoliaceae), *Hedyosmum* (Chloranthaceae), *Clethra revolute* (Clethraceae), *Clusia ducu* and *Tovomita weddeliana* (Clusiaceae), *Weinmannia* (Cunoniaceae), *Purdiaea nutans* (Clethraceae), *Myrica pubescens* (Myricaceae), *Myrsine coriacea* (Myrsinaceae), *Podocarpus oleifolius* and *Prumnopitys montana* (Podocarpaceae) amongst others. The upper forest line is formed by *Ilex* (Aquifoliaceae), *Puya eryngioides* (Bromeliaceae), *Hedyosmum* (Chloranthaceae), *Gaultheria reticulate* (Ericaceae), *Orthrosanthus chimborazensis* (Iridaceae), and *Chusquea* (Poaceae).

In the páramo, *Gynoxis* (Asteraceae), *Puya* (Bromeliaceae), *Rhynchospora* vulcani (Cyperaceae), different Ericaceae, *Chusquea neurophylla* (Poaceae), and *Valeriana* (Valerianaceae) are found (Homeier et al. 2008). Cleef (1981), who studied the páramo vegetation in-depth, found that it is characterized by the following geobotanic and physiographic features: The vegetation is dominated by bunchgrasses of the genus *Calamagrostis*, stemrosettes (*Espeletia*, Asteraceae), and small-leaved shrubs. Azonal bogs are also present. The climate is basically humid, but annual precipitation ranges

from 700 to >3000 mm with mist and clouds being common. Diurnal temperature variations are large. Páramos exist mainly in Panamá and Costa Rica and in the northern Andes from Venezuela to Ecuador, with patches extending into Peru and Bolivia (Cleef 1981). Cleef (1981) distinguishes three páramo zones: the subpáramo (or shrubpáramo), the grasspáramo, and the superpáramo. The dominant plant families in the subpáramo are Ericaceae, Asteraceae, and Melastomataceae. The grasspáramo is formed by associations of Poaceae and Espeletiinae, with the most prominent grasses in this zone being *Calamagrostis effusa* and *Swallenochloa tesselata*. Both species are endemic to the northern Andean páramos. The superpáramo is the uppermost vegetation belt in the northern Andes and is located just below the nival belt. It is dominated by dwarfshrubs and sessile rosette plants. Characteristic endemic species in this belt belong to the genera *Senecio* and *Draba* (Cleef 1981).

The upper forest line (UFL) is defined as the maximum altitude where continuous forest occurs (Bakker, Olivera, and Hooghiemstra 2008). The position of the UFL and its altitudinal fluctuations over time are often used to infer climatic changes (e.g. Bakker, Olivera, and Hooghiemstra 2008; Hooghiemstra and Ran 1994b). Its position differs strongly in different areas due to local conditions. In the Colombian Cordillera Oriental, the UFL is situated between 3000 and 3500m (Cleef 1981). In northern Ecuador, the natural UFL is presently located between 3600 and 3700 m (Moscol Olivera and Hooghiemstra 2010). In southern Ecuador, in the Huancabamba Depression, where the Andes are lower, the UFL is situated between 2700 and 3400 m (Richter et al. 2008).

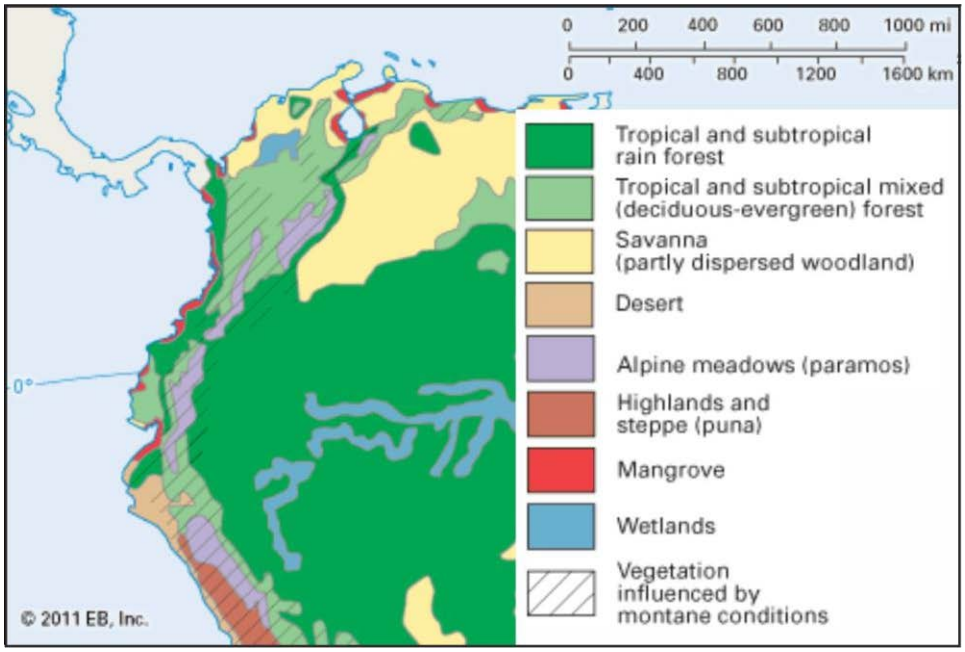

Figure 1.1. Vegetation distribution in northwestern South America, modified from Encyclopaedia Britannica (2011).

1.1.1 Pollen rain studies

When reconstructing past environments based on fossil pollen assemblages, it is essential to understand how the present vegetation is represented in the pollen rain of the study area. As already noted by Von Post (1916) cited in Parsons and Prentice (1981), pollen percentages do not directly correspond to vegetation percentages, because pollen percentages underly a production bias (differential pollen production) and a dispersal bias (differential dispersal of pollen types dependant on basin size). Simulations of particle dispersal showed that the larger the basin size, the better the representation of lighter pollen grains (e.g. *Pinus*) (Prentice 1985). Therefore, pollen rain studies are an important tool in order to investigate the pollen-vegetation relationship.

Several pollen rain studies have shown that pollen diversity in the Northern Andes generally reflects plant diversity of the surrounding vegetation, and that altitudinal vegetation belts are well reflected in the pollen rain (Weng, Hooghiemstra, and Duivenvoorden 2007; Jantz 2014). This implies that fossil palynological assemblages are a suitable proxy for reconstructing past Andean environments.

A comprehensive pollen rain study of the Northern Andes was conducted by Grabandt (1980) in the Eastern Cordillera of Colombia. Although she gained valuable insights into pollen representation of many montane forest taxa (see also table 1.1), the composition of the forests she studied is rather site-specific. *Quercus*, which is a dominant element, has its southern limit of distribution in Colombia and immigrated only recently into the southern Hemisphere. Thus, montane forest communities further south might have a quite different composition (Weng, Bush, and Silman 2004). Albeit some differences, the pollen rain from Colombia (Grabandt 1980) and Peru (Weng, Bush, and Silman 2004) also have remarkable similarities. Asteraceae, Poaceae, *Myrica* and *Myrsine* showed maximum abundances at high elevations (>2700), whereas *Hedyosmum* was most frequent at mid-elevations (1600-2000m). *Alchornea, Acalypha* and Rubiaceae were most abundant at premontane elevations (1000-1600m).

In a study comparing modern pollen spectra to the vegetation in northern Ecuador, Moscol Olivera, Duivenvoorden, and Hooghiemstra (2009) found that *Clusia, Ilex, Weinmannia, Peperomia* and *Clethra* are best suited to infer the local presence of forest from pollen records. The presence of páramo vegetation is indicated by *Puya*, Apiaceae, Poaceae, and Cyperaceae pollen. Hansen et al. (2003) found in pollen surface samples from Cajas National Park, Western Cordillera in Ecuador, that the main pollen and spore types in the upper páramo are *Huperzia, Plantago, Polylepis*, Poaceae, Cyperaceae, and Asteraceae. In both the Andean forest and páramo, pollen from wind-dispersed plants were overrepresented, e.g. *Alnus, Myrica, Podocarpus*, and *Alchornea* in páramo and *Lycopodium* and *Pityrogramma* fern spores in forest (Moscol Olivera, Duivenvoorden, and Hooghiemstra 2009). Other pollen rain studies indicate an over-representation of arboreal taxa above the upper forest line (Moscol Olivera, Duivenvoorden, and Hooghiemstra 2009; Hansen

and Rodbell 1995; Weng, Bush, and Silman 2004; Jansen et al. 2013) and upslope wind dispersal of *Alnus* and Urticaceae/Moraceae (Niemann, Brunschön, and Behling 2010). Pollen representation is generally correlated with pollination syndrome: wind-dispersed (anemophilous) pollen taxa are over-represented, whereas pollen taxa with other pollination syndromes (e.g. insect-pollination) are often under-represented (Moscol Olivera, Duivenvoorden, and Hooghiemstra 2009, see also table 1.1).

Recently, differences in the pollen rain trapped in moss polsters compared to lake sediments were discovered. Moss polsters contain higher percentages of pollen from entomophilous taxa than lake sediments (Weng, Bush, and Silman 2004). Furthermore, the pollen rain in moss polsters reflects the local vegetation, while the pollen rain in lake sediments represents the regional vegetation within a radius of up to 2km for lakes located in the upper montane forest and up to 40km for lakes in the páramo (Hagemans et al. 2019).

Concerning this study where a marine sediment core is analyzed, the interpretation is challenging because of the larger pollen source area and the mixing up of the pollen signal from different vegetation belts. When using modern pollen rain studies for the interpretation of fossil pollen records, it must also be kept in mind that the fossil plant communities are potentially non-analogous to present-day ones.

Table 1.1. Pollination syndromes and representation in the pollen rain of selected northern Andean taxa.

Pollen/spore type	pollination syndrome	representation	References
Alchornea	anemophilous	well- to over-represented	Grabandt (1980), Hagemans et al. (2019), Moscol Olivera, Duivenvoorden, and Hooghiemstra (2009)
Alnus	anemophilous	well- to over-represented	Grabandt (1980), Moscol Olivera, Duivenvoorden, and Hooghiemstra (2009)
Amaranthaceae/ Chenopodiaceae	anemophilous/ entomophilous	well- to over-represented	Moscol Olivera, Duivenvoorden, and Hooghiemstra (2009)
Asteraceae	predominantly entomophilous	slightly over-represented	Grabandt (1980)
Bocconia	entomophilous	well- to over-represented	Moscol Olivera, Duivenvoorden, and Hooghiemstra (2009)
Bromeliaceae	entomophilous	under- to well-represented	Moscol Olivera, Duivenvoorden, and Hooghiemstra (2009)
Caryophyllaceae	entomophilous	under-represented	Hagemans et al. (2019)
Clethra	entomophilous	under- to over-represented	Hansen et al. (2003), Moscol Olivera, Duivenvoorden, and Hooghiemstra (2009)
Cyatheaceae	anemophilous	over-represented	Grabandt (1980), Moscol Olivera, Duivenvoorden, and Hooghiemstra (2009)
Cyperaceae	anemophilous	well-represented	Moscol Olivera, Duivenvoorden, and Hooghiemstra (2009)
Dodonaea	anemophilous	over-represented	Moscol Olivera, Duivenvoorden, and Hooghiemstra (2009)

Elaphoglossum	anemophilous	well- to over-represented	Moscol Olivera, Duivenvoorden, and Hooghiemstra (2009)
Ericaceae	entomophilous/ ornithophilous	under- to over-represented	Grabandt (1980), Hansen et al. (2003), Moscol Olivera, Duivenvoorden, and Hooghiemstra (2009)
Hedyosmum	anemophilous/ entomophilous	well- to over-represented	Grabandt (1980), Moscol Olivera, Duivenvoorden, and Hooghiemstra (2009)
Ilex	entomophilous	under- to over-represented	Grabandt (1980), Moscol Olivera, Duivenvoorden, and Hooghiemstra (2009)
Iridaceae	entomophilous	well-represented	Moscol Olivera, Duivenvoorden, and Hooghiemstra (2009)
Jamesonia	anemophilous	well-represented	Moscol Olivera, Duivenvoorden, and Hooghiemstra (2009)
Lycopodium	anemophilous	well- to over-represented	Moscol Olivera, Duivenvoorden, and Hooghiemstra (2009)
Melastomata-ceae	entomophilous	well- to over-represented	Grabandt (1980), Moscol Olivera, Duivenvoorden, and Hooghiemstra (2009)
Myrica	anemophilous	well- to over-represented	Grabandt (1980), Hagemans et al. (2019), Moscol Olivera, Duivenvoorden, and Hooghiemstra (2009)
Myrsine	entomophilous	well- to over-represented	Moscol Olivera, Duivenvoorden, and Hooghiemstra (2009)
Myrtaceae	entomophilous/ ornithophilous	well- to over-represented	Grabandt (1980), Moscol Olivera, Duivenvoorden, and Hooghiemstra (2009)
Pityrogramma	anemophilous	over-represented	Moscol Olivera, Duivenvoorden, and Hooghiemstra (2009)
Poaceae	anemophilous	well- to over-represented	Moscol Olivera, Duivenvoorden, and Hooghiemstra (2009)
Podocarpus	anemophilous	well- to over-represented	Hagemans et al. (2019), Moscol Olivera, Duivenvoorden, and Hooghiemstra (2009)
Polylepis/ Acaena	entomophilous	well- to over-represented	Moscol Olivera, Duivenvoorden, and Hooghiemstra (2009)
Polypodium	anemophilous	well- to over-represented	Moscol Olivera, Duivenvoorden, and Hooghiemstra (2009)
Puya	entomophilous/ ornithophilous	under- to over-represented	Hagemans et al. (2019), Moscol Olivera, Duivenvoorden, and Hooghiemstra (2009)
Rosaceae	entomophilous	under-represented	Moscol Olivera, Duivenvoorden, and Hooghiemstra (2009)
Styloceras	n.a.	under-represented	Moscol Olivera, Duivenvoorden, and Hooghiemstra (2009)
Urticaceae/ Moraceae	anemophilous	well- to over-represented	Hagemans et al. (2019), Moscol Olivera, Duivenvoorden, and Hooghiemstra (2009)

1.1.2 Adaptations of the Andean vegetation to topographic and climatic changes

The closure of the CAS enabled northern-hemisphere taxa the migration into South America (Hooghiemstra 1989). From the mid-Pliocene onward, the number of taxa with a Holarctic and Asian origin increased. Although immigration of plant taxa from southern South America into the northern Andean montane rain forest presumably occurred even earlier, the present-day northern Andean flora contains more immigrants from the north than from the south (Hooghiemstra, Wijninga, and Cleef 2006). Several Northern Hemisphere tree species considerably changed the

vegetation in the northern Andes, e.g. *Alnus* which reached the high plain of Bogotá around 2.7 Ma and replaced *Myrica* swamp forests (Hooghiemstra 1989). *Quercus* came to the area only around 245 thousand years ago (ka) and further changed the composition of the Andean forest (Hooghiemstra and Ran 1994b).

With the gradual uplift of the northern Andes, new high elevation environments with cold climatic conditions evolved. The primary páramo flora consisted of local neotropical elements which became gradually enriched with elements from the Antarctic and Holarctic flora. The glacial-interglacial cycles of the Pleistocene caused repeated isolation and connection of páramos. Van der Hammen, Werner, and van Dommelen (1973) proposed that these cycles enhanced speciation resulting in the highly diverse páramo flora.

A globally observed phenomenon today is that species shift their distribution to higher latitudes and/or altitudes due to global warming (Thuiller 2007). In the South American tropics, this response was investigated with a vegetation survey on Chimborazo, Ecuador's highest mountain, first conducted by Alexander von Humboldt in 1802 and repeated by Morueta-Holme et al. (2015). The study showed that the upper limit of plant growth shifted from 4600m to ~5200m within 220 years, the elevation of vegetation zones increased, and the upper range limits of individual taxa moved upwards (Morueta-Holme et al. 2015).

Pollen records revealed oscillations of the upper forest line (UFL) in response to the glacial-interglacial cycles of the Pleistocene (Hooghiemstra and Ran 1994b; Hooghiemstra et al. 1993; Hooghiemstra 1989). Over the past 3.5 Ma, the UFL, which corresponds to the 9.5 °C isotherm, shifted between 1700 and 3700 m in the area of Bogotá, where presently, the UFL is located at 3100 m (Hooghiemstra 1989). At longer time scales, warm conditions prevailed between 735 and 569 ka and the UFL fluctuated between 2100 and 2700 m. Between 569 and 350 ka, the climate was colder and the UFL oscillated between 1800 and 2500 m. From 350 to 186 ka, the climate was warmer again and the UFL shifted from 2000 to 2600 m in the first part and from 2600 to 2900 in the second part of this interval. Between 186 and 24 ka, warm conditions continued to prevail and the UFL oscillated mostly between 2000 and 3000 m (Hooghiemstra and Ran 1994b).

1.2 Modern climate

1.2.1 Climate regimes in Ecuador

From the Pacific coast to the Andean Cordilleras, two main climatic regions with seven climatic regimes can be distinguished in Ecuador (Pourrut et al. 1995, compare figure 1.2). These are the coastal region with three climatic regimes and the Andean region with four climatic regimes. The three climatic regimes of the coastal region are:

1. Tropical megathermic arid to semi-arid climate: This type of climate has one rainy season between January and April and one pronounced dry season, an annual mean temperature > 22°C, and < 500 mm annual precipitation. It occurs along the coastal strip of southern Ecuador (figure 1.2). Heavy rain due to episodic El Niño events causes temporary greening of the otherwise barren landscape.
2. Tropical megathermic dry to semi-humid climate: This type of climate has one rainy season between December and May and one pronounced dry season, an annual mean temperature > 22°C, and 500-1000 mm annual precipitation. This climate zone lies east of the previously described one. The vegetation consists mainly of dry forest.
3. Tropical megathermic humid climate: This type of climate has one rainy season between December and May and one pronounced dry season, an annual mean temperature > 22°C, and 1000-2000 mm annual precipitation. This climate zone stretches approximately from Esmeraldas to the Gulf of Guayaquil. The vegetation consists of a dense broadleaf forest.

The four climatic regimes of the Andean region according to Pourrut et al. (1995) are:

4. Tropical megathermic very humid climate: This type of climate has one rainy season and one pronounced dry season, an annual mean temperature > 22°C, and > 2000 mm annual precipitation. This climate zone is present on the outer flanks of both cordilleras between 500 and 1500 m.a.s.l. and is directly influenced by very humid air masses. The vegetation is primarily forested.
5. Equatorial mesothermic semi-humid to humid climate: This type of climate has two annual peaks of precipitation between February and May and October to November, one pronounced dry season from June to September, an annual mean temperature of 12-22°C, and 500-2000 mm annual precipitation. The relative humidity is between 65 and 85%. The vegetation in this zone consists of Andean forest.
6. Equatorial mesothermic dry climate: This type of climate has two annual peaks of precipitation, an annual mean temperature of 12-22°C, and < 500 mm annual precipitation. This climate zone occurs in the sheltered interandean valleys on lower altitudes. Precipitation is rather low here, because much of the transported humidity is lost on the Andean flanks (Vuille, Bradley, and Keimig 2000).
7. Equatorial cold climate of the high mountains: This type of climate has two annual peaks of precipitation, an annual mean temperature < 12°C, and 800-2000 mm annual precipitation. This climate zone occurs above 3000 m.a.s.l. The relative humidity is above 80%. The natural vegetation is a shrub belt which at higher altitudes turns into a dense, water-saturated herbaceous layer, the páramo (Pourrut et al. 1995).

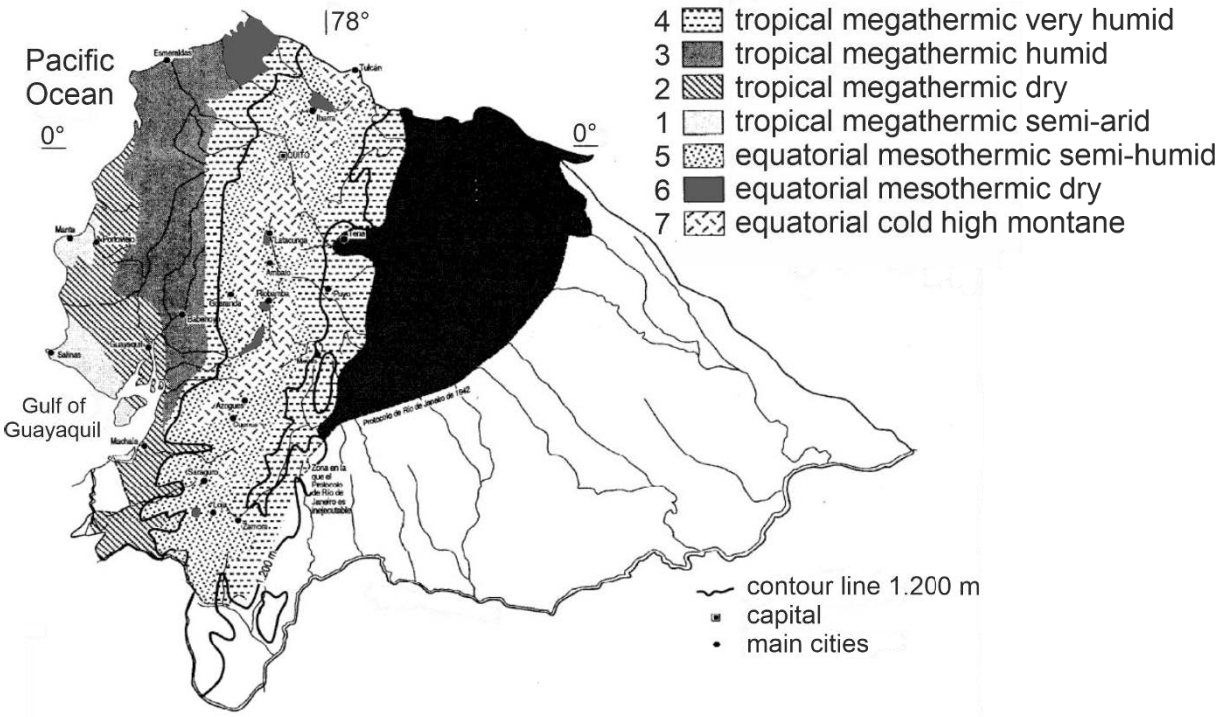

Figure 1.2. The main climate regimes of Ecuador, modified after Pourrut et al. (1995). Numbers of the climate regimes in the legend refer to numbers in the text.

1.2.2 Precipitation regimes

The annual precipitation patterns in Ecuador are determined by solar radiation which controls meridional shifts of the ITCZ. Precipitation is strongly modified by the topography of the Andes, ocean currents and sea surface temperature fluctuations and the valley winds (Bendix and Lauer 1992). The diverse influences of so many factors are the reason why so many distinct climate/precipitation regimes exist in this relatively small area. Precipitation in the coastal region of southern Ecuador and northern Peru is mainly modulated by El Niño dynamics (based on coastal sea surface temperatures offshore Ecuador and Peru), while precipitation in the western Andes is also influenced by El Niño (based on sea surface temperatures in the central Pacific) and the Pacific Decadal Oscillation (Moran-Tejeda et al. 2016). The climate divide over the high Andes shifts during the course of the year. During March/April (rainy season), the Eastern Cordillera acts as climate divide, because precipitation in the mountains has monsoonal character and originates from humid air masses over the warm Pacific Ocean. In contrast, the Western Cordillera is the climate divide in October, when humid air masses arrive in the high mountains mainly from the eastern lowlands (Bendix and Lauer 1992).

The lowlands on Colombia's Pacific coast belong to the rainiest regions on earth, with mean annual precipitation in excess of 12000 mm. This high precipitation is a result of the interaction of the

Choco jet with the dynamics of mesoscale convective systems, which deliver large amounts of moisture to the region (Poveda, Waylen, and Pulwarty 2006).

1.2.3 El Niño

As mentioned above, precipitation variability in western equatorial South America is partly related to sea surface temperature anomalies (SSTA) in the tropical Pacific. Temperature variability in the Andes depends even more on tropical Pacific SSTA. Only in the northernmost part of the Ecuadorian Andes (north of the equator), temperatures rather follow tropical North Atlantic SSTA, which are in turn related to Pacific SSTA (Vuille, Bradley, and Keimig 2000). The influence of Pacific SSTs on Andean temperatures is especially pronounced during El Niño (La Niña) years when the tropical Andes experience warming (cooling) up to 1°C (Garreaud 2009). Although the mechanism and its cause are not fully explored, it is known that the El Niño-Southern Oscillation (ENSO) is responsible for the recurring Pacific SSTA. According to Trenberth (1997), El Niño can be defined as an SSTA in the Central Pacific, where the 5-month running average exceeds 0.4°C for at least six months. The Southern Oscillation is the atmospheric component of this phenomenon. Thus, El Niño corresponds to the warm phase of ENSO with a deepened thermocline in the eastern Pacific, whereas La Niña is the basinwide cooling of the tropical Pacific (with a shallow thermocline in the eastern Pacific) and the cold phase of ENSO (Trenberth 1997). In the northwestern part of the Andes, the influence of ENSO is most prominent from December to February. It is expressed by below- (above-) average precipitation during El Niño (La Niña) years (Vuille, Bradley, and Keimig 2000; Moran-Tejeda et al. 2016). During El Niño years, the descending branch of the Walker cell moves eastward over Colombia and northern Ecuador suppressing convection, and the ITCZ shifts southwards. The westerly low level jet that normally flows from the Pacific Ocean to inland Colombia is weakened due to a reduced temperature gradient between Colombia and the EEP cold tongue. Therefore, the water vapor advection is decreased during El Niño (Waylen and Poveda 2002). In the coastal areas of northern Peru and Ecuador, this signal is reversed. The positive sea surface temperature anomalies in the eastern equatorial Pacific during El Niño cause a southward expansion and intensification of the ITCZ. This leads to exceptionally high rainfall, river runoff and flooding. On the western Andean slopes near 1°-3°S up to 1800 m, the precipitation response to ENSO is similar as in the coastal lowlands, which can be explained by the proximity of this region to the ocean and the exposure of the Andean slopes to Pacific air masses (Vuille, Bradley, and Keimig 2000; Bendix and Bendix 2006). High SSTs combined with large SST gradients offshore Ecuador and warm SST bubbles cause regional differences in moist instability and lead to heavy rainfall. Heavy precipitation during El Niño is

caused by both large scale circulation changes (reversal of the Walker circulation) and regional dynamics (extended land-sea-breeze system) (Bendix and Bendix 2006).

1.2.4 Atmospheric circulation

At higher levels, easterlies prevail (figure 1.3 b). The lower tropospheric flow is blocked by the Andes. Consequently, coastal areas and the western Andean slopes are mainly controlled by air masses from the Pacific, while the eastern Andes are influenced by the easterly trade winds, transporting moisture from the tropical Atlantic and Amazon (Vuille, Bradley, and Keimig 2000). The hydro-climatic cycle in northwestern South America is controlled by the annual migration of the ITCZ, which is in turn related to the dynamics of the trade winds. The westerly Choco jet at 5°N and its seasonal variability influences the regional climate. It is thermally driven by the SST gradient between the warmer Colombian Pacific and the colder EEP cold tongue. The Choco jet is further enhanced by the change of direction of the cross-equatorial southeast trade winds which become westerlies north of the equator (Poveda, Waylen, and Pulwarty 2006). Another easterly jet exists at the 600-700 hPa level over South America and the eastern equatorial Pacific (Hastenrath 1999). Analysis of pollen samples from Laguna Pallcacocha (~4000m), western Cordillera in Ecuador, suggests that this area is a climate divide with changing wind patterns which alternate between westerly and easterly winds (Hansen et al. 2003).

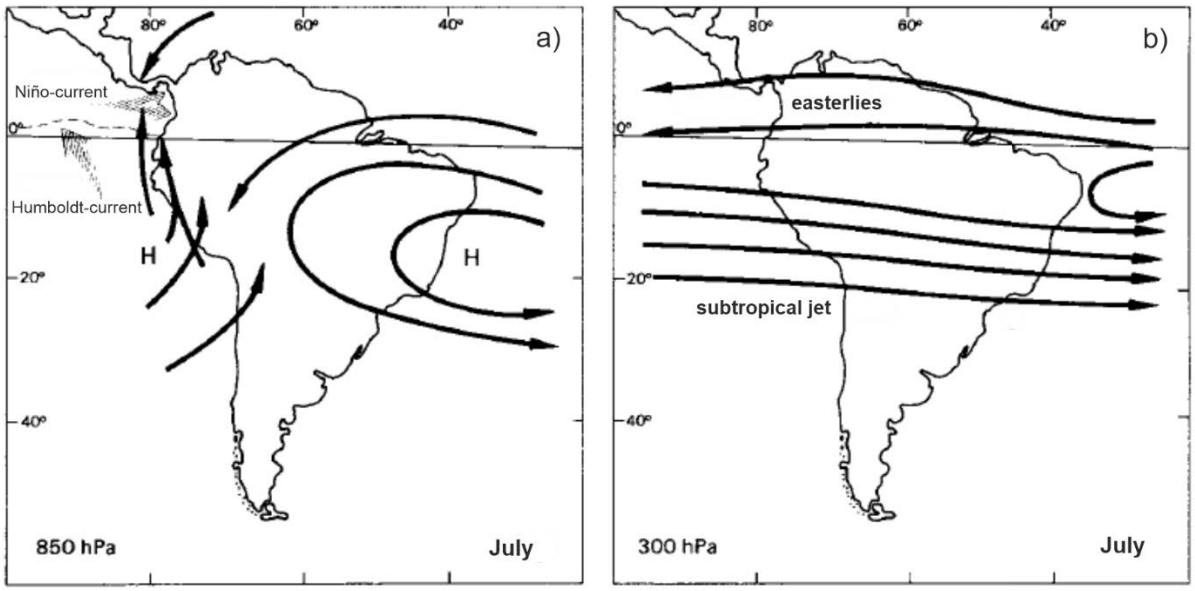

Figure 1.3. Atmospheric circulation patterns over South America in July a) at 850hPa (lower atmosphere) and b) at 300 hPa (upper atmosphere), modified after Bendix and Lauer (1992). Direction of the oceanic Humboldt- and Niño-current are indicated in gray.

1.3 Modern oceanographic setting of the eastern equatorial Pacific

The Eastern Equatorial Pacific (EEP) Ocean has two eastern boundary currents, the California Current along Baja California in the north and the Peru Current along Peru and Ecuador to the south, both with relatively cold surface waters (Wyrtki 1967; Fiedler and Talley 2006). They turn west near the equator and supply the zonal North and South Equatorial Currents (figure 1.4). The South Equatorial Current (SEC) is driven by the southeast trade winds. Since the trade winds cross the equator into the Northern Hemisphere, the SEC extends to about 4°N. However, farther to the south, the SEC is strongest and extends to a depth of 200 m (Wyrtki 1967). The eastern origin of the SEC remains unknown, although it is assumed that part of it comes from equatorial upwelling, part from the North Equatorial Countercurrent (NECC), and part from the Peru coast (Kessler 2006).

The westward flowing North and South Equatorial Currents are opposed by two eastward flowing currents, the North Equatorial Countercurrent (NECC) and the Equatorial Undercurrent (EUC). The 300 to 700 km wide NECC flows east between 4°N and 10°N, separating the North and South Equatorial Currents (Wyrtki 1967). The NECC splits and turns south into the SEC and north into the NEC, while only a small fraction of the NECC continues to the east (Kessler 2006). The EUC flows along the equator below the SEC at depths of 50 to 300 m (Wyrtki 1967). A large part of the high-salinity, high-oxygen waters of the EUC flows southeast and turns into the Peru Undercurrent (PUC), feeding the seasonal coastal upwelling. Although most of the EUC water flows to the Peruvian coast, a substantial portion of the EUC is lost downstream by upwelling (Kessler 2006).

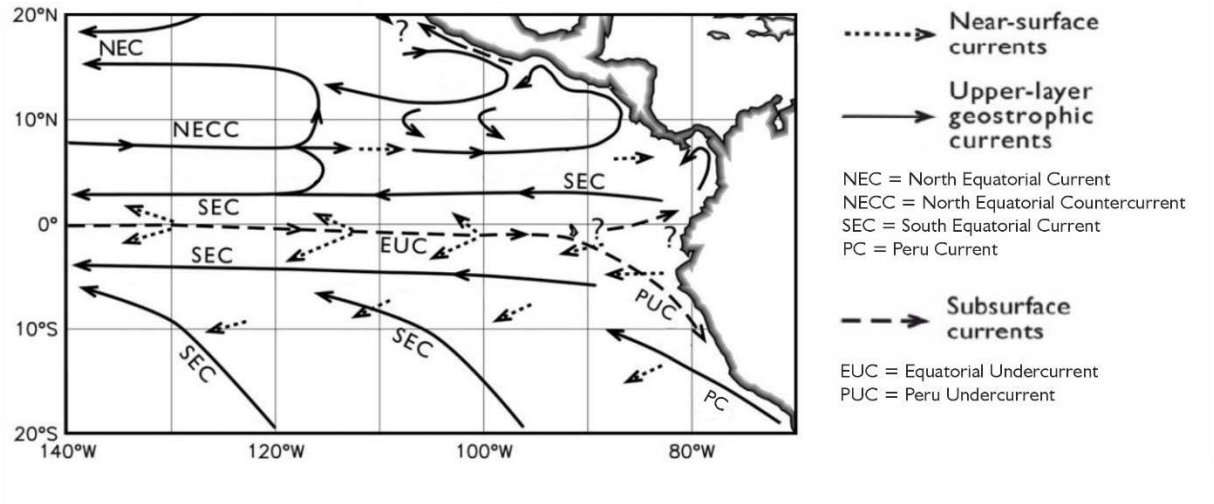

Figure 1.4. Main ocean circulation of the Eastern Equatorial Pacific, modified after Kessler (2006). Question marks indicate areas with unknown circulation patterns.

Upwelling along the coast of Peru is maintained by the interplay of the Peru Current, the westward wind drift and the subsurface PUC (Wyrtki 1967). The Eastern Equatorial Pacific cold tongue (EEP CT) is located slightly south of the equator east of 120°W. Its surface waters are characterized by equatorial upwelling and seasonal advection of cool water from the Peru Current (Fiedler and Talley 2006). A positive feedback exists between cool SST of the EEP and stratus clouds: The cool SST favor the formation of stratus clouds, which reduces insolation. This in turn keeps the SST cool. In the EEP, the ocean circulation is modified by the weaker and more southerly trade winds compared to the central Pacific. East of 85°W, the SEC is weak. The EUC is shallower in the EEP. East of 90°W, the zonal winds are weak or westerly (Kessler 2006).

The lowest surface salinity of the EEP is found in the Gulf of Panama, due to extreme local rainfall and additional westward transport of water vapor over the Isthmus of Panama. Further, a zonal band of low-salinity surface water is found along the mean position of the ITCZ, where precipitation is high. It is located around 5-7°N east of 100°W and at 10-11°N west of 110°W. The Eastern Tropical Pacific is characterized by a shallow thermocline with a large temperature difference between the top and the bottom. During El Niño events, the thermocline in the EEP deepens by 5-10m, whereas it shoals in the western tropical Pacific and in the subtropics (Fiedler and Talley 2006).

1.4 **Carnegie Ridge and Ocean Drilling Program Site 1239**

The Carnegie Ridge is an east-west oriented submarine ridge in the Eastern Equatorial Pacific which is about 1350 km long and 300 km wide (Rincón-Martínez 2013). The eastern part of Carnegie Ridge is affected by a higher degree of dissolution compared to the western Ridge. Dissolution by corrosive waters occurs because the northward flowing Pacific Bottom Water is rather cool and has a high CO_2 and organic carbon content (Pazmiño Manrique 2005). However, whereas dissolution occurs at the lysocline (2700-2800 m) and below, sediment deposition of calcareous material on the Ridge takes place above these depths (Rincón-Martínez 2013). Relatively constant sedimentation rates on the eastern Ridge were revealed by seismic profiles. Although most of the terrigenous sediments from the river delta systems along the South American coast end up in the Ecuadorian Trench, the eastern Ridge receives a moderate load. Maximum flux rates of terrigenous sediments are found at the mouths of the Magdalena, Esmeraldas, and Guayaquil rivers. The distribution of opal silica, which consists of the remains of diatoms and radiolarians, is correlated to surface productivity and is low on the eastern Ridge (Pazmiño Manrique 2005).

Ocean Drilling Program (ODP) Site 1239 is situated at 0°40.32'S, 82°4.86'W, about 120 km offshore Ecuador on the eastern side of Carnegie Ridge at a water depth of 1414 m. The area of Site 1239 is covered with thick sediments, mainly foraminifer-nannofossil ooze accompanied by

some diatom ooze, clay, micrite and ash layers. The sedimentation rates at Site 1239 are up to 10 cm/ky. Downslope sediment transport is possible along the steep basaltic flanks of Carnegie Ridge (Shipboard Scientific Party 2003). A tectonic backtracking of the Nazca plate reveals that Site 1239 was located about 200 km further west and slightly southwards compared to a fixed South America at 5 Ma (Pisias 1995). This change must be considered when interpreting the presented data. Presently, Site 1239 is located under the eastern border of the EEP CT in an upwelling system with relatively high salinity surface-waters close to the equator. To the north in contrast, the warm, low-salinity waters of Panama Basin are found. These two water bodies are separated by the equatorial front (EF) (Shipboard Scientific Party 2003).

1.5 Pollen transport to ODP Site 1239

There are basically two transport mechanisms for pollen grains to reach the site of deposition, by wind (aeolian transport) and by water (fluvial transport; Dupont 1999). For ODP Site 1239, Rincón-Martínez et al. (2010) found that fluvial transport of terrigenous sediment prevailed during Pleistocene interglacials, while the input of terrestrial material decreased during the drier glacial stages. Consequently, transport of pollen and spores to the study site is also predominantly fluvial (González, Urrego, and Martínez 2006).

Western equatorial South America is characterized by high amounts of precipitation, both, within the range of the ITCZ and of orographic nature. These heavy rains cause any pollen floating in the air to be washed out and transported by the several rivers draining the land west of the Andean Cordilleras. The northern coastal plain of Ecuador is drained by the Esmeraldas and Cayapas River, while several smaller rivers drain the southern coastal plain, eventually converging in the Guayas River (Balslev 1988). Major aeolian pollen transport to the ocean can be excluded due to the prevailing westerly winds. Furthermore, aeolian transport of terrigenous sediments was shown to be predominant only south of 5°S (Saukel et al. 2011). However, a small fraction might be transported by the SE trade winds. Transport within the ocean is directed by ocean currents. Once the palynomorphs reach the ocean, they presumably pass the narrow Peru-Chile Trench in nepheloid layers at subsurface depths. While some pollen transport from the Bay of Guayaquil northwards via the Coastal Current is possible, the Peru-Chile Current is located too far from the coast to have a significant influence on palynomorph transport.

The main source area of palynomorphs at ODP Site 1239 is considered to be western Ecuador, northernmost Peru, and southwestern Colombia, which is broadly the catchment area of the main rivers and their tributaries in this area. The development of the catchment area towards its present state is closely related to Andean uplift. As known from the eastern Cordillera of Peru, Andean-Amazonian drainage patterns began to set up in late Cretaceous to early Paleocene times already

(Hurtado et al. 2018). If a similar orographic history is postulated for the Western Cordillera of Ecuador, present-day drainage patterns might have been established well before the Pliocene.

1.6 Thesis outline

This thesis was written in a cumulative form, with two peer-reviewed and published manuscripts (Chapters 4 and 5) and one chapter about the uplift history of the Northern and Central Andes (Chapter 3). The thesis ends with a comprehensive conclusion, where the parts are put together and links across the chapters are described.

Overview of the manuscripts and contributions:

1) Chapter 3: **Andean uplift**

   This chapter gives an overview of the current state of knowledge on the timing of uplift of the Northern and Central Andes. It therefore has the character of a review paper rather than a manuscript presenting original research.

   The chapter was designed and written by Friederike Grimmer.

2) Chapter 4: **"Early Pliocene vegetation and hydrology changes in western equatorial South America"**

   Friederike Grimmer, Lydie Dupont, Frank Lamy, Gerlinde Jung, Catalina González, and Gerold Wefer.

   Published in *Climate of the Past*

   In this manuscript, pollen data from ODP Site 1239 from the time window between 4.7 and 4.2 Ma are presented and discussed. Additionally, Fe/K data support the hydrological interpretation. This paper focuses on the question of an early Pliocene shift of the Intertropical Convergence Zone (ITCZ) in the context of the progressive closure of the Central American Seaway (CAS) and the uplift of the Northern Andes. Furthermore, the origin of páramo vegetation in the study area is assessed.

   The idea for this study was conceived by Lydie Dupont and Friederike Grimmer. The sample preparation and the microscopic analysis was carried out by Friederike Grimmer (53 samples) and Lydie Dupont (16 samples). The X-ray fluorescence (XRF) core scanning data was provided by Frank Lamy. Friederike Grimmer analyzed the data and prepared the manuscript with contributions from all co-authors.

3) Chapter 5: **"Piacenzian environmental change and the onset of cool and dry conditions in tropical South America"**

Friederike Grimmer, Lydie M. Dupont, Gerlinde Jung, and Gerold Wefer

Published in *Paleoceanography and Paleoclimatology*

This manuscript focuses on late Pliocene vegetation and climate change in western equatorial South America, a time when the atmospheric circulation presumably strengthened and the global climate started to cool.

The idea for this study was conceived by Lydie Dupont and Friederike Grimmer. Friederike Grimmer carried out the sample preparation and the microscopic analysis of 83 samples. Lydie Dupont carried out the sample preparation and the microscopic analysis of 5 samples. Friederike Grimmer analyzed the data and prepared the manuscript with contributions from all co-authors.

1.7 References

Abels, H. A., and M. Ziegler. 2018. 'Paleoclimate.' in C. Hoorn, A. L. Perrigo and A. Antonelli (eds.), *Mountains, Climate and Biodiversity* (Wiley-Blackwell).

Bacon, C. D., D. Silvestro, C. Jaramillo, B. T. Smith, P. Chakrabarty, and A. Antonelli. 2015. 'Biological evidence supports an early and complex emergence of the Isthmus of Panama', *Proceedings of the National Academy of Sciences of the United States of America*, 112: 6110-5.

Bakker, J., M. M. Olivera, and H. Hooghiemstra. 2008. 'Holocene environmental change at the upper forest line in northern Ecuador', *Holocene*, 18: 877-93.

Balslev, H. 1988. 'Distribution Patterns of Ecuadorean Plant-Species', *Taxon*, 37: 567-77.

Bendix, A. , and J. Bendix. 2006. 'Heavy rainfall episodes in Ecuador during El Nino events and associated regional atmospheric circulation and SST patterns', *Advances in Geosciences*, 6: 43-49.

Bendix, J., and W. Lauer. 1992. 'Die Niederschlagsjahreszeiten in Ecuador und ihre klimadynamische Interpretation', *Erdkunde*, 46: 118-34.

Bonham, S. G., A. M. Haywood, D. J. Lunt, M. Collins, and U. Salzmann. 2009. 'El Nino-Southern Oscillation, Pliocene climate and equifinality', *Philos Trans A Math Phys Eng Sci*, 367: 127-56.

Brierley, C. M., A. V. Fedorov, Z. Liu, T. D. Herbert, K. T. Lawrence, and J. P. Lariviere. 2009. 'Greatly expanded tropical warm pool and weakened Hadley circulation in the early Pliocene', *Science*, 323: 1714-8.

Britannica. 2011. "Vegetation zones of South America." In *Encyclopaedia Britannica*.

Burke, K. D., J. W. Williams, M. A. Chandler, A. M. Haywood, D. J. Lunt, and B. L. Otto-Bliesner. 2018. 'Pliocene and Eocene provide best analogs for near-future climates', *Proceedings of the National Academy of Sciences of the United States of America*, 115: 13288-93.

Bush, M. B. 2001. 'The Influence of Biogeographic and Ecological Heterogeneity on Amazonian Pollen Spectra', *Journal of Tropical Ecology*, 17: 729-43.

Cannariato, K. G., and A. C. Ravelo. 1997. 'Pliocene-Pleistocene evolution of eastern tropical Pacific surface water circulation and thermocline depth', *Paleoceanography*, 12: 805-20.

Chaisson, W. P., and A. C. Ravelo. 2000. 'Pliocene development of the east-west hydrographic gradient in the equatorial Pacific', *Paleoceanography*, 15: 497-505.

Chiessi, C. M., S. Mulitza, N. K. Taniguchi, M. Prange, M. C. Campos, C. Haggi, E. Schefuss, T. M. L. Pinho, T. Frederichs, R. C. Portilho-Ramos, S. H. M. Sousa, S. Crivellari, and F. W. Cruz. 2021. 'Mid- to Late Holocene Contraction of the Intertropical Convergence Zone Over Northeastern South America', *Paleoceanography and Paleoclimatology*, 36: 1-20.

Cleef, A. 1981. 'The Vegetation of the Páramos of the Colombian Cordillera Oriental', Mededelingen van het Botanisch Museum en Herbarium van de Rijksuniversiteit te Utrecht.

Coates, A.G., L.S. Collins, M.-P. Aubry, and W.A. Berggren. 2004. 'The Geology of the Darien, Panama, and the late Miocene-Pliocene collision of the Panama arc with northwestern South America', *GSA Bulletin*, 116: 1327-44.

Cuatrecasas, J. 1934. 'Observaciones geobotanicas en Colombia', *Trabajos del Museo Nacional de Ciencias Naturales*, Serie Botánica: 144.

———. 1958. 'Aspectos de la vegetación naturel de Colombia', *Rev. Acad. Colomb. Cienc. Ex. Fis. Nat.*, 10: 221-64.

Dowsett, H., A. Dolan, D. Rowley, R. Moucha, A. M. Forte, J. X. Mitrovica, M. Pound, U. Salzmann, M. Robinson, M. Chandler, K. Foley, and A. Haywood. 2016. 'The PRISM4 (mid-Piacenzian) paleoenvironmental reconstruction', *Climate of the Past*, 12: 1519-38.

Dupont, L. M. 1999. 'Pollen and spores in marine sediments from the East Atlantic. A view from the ocean into the African continent. .' in G. Fischer and G. Wefer (eds.), *Use of Proxies in Paleoceanography: Examples from the South Atlantic.* (Springer Verlag: Berlin Heidelberg).

Fedorov, A. V., P. S. Dekens, M. McCarthy, A. C. Ravelo, P. B. deMenocal, M. Barreiro, R. C. Pacanowski, and S. G. Philander. 2006. 'The Pliocene paradox (mechanisms for a permanent El Niño)', *Science*, 312: 1485-9.

Fiedler, P. C., and L. D. Talley. 2006. 'Hydrography of the eastern tropical Pacific: A review', *Progress in Oceanography*, 69: 143-80.

Fischer, H., K. J. Meissner, A. C. Mix, N. J. Abram, J. Austermann, V. Brovkin, E. Capron, D. Colombaroli, A. L. Daniau, K. A. Dyez, T. Felis, S. A. Finkelstein, S. L. Jaccard, E. L. McClymont, A. Rovere, J. Sutter, E. W. Wolff, S. Affolter, P. Bakker, J. A. Ballesteros-Canovas, C. Barbante, T. Caley, A. E. Carlson, O. Churakova, G. Cortese, B. F. Cumming, B. A. S. Davis, A. de Vernal, J. Emile-Geay, S. C. Fritz, P. Gierz, J. Gottschalk, M. D. Holloway, F. Joos, M. Kucera, M. F. Loutre, D. J. Lunt, K. Marcisz, J. R. Marlon, P. Martinez, V. Masson-Delmotte, C. Nehrbass-Ahles, B. L. Otto-Bliesner, C. C. Raible, B. Risebrobakken, M. F. S. Goni, J. S. Arrigo, M. Sarnthein, J. Sjolte, T. F. Stocker, P. A. V. Alvarez, W. Tinner, P. J. Valdes, H. Vogel, H. Wanner, Q. Yan, Z. C. Yu, M. Ziegler, and L. P. Zhou. 2018. 'Palaeoclimate constraints on the impact of 2 degrees C anthropogenic warming and beyond', *Nature Geoscience*, 11: 615-15.

Flesche Kleiven, H., E. Jansen, T. Fronval, and T. M. Smith. 2002. 'Intensification of Northern Hemisphere glaciations in the circum Atlantic region (3.5-2.4 Ma) - ice-rafted detritus evidence', *Palaeogeography Palaeoclimatology Palaeoecology*, 184: 213-23.

Ford, H. L., A. C. Ravelo, P. S. Dekens, J. LaRiviere, and M. W. Wara. 2015. 'The evolution of the equatorial thermocline and the early Pliocene El Padre mean state', *Geophysical Research Letters*, 42: 4878-87.

Garreaud, R. D. 2009. 'The Andes climate and weather', *Advances in Geosciences*, 7: 1-9.

González, C., L. E. Urrego, and J. I. Martínez. 2006. 'Late Quaternary vegetation and climate change in the Panama Basin: Palynological evidence from marine cores ODP 677B and TR 163-38', *Palaeogeography, Palaeoclimatology, Palaeoecology*, 234: 62-80.

Grabandt, R. A. J. 1980. 'Pollen Rain in Relation to Arboreal Vegetation in the Colombian Cordillera Oriental', *Review of Palaeobotany and Palynology*, 29: 65-147.

Groeneveld, J., S. Steph, R. Tiedemann, D. Garbe-Schönberg, D. Nürnberg, and A. Sturm. 2006. 'Pliocene mixed-layer oceanography for Site 1241, using combined Mg/Ca and $d^{18}O$ analyses of *Globigerinoides sacculifer*', *Proceedings of the Ocean Drilling Program, Scientific Results*, 202.

Grubb, P. J., J. R. Lloyd, T. D. Pennington, and T. C. Whitmore. 1963. 'A comparison of montane and lowland rain forest in Ecuador', *Journal of Ecology*, 51: 567-601.

Hagemans, K., C.-D. Tóth, M. Ormaza, W. D. Gosling, D. H. Urrego, S. León-Yánez, F. Wagner-Cremer, and T. H. Donders. 2019. 'Modern pollen-vegetation relationships along a steep temperature gradient in the Tropical Andes of Ecuador', *Quaternary Research*: 1-13.

Hansen, B. C. S., and D. T. Rodbell. 1995. 'A late Glacial Holocene Pollen Record from the Eastern Andes of Northern Peru', *Quaternary Research*, 44: 216-27.

Hansen, B. C. S., D. T. Rodbell, G. O. Seltzer, B. León, K. R. Young, and M. Abbott. 2003. 'Late-glacial and Holocene vegetational history from two sites in the western Cordillera of southwestern Ecuador', *Palaeogeography, Palaeoclimatology, Palaeoecology*, 194: 79-108.

Hastenrath, S. 1999. 'Equatorial Mid-Tropospheric Easterly Jet over the eastern Pacific', *Journal of the Meteorological Society of Japan*, 77: 701-09.

Haug, G. H., K. A. Hughen, D. M. Sigman, L. C. Peterson, and U. Röhl. 2001. 'Southward Migration of the Intertropical Convergence Zone Through the Holocene', *Science*, 293: 1304-8.

Haug, G. H., and R. Tiedemann. 1998. 'Effect of the formation of the Isthmus of Panama on Atlantic Ocean thermohaline circulation', *Nature*, 393: 673-76.

Haywood, A. M., M. A. Chandler, P. J. Valdes, U. Salzmann, D. J. Lunt, and H. J. Dowsett. 2009. 'Comparison of mid-Pliocene climate predictions produced by the HadAM3 and GCMAM3 General Circulation Models', *Global and Planetary Change*, 66: 208-24.

Haywood, A. M., and P. J. Valdes. 2004. 'Modelling Pliocene warmth: contribution of atmosphere, oceans and cryosphere', *Earth and Planetary Science Letters*, 218: 363-77.

Homeier, J., F.A. Werner, S.R. Gradstein, S.-W. Breckle, and M. Richter. 2008. 'Potential Vegetation and Floristic Composition of Andean Forests in South Ecuador, with a Focus on the RBSF.' in E. Beck, J. Bendix, I. Kottke, F. Makeschin and R. Mosandl (eds.), *Gradients in a Tropical Mountain Ecosystem of Ecuador* (Springer: Heidelberg).

Hooghiemstra, H. 1989. 'Quaternary and Upper-Pliocene Glaciations and Forest Development in the Tropical Andes - Evidence from a Long High-Resolution Pollen Record from the Sedimentary Basin of Bogotá, Colombia', *Palaeogeography Palaeoclimatology Palaeoecology*, 72: 11-26.

Hooghiemstra, H., J. L. Melice, A. Berger, and N. J. Shackleton. 1993. 'Frequency spectra and paleoclimatic variability of the high-resolution 30-1450 ka Funza I pollen record (Eastern Cordillera, Colombia)', *Palaeogeography Palaeoclimatology Palaeoecology*, 72: 11-26.

Hooghiemstra, H., and E. Th. H. Ran. 1994b. 'Upper and middle Pleistocene climatic change and forest development in Colombia: pollen record Funza II (2-158 m core interval)', *Palaeogeography, Palaeoclimatology, Palaeoecology*, 109: 211-46.

Hooghiemstra, H., and T. van der Hammen. 1998. 'Neogene and Quaternary development of the neotropical rain forest: the forest refugia hypothesis, and a literature overview', *Earth-Science Reviews*, 44: 147-83.

———. 2004. 'Quaternary Ice-Age dynamics in the Colombian Andes: developing an understanding of our legacy', *Philosophical Transactions of the Royal Society of London Series B-Biological Sciences*, 359: 173-80.

Hooghiemstra, H., V. M. Wijninga, and A. M. Cleef. 2006. 'The Paleobotanical Record of Colombia: Implications for Biogeography and Biodiversity', *Annals of the Missouri Botanical Garden*, 93: 297-325.

Hovan, S. A. . 1995. 'Late Cenozoic atmospheric circulation intensity and climatic history recorded by Eolian deposition in the Eastern Equatorial Pacific Ocean, Leg 138', *Proceedings of the Ocean Drilling Program, Scientific Results*, 138: 615-25.

Humboldt, A., and A. Bonpland. 1807. *Ideen zu einer Geographie der Pflanzen nebst einem Naturgemälde der Tropenländer: auf Beobachtungen und Messungen gegründet, welche vom 10ten Grade nördlicher bis zum 10ten Grade südlicher Breite, in den Jahren 1799, 1800, 1801, 1802 und 1803 angestellt worden sind* (Cotta: Tübingen).

Hurtado, C., M. Roddaz, R. Ventura Santos, P. Baby, P.-O. Antoine, and E.L. Dantas. 2018. 'Late Cretaceous-early Paleocene drainage shift of Amazonian rivers driven by Equatorial Atlantic Ocean opening and Andean uplift as deduced from the provenance of northern Peruvian sedimentary rocks (Huallaga basin)', *Gondwana Research*, 63: 152-68.

IPCC. 2019. "Technical Summary." In *IPCC Special Report on the Ocean and Cryosphere in a Changing Climate*, edited by H.-O. Pörtner, D.C. Roberts, V. Masson-Delmotte, P. Zhai, E. Poloczanska, K. Mintenbeck, M. Tignor, A. Alegría, M. Nicolai, A. Okem, J. Petzold, B. Rama and N.M. Weyer.

Jansen, B., E. J. de Boer, A. M. Cleef, H. Hooghiemstra, M. Moscol-Olivera, F. H. Tonneijck, and J. M. Verstraten. 2013. 'Reconstruction of late Holocene forest dynamics in northern Ecuador from biomarkers and pollen in soil cores', *Palaeogeography Palaeoclimatology Palaeoecology*, 386: 607-19.

Jantz, N. 2014. 'Representativeness of tree diversity in the modern pollen rain of Andean montane forests', *Journal of Vegetation Science*, 25: 481-90.

Jaramillo, C. 2018. 'Evolution of the Isthmus of Panama: Biological, Paleoceanographic and Paleoclimatological Implications.' in C. Hoorn, A. L. Perrigo and A. Antonelli (eds.), *Mountains, Climate and Biodiversity* (John Wiley & Sons Ltd.).

Jaramillo, C., C. Montes, A. Cardona, D. Silvestro, A. Antonelli, and C. D. Bacon. 2017. 'Comment (1) on "Formation of the Isthmus of Panama" by O'Dea *et al.*', *Science Advances*, 3: 1-8.

Jørgensen, P. M., and S. León-Yánez. 1999. *Catalogue of the vascular plants of Ecuador = Catálogo de las plantas vasculares del Ecuador* (Missouri Botanical Garden Press: St. Louis, Missouri).

Kessler, W. S. 2006. 'The circulation of the eastern tropical Pacific: A review', *Progress in Oceanography*, 69: 181-217.

Lawrence, K. T., Z. Liu, and T. D. Herbert. 2006. 'Evolution of the eastern tropical Pacific through Plio-Pleistocene glaciation', *Science*, 312: 79-83.

Madriñán, S., A. J. Cortes, and J. E. Richardson. 2013. 'Páramo is the world's fastest evolving and coolest biodiversity hotspot', *Frontiers in Genetics*, 4: 1-7.

Molnar, P. 2017. 'Comment (2) on "Formation of the Isthmus of Panama" by O'Dea *et al.*', *Science Advances*, 3: 1-4.

Montes, C., G. A. Bayona, A. Cardona, D. M. Buchs, C. A. Silva, S. Morón, N. Hoyos, D. A. Ramirez, C. A. Jaramillo, and V. Valencia. 2012. 'Arc-continent collision and orocline formation: Closing of the Central American seaway', *Journal of Geophysical Research*, 117: 1-25.

Montes, C., A. Cardona, C. Jaramillo, A. Pardo, J.C. Silva, V. Valencia, C. Ayala, L.C. Pérez-Angel, L.A. Rondriguez-Parra, V. Ramirez, and H. Nino. 2015. 'Middle Miocene closure of the Central American Seaway', *Paleoceanography*, 348: 226-29.

Montes, C., A. Cardona, R. McFadden, S. E. Moron, C. A. Silva, S. Restrepo-Moreno, D. A. Ramirez, N. Hoyos, J. Wilson, D. Farris, G. A. Bayona, C. A. Jaramillo, V. Valencia, J. Bryan, and J. A. Flores. 2012. 'Evidence for middle Eocene and younger land emergence in central Panama: Implications for Isthmus closure', *Geological Society of America Bulletin*, 124: 780-99.

Moran-Tejeda, E., J. Bazo, J. I. Lopez-Moreno, E. Aguilar, C. Azorin-Molina, A. Sanchez-Lorenzo, R. Martinez, J. J. Nieto, R. Mejia, N. Martin-Hernandez, and S. M. Vicente-Serrano. 2016. 'Climate trends and variability in Ecuador (1966-2011)', *International Journal of Climatology*, 36: 3839-55.

Morueta-Holme, N., K. Engemann, P. Sandoval-Acuna, J. D. Jonas, R. M. Segnitz, and J. C. Svenning. 2015. 'Strong upslope shifts in Chimborazo's vegetation over two centuries since Humboldt', *Proceedings of the National Academy of Sciences of the United States of America*, 112: 12741-5.

Moscol Olivera, M. , J. Duivenvoorden, and H. Hooghiemstra. 2009. 'Pollen rain and pollen representation across a forest-páramo ecotone in northern Ecuador', *Review of Palaeobotany and Palynology*, 157: 285-300.

Moscol Olivera, M., and A. Cleef. 2009. 'Vegetation composition and altitudinal distribution of Andean rain forests in El Angel and Guandera reserves, northern Ecuador', *Phytocoenologia*, 39: 175-204.

Moscol Olivera, M., and H. Hooghiemstra. 2010. 'Three millennia upper forest line changes in northern Ecuador: Pollen records and altitudinal vegetation distributions', *Review of Palaeobotany and Palynology*, 163: 113-26.

Niemann, H., C. Brunschön, and H. Behling. 2010. 'Vegetation/modern pollen rain relationship along an altitudinal transect between 1920 and 3185 m a.s.l. in the Podocarpus National Park region, southeastern Ecuadorian Andes', *Review of Palaeobotany and Palynology*, 159: 69-80.

O'Dea, A. , A.H. Lessios, A.G. Coates, R.I. Eytan, S.A. Restrepo-Moreno, A.L. Cione, L.S. Collins, A. de Queiroz, D.W. Farris, R.D. Norris, R.F. Stallard, M.O. Woodburne, O. Aguilera, M.-P. Aubry, W.A. Berggren, A.F. Budd, M.A. Cozzuol, S.E. Coppard, H. Duque-Caro, S. Finnegan, G.M. Gasparini, E.L. Grossman, K.G. Johnson, L.D. Keigwin, N. Knowlton, E.G. Leigh, J.S. Leonard-Pingel, P.B. Marko, N.D. Pyenson, P.G. Rachello-Dolmen, E. Soibelzon, L. Soibelzon, J.A. Todd, G.J. Vermeij, and J.B.C. Jackson. 2016. 'Formation of the Isthmus of Panama', *Science Advances*, 2: 1-11.

Pagani, M., Z. H. Liu, J. LaRiviere, and A. C. Ravelo. 2010. 'High Earth-system climate sensitivity determined from Pliocene carbon dioxide concentrations', *Nature Geoscience*, 3: 27-30.

Parsons, R. W., and I. C. Prentice. 1981. 'Statistical Approaches to R-Values and the Pollen-Vegetation Relationship', *Review of Palaeobotany and Palynology*, 32: 127-52.

Pazmiño Manrique, N. A. 2005. 'Sediment distribution and depositional processes on the Carnegie Ridge', Texas A&M University.

Pérez-Escobar, O. A. , A. Zizka, M. A. Bermudez, A. S. Meseguer, F. L. Condamine, C. Hoorn, H. Hooghiemstra, Y. Pu, D. Bogarin, L. M. Boschman, R. T. Pennington, A. Antonelli, and G. Chomicki. 2022. 'The Andes through time: evolution and distribution of Andean floras', *Trends in Plant Science*, 27: 364-78.

Pisias, N. 1995. 'Paleoceanography of the eastern equatorial Pacific during the Neogene: Synthesis of Leg 138 drilling results', *Proceedings of the Ocean Drilling Program, Scientific Results*, 138: 5-21.

Pourrut, P., O. Róvere, I. Romo, and H. Villacrés. 1995. 'Artículo III Clima del Ecuador.' in P. Pourrut (ed.), *El Agua en el Ecuador Clima, precipitaciones, escorrentía* (Estudios de Geografía: Quito).

Poveda, G., P. R. Waylen, and R. S. Pulwarty. 2006. 'Annual and inter-annual variability of the present climate in northern South America and southern Mesoamerica', *Palaeogeography Palaeoclimatology Palaeoecology*, 234: 3-27.

Prentice, I. C. 1985. 'Pollen Representation, Source Area, and Basin Size: Toward a Unified Theory of Pollen Analysis', *Quaternary Research*, 23: 76-86.

Prescott, C. L., A. M. Haywood, A. M. Dolan, S. J. Hunter, J. O. Pope, and S. J. Pickering. 2014. 'Assessing orbitally-forced interglacial climate variability during the mid-Pliocene Warm Period', *Earth and Planetary Science Letters*, 400: 261-71.

Ravelo, A. C., K. T. Lawrence, A. Fedorov, and H. L. Ford. 2014. 'Comment on "A 12-million-year temperature history of the tropical Pacific Ocean"', *Science*, 346.

Richter, M., K.-H. Diertl, T. Peters, and R. W. Bussmann. 2008. 'Vegetation Structures and Ecological Features of the Upper Timberline Ecotone.' in E. Beck, J. Bendix, I. Kottke, F. Makeschin and R. Mosandl (eds.), *Gradients in a Tropical Mountain Ecosystem of Ecuador* (Springer: Heidelberg).

Rincón-Martínez, D. 2013. 'Eastern Pacific background state and tropical South American climate history during the last 3 million years', Universität Bremen.

Rincón-Martínez, D., F. Lamy, S. Contreras, G. Leduc, E. Bard, C. Saukel, T. Blanz, A. Mackensen, and R. Tiedemann. 2010. 'More humid interglacials in Ecuador during the past 500 kyr linked to latitudinal shifts of the equatorial front and the Intertropical Convergence Zone in the eastern tropical Pacific', *Paleoceanography*, 25: 1-15.

Robinson, M., H. Dowsett, and M. Chandler. 2008. 'Pliocenen Role in Assessing Future Climate Impacts', *EOS Transactions, American Geophysical Union*, 89: 501-12.

Saukel, C., F. Lamy, J. B. W. Stuut, R. Tiedemann, and C. Vogt. 2011. 'Distribution and provenance of wind-blown SE Pacific surface sediments', *Marine Geology*, 280: 130-42.

Schneider, T., T. Bischoff, and G. H. Haug. 2014. 'Migrations and dynamics of the intertropical convergence zone', *Nature*, 513: 45-53.

Seki, O., G. L. Foster, D. N. Schmidt, A. Mackensen, K. Kawamura, and R. D. Pancost. 2010. 'Alkenone and boron-based Pliocene pCO(2) records', *Earth and Planetary Science Letters*, 292: 201-11.

Sepulchre, P., T. Arsouze, Y. Donnadieu, J. C. Dutay, C. Jaramillo, J. Le Bras, E. Martin, C. Montes, and A. J. Waite. 2014. 'Consequences of shoaling of the Central American Seaway determined from modeling Nd isotopes', *Paleoceanography*, 29: 176-89.

Shipboard Scientific Party. 2003. "Site 1239." In *Proceedings of the Ocean Drilling Program, Initial Reports*, edited by A.C. Mix, R. Tiedemann and P. Blum, 1-93. College Station, Texas: Ocean Drilling Program.

Song, Z. Y., M. Latif, W. Park, U. Krebs-Kanzow, and B. Schneider. 2017. 'Influence of seaway changes during the Pliocene on tropical Pacific climate in the Kiel climate model: mean state, annual cycle, ENSO, and their interactions', *Climate Dynamics*, 48: 3725-40.

Steph, S., R. Tiedemann, M. Prange, J. Groeneveld, D. Nurnberg, L. Reuning, M. Schulz, and G. H. Haug. 2006. 'Changes in Caribbean surface hydrography during the Pliocene shoaling of the Central American Seaway', *Paleoceanography*, 21: 1-25.

Steph, S., R. Tiedemann, M. Prange, J. Groeneveld, M. Schulz, A. Timmermann, D. Nürnberg, C. Rühlemann, C. Saukel, and G. H. Haug. 2010. 'Early Pliocene increase in thermohaline overturning: A precondition for the development of the modern equatorial Pacific cold tongue', *Paleoceanography*, 25.

Thuiller, W. 2007. 'Biodiversity: climate change and the ecologist', *Nature*, 448: 550-2.

Tiedemann, R., and A. Mix. 2007. "Leg 202 Synthesis southeast pacific paleoceanography." In *Proc. ODP, Sci. Results, 202*, edited by R. Tiedemann, A.C. Mix, C. Richter and W.F. Ruddiman, 1-56. College Station, TX (Ocean Drilling Program).

Trenberth, K. E. 1997. 'The definition of El Nino', *Bulletin of the American Meteorological Society*, 78: 2771-77.

Van der Hammen, T. 1974a. 'The Pleistocene Changes of Vegetation and Climate in Tropical South America', *Journal of Biogeography*, 1: 3-26.

Van der Hammen, T., J. H. Werner, and H. van Dommelen. 1973. 'Palynological record of the upheaval of the Northern Andes: a study of the Pliocene and Lower Quaternary of the Colombian early evolution of its high-Andean biota', *Review of Palaeobotany and Palynology*, 16: 1-122.

Vuille, M., R.S. Bradley, and F. Keimig. 2000. 'Climate variability in the Andes of Ecuador and its relation to tropical Pacific and Atlantic Sea surface temperature anomalies', *Journal of Climate*, 13: 2520-35.

Wara, M. W., A. C. Ravelo, and M. L. Delaney. 2005. 'Permanent El Niño-like conditions during the Pliocene warm period', *Science*, 309: 758-61.

Waylen, P., and G. Poveda. 2002. 'El Niño-Southern Oscillation and aspects of western South American hydro-climatology', *Hydrological Processes*, 16: 1247-60.

Webb, T. 1980. 'The reconstruction of climatic sequences from botanical data', *The Journal of Interdisciplinary History*, 10: 749-72.

Weng, C., H. Hooghiemstra, and J. F. Duivenvoorden. 2007. 'Response of pollen diversity to the climate-driven altitudinal shift of vegetation in the Colombian Andes', *Philosophical Transactions of the Royal Society B: Biological Sciences*, 362: 253-62.

Weng, C. Y., M. B. Bush, and M. R. Silman. 2004. 'An analysis of modern pollen rain on an elevational gradient in southern Peru', *Journal of Tropical Ecology*, 20: 113-24.

White, S. M., and A. C. Ravelo. 2020. 'The Benthic B/Ca Record at Site 806: New Constraints on the Temperature of the West Pacific Warm Pool and the "El Padre" State in the Pliocene', *Paleoceanography and Paleoclimatology*, 35: 1-18.

Wyrtki, K. 1967. 'Circulation and Water Masses in Eastern Equatorial Pacific Ocean', *International Journal of Oceanology and Limnology*, 1: 117-47.

Zubakov, V. A., and I. I. Borzenkova. 1988. 'Pliocene Paleoclimates - Past Climates as Possible Analogs of Mid-21st Century Climate', *Palaeogeography Palaeoclimatology Palaeoecology*, 65: 35-49.

2 Methods

2.1 Stratigraphy (age model)

Orbital tuning is a method where the observation that cyclic changes in climate records respond to variations in insolation is used to date Neogene sediments. The main orbital parameters used for astronomical tuning are the eccentricity of the Earth's orbit with periods of 413, 95 and 123 thousand years (k.y.), the obliquity/tilt of the Earth's axis with a period of 41 k.y., and the precession of the Earth's axis with a period of 23 and 19 k.y. (Berger 1988).

For the age model of ODP Site 1239, its benthic $\delta^{18}O$ and $\delta^{13}C$ records were correlated to the orbitally tuned isotope record of Site 1241 (Tiedemann et al. 2007). The orbitally tuned age model of ODP Site 1241 was generated by correlation of variations in Earth's orbital parameters (Laskar, Joutel, and Boudin 1993) with different sedimentary parameters (variations in gamma ray attenuation density, percent sand of the carbonate fraction, benthic $\delta^{13}C$). The age model of Site 1239 is not orbitally tuned as a composite depth for the Miocene to Pliocene interval is missing (Tiedemann et al. 2007). The initial age model of Site 1239 is based on biostratigraphic information (Shipboard Scientific Party 2003). Subsequently, the benthic $\delta^{18}O$ and $\delta^{13}C$ records of Hole 1239A and site 1241 were matched by visually identifying isotope stages. This approach resulted in an indirectly orbitally tuned age model for Site 1239 for the time interval from 2.7 to 5 Ma (Tiedemann et al. 2007, compare table 2.1). Ages between the age-depth control points were determined through linear interpolation. For the time interval between 0.5 and 0 Ma, an age model was constructed by Rincón-Martínez (2013) based on the benthic oxygen isotope record tuned to the LR04 benthic stack (Lisiecki and Raymo 2005). Thus, a Holocene age could be assigned to the surface/subsurface samples taken from Hole 1239B.

Table 2.1. Age-depth control points (Tiedemann et al. 2007) and cumulative offset (Shipboard Scientific Party 2003) for Hole 1239A.

Age (ka)	Depth (mcd)	Cumulative offset (m)
2700	150.73	12.8
2766	162.29	13.05
2896	176.15	15.0
2999	190.18	15.16
3107	208.51	16.88
3204	222.41	17.74
3361	249.34	20.32
3424	257.70	21.18
3561	271.77	22.04

3630	277.48	22.04
3769	292.48	23.76
3876	300.24	24.62
3989	307.04	24.62
4077	317.52	25.48
4183	326.56	26.34
4247	331.92	27.2
4307	336.03	27.2
4386	341.78	28.06
4446	347.11	28.06
4553	352.34	28.92
4696	362.60	29.78
4767	369.23	29.78
4863	375.77	30.64
4956	385.43	31.5

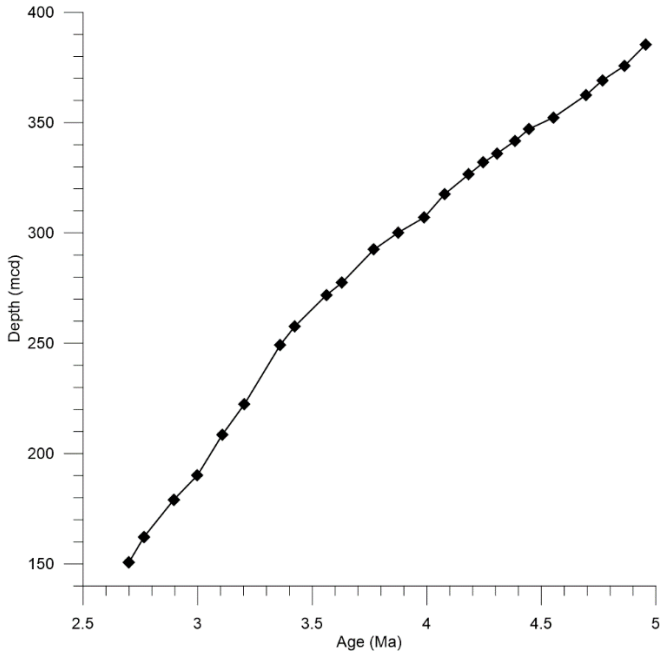

Figure 2.1. Age-depth model of ODP Site 1239A from 2.7 to 4.96 Ma after Tiedemann et al. (2007).

2.2 Palynological analysis

2.2.1 Underlying assumptions

Pollen and spores are a useful tool to study past environments. The fossil record is rich in pollen because they are produced in large numbers and they are extremely resistant to decay (Spicer 2018).

The interpretation of fossil pollen records in terms of climate requires some underlying assumptions. Among these are that evolutionary changes at the species or genus level are absent or negligible, and that present and past biological responses (e.g. abundances) to climatic variables are comparable (Spicer 2018; Webb 1980). There are, however, several non-climatic factors affecting the vegetation, amongst others soil, fires, human impact, and species invasions (Webb 1980). Also, as Hooghiemstra and Ran (1994b) note, the tree species composition of the Andean forest around the high plain of Bogotá was different in the Pleistocene compared to present day. Still, the overall ecology and altitudinal zonation of the vegetation was similar enough in order to reconstruct the vegetation and climate of this region based on comparison with present day conditions (Hooghiemstra and Ran 1994b).

When using a taxon based approach, correct pollen identification is indispensable. With the light microscope, pollen grains can often be identified down to the genus level at its best due to the lack of further morphological differences (Spicer 2018).

2.2.2 Sampling and preparation of pollen samples

Marine sediment core ODP Leg 202 Site 1239 was recovered during ODP cruise 202 in 2003 from a water depth of 1414m (Shipboard Scientific Party 2003). For pollen analysis, samples were ordered from the International Ocean Discovery Program's (IODP) Gulf Coast Repository (GCR), located at Texas A&M University, College Station, Texas, USA.

From Hole 1239A, 148 subsamples of 4.5-9.5 cm^3 volume were taken. The samples cover the time period from 6.515 Ma to 28 ka. Additionally, two surface /subsurface samples of Holocene age were taken from Hole 1239B. Two time windows were sampled at a higher resolution, 4.7 to 4.2 Ma and 3.6 to 2.7 Ma. During the time window 4.7 to 4.2 Ma (334 – 301 mbsf), the average temporal resolution is one sample per 9 ka (excluding the coring gap between 319 and 323 mbsf). This equals a distance of 64 cm between core samples. For the time window from 3.6 to 2.7 Ma, the temporal resolution is about 11 ka. This equals a sampling interval of 137 cm.

Standard analytical methods were used to process the samples (Faegri and Iversen 1989). The volume of each sample was measured in a cylinder by displacement of the water column. Carbonates were removed with dissolved HCl (10%). Two tablets with a known number of exotic *Lycopodium* spores (batch no. 177745 containing 18,584 ± 829 spores per tablet) were added to each sample in order to determine the pollen concentration (grains/cm^3). Silicates were removed with pure HF (40%). The samples were neutralized with KOH (40-50%). Finally, they were sieved over a screen with an 8x3 µm mesh in an ultrasound bath until all clay clumps were removed. Samples were mounted in glycerin, and 246 pollen grains and spores were counted on average per sample (minimum: 97, maximum: 452) with a Zeiss Axioskop at 400× and 1,000× (oil immersion)

magnification. Due to variable pollen and spore counts, most percentages were plotted with 95% confidence intervals (after Maher 1972), whose size depends on the pollen and spore sum. The pollen concentration was determined according to the technique of Stockmarr (1971):

$$\frac{37168 \times palynomorphs\ counted\ on\ a\ slide}{number\ of\ Lycopodium\ spores\ counted} = number\ of\ palynomorphs\ in\ the\ sediment\ sample$$

$$\frac{number\ of\ palynomorphs\ in\ the\ sediment\ sample}{volume\ of\ the\ sample} = pollen\ concentration$$

2.2.3 Pollen identification, grouping and statistical analyses

In this study, the following literature and databases were used for pollen identification:

- Colinvaux, De Oliveira, and Moreno Patino (1999), Hooghiemstra (1984), Murillo and Bless (1974), Murillo and Bless (1978), Roubik and Moreno P. (1991)
- The reference collection for Neotropical species from the Department of Palynology and Climate Dynamics in Göttingen
- Neotropical Pollen Database (Bush and Weng 2007)

Most pollen types were identified to the genus or family level. Therefore, only an assignment to broad altitudinal belts was possible. Pollen types were grouped according to ecosystem or habitat type which they most commonly occur in (Van der Hammen, Werner, and van Dommelen 1973; Marchant et al. 2002; Flantua et al. 2014). Some types need permanently humid conditions for their growth. These types were summarized in the group of 'humid indicators'. Some types such as Poaceae and Asteraceae are most abundant in the páramo. However, they may also occur in open vegetation types at lower altitudes in larger quantities. Although a pollen rain study across the Colombian Cordillera showed that the tree- and shrub-like Asteraceae of the páramo are the greatest pollen producers compared to other Asteraceae occurring at lower altitudes (Van der Hammen, Werner, and van Dommelen 1973), the family was not included in the páramo sum.

Table 2.2. Grouping of pollen and spore types according to their main ecological affinity.

Vegetation type	Pollen Taxa	Spore Taxa
Páramo (>3200m)	*Draba, Orthrosanthus, Polylepis/Acaena, Puya, Ranunculus, Sisyrinchium, Valeriana triphylla T*	*Cystopteris diaphana T, Jamesonia/Eriosorus, Huperzia*
Upper montane forest (2300-3200m)	Acanthaceae, Alnus, *Bocconia, Clethra, Daphnopsis, Dodonaea viscosa, Hedyosmum,* Melastomataceae, *Morella, Myrsine,* Podocarpaceae	*Elaphoglossum, Grammitis, Hypolepis hostilis T, Lophosoria quadripinnata,*

Lower montane forest (1000-2300m)	*Alchornea, Croton, Erythrina,* Malpighiaceae, *Passiflora, Styloceras T*, Urticaceae/Moraceae, *Vernonia T*	*Ctenitis subincisa*, Cyatheaceae excl. *Cyathea horrida, Pteris grandifolia T, Pteris podophylla T, Saccoloma elegans T, Thelypteris*
Lowland rainforest (<1000m)	*Arecaceae, Cordia lanata T, Socratea, Wallichia, Wettinia*	*Pityrogramma-Pteris altissima T, Pityrogramma*, Polypodiaceae
Broad range taxa	Amaranthaceae, *Ambrosia/Xanthium,* Anacardiaceae T, Apocynaceae, *Artemisia, Bomarea*, Bromeliaceae, *Calandrinia*, Caryophyllaceae, Cyperaceae, Ericaceae, Euphorbiaceae T, *Ilex*, Liguliflorae (Asteraceae), Liliaceae, Malvaceae, *Monnina*, Myrtaceae, Nyctaginaceae, Poaceae, *Polygonum (Persicaria T)*, Proteaceae, Rosaceae, *Salacia, Thevetia, Tournefortia*, Tubuliflorae (Asteraceae)	*Anemia T, Anthoceros, Cystopteris-Hypolepis, Hymenophyllum trichophyllum*, Lycopodiaceae excl. *Huperzia*, *Saccoloma elegans T, Schizaea pennula, Selaginella*
Humid indicators	*Alnus,* Cyperaceae, *Hedyosmum, Ilex*, Malpighiaceae, *Myrica, Pachira, Ranunculus*	*Ctenitis subincisa T,* Cyatheaceae, *Cystopteris diaphana T, Hymenophyllum T, Pityrogramma-Pteris altissima T, Selaginella, Thelypteris*

Pollen diagrams were created in TILIA (Grimm 1991) and Grapher™ (Golden Software, LLC). Percentages are based on the pollen sum. This includes all pollen and fern spores and unidentifiable ones. Confidence intervals for pollen percentages were calculated after the method of Maher (1972) and for pollen concentrations after Maher (1981). The zonation of the pollen diagrams was done by constrained incremental sum-of-squares cluster analysis (CONISS) of pollen percentage curves, applying the square root transformation method (Edwards & Cavalli–Sforza's chord distance) in TILIA (Grimm 1991).

2.3 References

Berger, A. 1988. 'Milankovitch Theory and Climate', *Reviews of Geophysics*, 26: 624-57.

Bush, Mark B., and Chengyu Weng. 2007. 'Introducing a new (freeware) tool for palynology', *Journal of Biogeography*, 34: 377-80.

Colinvaux, P., P. E. De Oliveira, and J. E. Moreno Patino. 1999. *Amazon Pollen Manual and Atlas* (Harwood Academic Publishers: Amsterdam).

Faegri, K., and J. Iversen. 1989. *Textbook of Pollen Analysis* (John Wiley & Sons: Chichester).

Flantua, S., H. Hooghiemstra, J.H. Van Boxel, M. Cabrera, Z. González-Carranza, and C. González-Arango. 2014. 'Connectivity dynamics since the last glacial maximum in the northern Andes: a pollen-driven framework to assess potential migration.' in W. D. Stevens, O. M. Montiel and P. H. Raven (eds.), *Paleobotany and Biogeography: A Festschrift for Alan Graham in His 80th Year* (Missouri Botanical Garden Press: St. Louis).

Grimm, EC. 1991. "Tilia and Tiliagraph." In. Springfield: Illinois State Museum.

Hooghiemstra, H. 1984. *Vegetational and Climatic History of the High Plain of Bogotá, Colombia: A Continuous Record of the Last 3.5 Million Years* (A.R. Gantner Verlag K.G.: Vaduz).

Hooghiemstra, H., and E. Th. H. Ran. 1994b. 'Upper and middle Pleistocene climatic change and forest development in Colombia: pollen record Funza II (2-158 m core interval)', *Palaeogeography, Palaeoclimatology, Palaeoecology*, 109: 211-46.

Laskar, J., F. Joutel, and F. Boudin. 1993. 'Orbital, Precessional, and Insolation Quantities for the Earth from -20 Myr to +10 Myr', *Astronomy & Astrophysics*, 270: 522-33.

Lisiecki, L. E., and M. E. Raymo. 2005. 'A Pliocene-Pleistocene stack of 57 globally distributed benthic $\delta^{18}O$ records', *Paleoceanography*, 20: 1-17.

Maher, L. J. 1972. 'Nomograms for computing 0.95 confidence limits of pollen data', *Review of Palaeobotany and Palynology*, 13: 85-93.

———. 1981. 'Statistics for Microfossil Concentration Measurements Employing Samples Spiked with Marker Grains', *Review of Palaeobotany and Palynology*, 32: 153-91.

Marchant, R., L. Almeida, H. Behling, J. C. Berrio, M. Bush, A. Cleef, J. Duivenvoorden, M. Kappelle, P. De Oliveira, A. Teixeira de Oliveira-Filho, S. Lozano-Garcia, H. Hooghiemstra, M.-P. Ledru, B. Ludlow-Wiechers, V. Markgraf, V. Mancini, M. Paez, A. Prieto, O. Rangel, and M. Salgado-Labouriau. 2002. 'Distribution and ecology of parent taxa of pollen lodged within the Latin American Pollen Database', *Review of Palaeobotany and Palynology*, 121: 1-75.

Murillo, M. T., and M. J. M. Bless. 1974. 'Spores of recent Colombian Pteridophyta. I. Trilete Spores', *Review of Palaeobotany and Palynology*, 18: 223-69.

———. 1978. 'Spores of recent Colombian Pteridophyta. II. Monolete Spores', *Review of Palaeobotany and Palynology*, 25: 319-65.

Rincón-Martínez, D. 2013. 'Eastern Pacific background state and tropical South American climate history during the last 3 million years', Universität Bremen.

Roubik, D. W., and J. E. Moreno P. 1991. *Pollen and spores of Barro Colorado Island [Panama]* (Missouri Botanical Garden: St. Louis, MO).

Shipboard Scientific Party. 2003. "Site 1239." In *Proceedings of the Ocean Drilling Program, Initial Reports*, edited by A.C. Mix, R. Tiedemann and P. Blum, 1-93. College Station, Texas: Ocean Drilling Program.

Spicer, R. A. 2018. 'Phytopaleoaltimetry: Using Plant Fossils to Measure Past Land Surface Elevation.' in C. Hoorn, A. L. Perrigo and A. Antonelli (eds.), *Mountains, Climate and Biodiversity* (Wiley-Blackwell).

Stockmarr, J. 1971. 'Tablets with spores used in absolute pollen analysis', *Pollen et Spores*, XIII: 615-21.

Tiedemann, R, A. Sturm, S. Steph, S.P. Lund, and J.S. Stoner. 2007. 'Astronomically calibrated timescales from 6 to 2.5 Ma and benthic isotope stratigraphies, sites 1236, 1237, 1239, and 1241', *Proceedings of the Ocean Drilling Program, Scientific Results*, 202.

Van der Hammen, T., J. H. Werner, and H. van Dommelen. 1973. 'Palynological record of the upheaval of the Northern Andes: a study of the Pliocene and Lower Quaternary of the Colombian early evolution of its high-Andean biota', *Review of Palaeobotany and Palynology*, 16: 1-122.

Webb, T. 1980. 'The reconstruction of climatic sequences from botanical data', *The Journal of Interdisciplinary History*, 10: 749-72.

3 Andean uplift

Mountains are complex features of the Earth and interesting study objects in many respects. Concerning this thesis the main aspects of mountains are their role in shaping regional and global climate, being the source of many rivers, and being a hotspot for the migration and evolution of species (Perrigo, Hoorn, and Antonelli 2019). Thus, for gathering a deeper understanding of the geological, biological and meteorological processes connected to the presence of mountains, it is essential to first understand mountain building itself. In Chapters 4 and 5 of this thesis, palynological analyses of Pliocene marine sediments are presented. These data are interpreted in terms of vegetation and climate change in western equatorial South America, from the lowlands to the páramos of the Western Andean Cordillera. In order to provide a solid base for this interpretation, it is necessary to understand the effects that Andean uplift had on climate and biodiversity. Furthermore, it is crucial to constrain as much as possible the timing of Andean uplift. This is especially important, because marine pollen data yield an integrated signal of the vegetation from the lowlands to the highest elevations. Thus, knowing dates and rates of uplift provides a framework for the interpretation of the pollen signal. Specifically, the possible altitudinal occurrence of pollen taxa can be better narrowed down when paleoelevation estimates are known. Also, results from climate modelling are much more useful when the timing of Andean uplift is well constrained.

Therefore, this chapter is structured in two main parts. The first section (3.1) deals with the impacts of Andean uplift on South American climate and biodiversity, focusing on the western (Pacific) side of the Northern and Central Andes which is most relevant for this study. The second section (3.2) treats the timing of Andean uplift, focusing again on the Northern and Central Andes. The chapter closes with a discussion where caveats and uncertainties of the paleoaltimetry proxies are described, followed by a conclusion which summarizes the most important points.

3.1 Impact of Andean uplift on South American climate and biodiversity

3.1.1 Effect of the Andes on climate

Land surfaces and climate are closely linked. Mountain uplift affects climate because it changes patterns of precipitation, temperature, and atmospheric circulation. The Andes run perpendicular to atmospheric circulation, which creates complex climatic patterns (Perrigo, Hoorn, and Antonelli 2019). Uplift of the Andes caused increased moisture transport out of the tropics and higher convective precipitation in the Andean lowlands and the eastern flanks (Aron and Poulsen 2018). Climate modelling results show that the Andes have a direct effect on South American climate after reaching around 50% of their modern heights (Insel, Poulsen, and Ehlers 2009). Several different

aspects of climate are influenced: The Andes block atmospheric flow at ~2000 m elevation, leading to a reversal of the main wind direction from westerly to easterly flow. Concomitant, the water vapor source over the Central Andes changes from a Pacific to an Atlantic source (Ehlers and Poulsen 2009; Poulsen, Ehlers, and Insel 2010). Andean uplift further caused the development of the southward flowing South American low-level jet (SALLJ) through mechanical blocking. Barrier jets like the SALLJ turn towards the north in the Northern Hemisphere and towards the south in the southern hemisphere. The SALLJ flows southward parallel to the eastern Andes and transports considerable moisture from the Amazon to the southern Andes (Vera et al. 2006). Finally, for elevations < 50% of the modern, precipitation is driven by local processes whereas for elevations > 50% of the modern, regional-scale processes govern precipitation (Insel, Poulsen, and Ehlers 2009). In addition to these large-scale climate features, small-scale phenomena such as gaps in mountain ranges have a considerable effect on climate as well. Andean valleys provide channels for moist air to flow across mountains into regions which would otherwise be dry (Aron and Poulsen 2018). Further, the uplift of mountains and plateaus may increase rates of chemical weathering (Graham, Gregory-Wodzicki, and Wright 2001).

The Andes have the largest effect on the climate of the interior of the South American continent. However, for this study, the western (Pacific) side as well as the effect of uplift on Pacific sea surface temperatures is more relevant and will therefore be the focus of the following paragraph.

At higher tropospheric levels, easterlies prevail throughout the year. The lower tropospheric flow which controls the precipitation field by transporting most of the water vapor is effectively blocked by the Andes. Hence, the coastal areas and the lower western slopes of the Ecuadorean Andes are mainly influenced by air masses from the Pacific (Vuille, Bradley, and Keimig 2000). High Andes block the air from the east, creating low level divergence and thereby reducing precipitation in coastal Ecuador and northern Peru (Xu, Wang, and Xie 2004). Changes in low-level winds and the onset of convective precipitation in the Central Andes are indicated by a decrease in $\delta^{18}O$ during the late Miocene, when climate conditions changed from arid to humid. In the Northern Andes in contrast, surface uplift has a minor influence on simulated rainfall rates (Poulsen, Ehlers, and Insel 2010).

Takahashi and Battisti (2007) show in experiments with an atmospheric general circulation model that subsidence of dry air west of the Andes cools sea surface temperatures through evaporation. This surface cooling is sufficient to establish a north-south asymmetry with the ITCZ being located north of the equator in the east Pacific. This state is reinforced through the wind-evaporation-SST mechanism (Xie and Philander 1994). This mechanism describes a feedback where convection is stronger in one hemisphere due to higher SSTs. This would in turn drive stronger surface wind speeds in the other hemisphere. These winds would cool the water by evaporation, reinforcing the

initial location of the convection (Xie and Philander 1994). Likewise, experiments by Xu, Wang, and Xie (2004) show that the Andes cause an increase of low-level stratus clouds over the Southeast Pacific in the austral cold season and shorten the time of the ITCZ at its southern position during the warm season. Both these features strengthen the latitudinal asymmetry of the eastern Pacific climate.

Climatic responses to Andean surface uplift may extend beyond South America (Garzione et al. 2008). For example, the ITCZ is located at 6°N on average because the Northern Hemisphere is warmer (Schneider, Bischoff, and Haug 2014). The presence of the Andes enables a feedback mechanism (as described above) which strengthens the northern position of the ITCZ over the Pacific. This influences the strength and distribution of monsoonal climates with Pacific teleconnections (Takahashi and Battisti 2007).

As described above, the topography of the Andes has a strong effect on climate, but finally it should be mentioned that conversely, climate patterns also control the topographic evolution of the Andes. Climatic patterns influence orogen morphology especially in the northern Andes, where high precipitation rates accompanied by fluvial erosion maintain a narrow mountain range. In the central Andes, tectonic activity dominates the landscape form (Montgomery, Balco, and Willett 2001).

3.1.2 Effects of Andean uplift on biodiversity

The effects of Andean uplift on the biota are numerous and diverse. Here I focus on the largest effects that Andean uplift had on biodiversity in the eastern Pacific-Northern Andean-Amazon region: Andean uplift fostered the development of new ecosystems and led to the dispersal of new species in the Amazon basin through changing river drainage patterns (Hoorn et al. 2010). In the Eastern Equatorial Pacific, Andean uplift generated shifts in the sea surface temperature (SST) gradient and ocean circulation, thereby contributing to enhanced marine productivity (Feng and Poulsen 2014).

Concerning floral and vegetation changes, the appearance and evolution of high Andean environments is most relevant in the context of this study. Palynological evidence for an open, páramo-like vegetation was first found in the Chocontá area in the central part of the Colombian Eastern Cordillera. This early páramo consisted of Poaceae, *Valeriana, Plantago*, Ranunculaceae, *Aragoa* and *Polylepis-Acaena* (Van der Hammen, Werner, and van Dommelen 1973). Hooghiemstra, Wijninga, and Cleef (2006) studied fossil plant assemblages on the high plain of Bogotá, Colombia, and concluded that páramo-like vegetation first appeared in the late Pliocene. Martinez et al. (2020) documented earliest existence of a non-analogue montane ecosystem on the Northern Central Andean Plateau since the Miocene and evidence of a puna-like ecosystem since the Pliocene. With

Andean uplift, new temperate environments were created which provided an opportunity for taxa from different floristic realms (e.g. Holarctic, Austral-Antarctic, Neotropics) to immigrate into these regions and on the other hand, for in situ evolution of new páramo taxa (Kroonenberg, Bakker, and Van der Wiel 1990). Immigration of Austral-Antarctic taxa to the northern Andes took place as soon as suitable high-Andean climatic conditions were present. The closure of the Isthmus of Panama further enabled the immigration of Holarctic taxa into the Andes (Kroonenberg, Bakker, and Van der Wiel 1990).

The question of whether diversification of the montane vegetation and mountain uplift are directly temporally related is not yet fully answered (Perrigo, Hoorn, and Antonelli 2019). Since the montane flora is a mixture of local neotropical elements and immigrants from other floristic realms, it seems most plausible to assume a species-poor early páramo flora that became only gradually enriched by more species (through immigration, long-distance dispersal and speciation of the existing taxa). Unfortunately, pollen is not diagnostic enough at the species level to set temporal constraints for speciation. However, molecular phylogenies of 176 páramo species indicate rapid diversification rates since the Plio-Pleistocene, most probably driven by interglacial range contractions during the Pleistocene (Madriñán, Cortes, and Richardson 2013).

3.2 Timing of Andean uplift

The Andes are the longest and second highest mountain chain in the world with a north-south extension from 10°N to 55°S, widths of the Cordilleras of 100-300 km and elevations of almost 7000 m (mean height: ~4000 m; Aron and Poulsen 2018; Restrepo-Moreno et al. 2019). The uplift of the Northern Andes and the formation of the Isthmus of Panama are fundamental for understanding the environmental and biotic history of northwestern South America and the eastern equatorial Pacific (Restrepo-Moreno et al. 2019). The changing topography altered the drainage patterns of rivers including the Amazon, Orinoco, and Magdalena-Cauca (Restrepo-Moreno et al. 2019).

By definition, the Northern Andes comprise the Venezuelan, Colombian, and Ecuadorean Cordilleras and the Central Andes include the Peruvian and the Bolivian parts (Pérez-Escobar et al. 2022). The Colombian Andes are located at the juncture of four tectonic plates, the Nazca, Cocos, Caribbean, and South American plate. The Nazca plate is subducted below the South American plate which causes present-day volcanism and seismicity in the Colombian and Ecuadorian Andes (Kroonenberg, Bakker, and Van der Wiel 1990). The Colombian Andes are arranged in three N- to NNE-oriented mountain chains: the Western, Central and Eastern Cordillera (Mora et al. 2020). The Central Cordillera of Colombia becomes the Eastern Cordillera (or Cordillera Real) in Ecuador. Thus, the Andes in Ecuador consist of only two parallel Cordilleras

which are separated by the Interandean Valley. While the Cordilleras typically reach elevations between 4000 (in southern Ecuador) and 6000 m, the Interandean Valley is 2600-2700 m high (Balslev 1988).

Morphotectonic activity across the Andes is an ongoing process since the late Cretaceous. Although the timing and mechanism of Andean uplift are still debated, it is accepted that convergence of the Nazca and South American Plates caused the Andes to rise (Gregory-Wodzicki 2000). The geological methodologies to investigate mountain uplift and related processes comprise two different approaches: thermochronology and paleoealtimetry. Whereas thermochronology is suitable to infer the rates and timing of geological activity, paleoaltimetric methods can yield dates of paleoaltitudes and rates of uplift (Perrigo, Hoorn, and Antonelli 2019). Paleoaltimetry itself comprises methods from a variety of subdisciplines including geochemistry, volcanology, and paleobotany (Graham, Gregory-Wodzicki, and Wright 2001). The uplift history of the Andes is complex and characterized as being episodic, asynchronous, and spatially heterogeneous (Restrepo-Moreno et al. 2019). The two contrasting theories regarding the timing of Andean uplift are rapid recent uplift vs. slow and continuous uplift (Barnes and Ehlers 2009).

For the interpretation of the paleovegetation record in terms of climate, it is essential to constrain the paleoaltitude of the Andes as much as possible. However, despite extensive research on the geodynamic and tectonic evolution of some parts of the Andes, the details of the timing and rate of Andean surface uplift remain controversial. Moreover, paleoelevation data of the Ecuadorean Andes are remarkably scarce. Therefore, the current state-of-the-art on the uplift histories of the Northern Andes as well as the adjacent Central Andes is described in the following section and an overview of uplift estimates is given in table 3.1.

Table 3.1. Overview of uplift estimates from the Northern and Central Andes, adapted from Gregory-Wodzicki (2000) and supplemented with more recent data.

Location	Method	Age (Ma)	Paleo-elevation	Modern Elevation	%M elev.†	S error§ (m)/ A error# (m)	Reference(s)
E.C., Colombia, Sal. de Tequendama I	Paleobotany	early-middle? Miocene	<700	2450	<29-36	±250¶¶/ ±1500	Wijninga (1996)
E.C., Colombia, Sal. de Tequendama II	Paleobotany	middle? Miocene	<700	2475	<29-36	±250¶¶/ ±1500	Wijninga (1996)
E.C., Colombia, Sal. de Tequendama	Paleobotany	middle? Miocene	0-500	2475	0-20	N.D./ ±1500	Van der Hammen et al. (1973)
E.C., Colombia, Rio Frio 17	Paleobotany	5.3 ± 1	1000	3165	32	±250+§§/ ±1500	Wijninga (1996)

E.C., Colombia, Subachoque 39	Paleobotany	ca. 4-5	1000	2820	35	±250+§§/ ±1500	Wijninga (1996)
E.C., Colombia, Facatativa 13	Paleobotany	3.7 ± 0.7	2000	2750	73	±250/ ±1500	Wijninga (1996)
E.C., Colombia, Facatativa 13	Paleobotany	3.7 ± 0.7	1500	2750	55	N.D./ ±1500	Van der Hammen et al. (1973)
E.C., Colombia, Rio Sotaquirá	Paleobotany	ca. 3-4	1600	2600	62	N.D./ ±1500	Van der Hammen et al. (1973)
E.C., Colombia, Guasca 103	Paleobotany	2.8 ± 0.5	2200	2650	83	±250/ ±1500	Wijninga (1996), Van der Hammen and Hooghiemstra (1997)
E.C., Colombia, Chocontá 4	Paleobotany	2.8 ± 0.5	2300	2690	86	N.D./ ±1500	Van der Hammen et al. (1973), Van der Hammen and Hooghiemstra (1997)
E.C., Colombia, Chocontá 1	Paleobotany	2.7 ± 0.6	2800	2800	100	N.D./ ±1500	Van der Hammen et al. (1973), Van der Hammen and Hooghiemstra (1997)
E.C., Colombia, Honda Group	Stratigraphy, sedimentology	11.8	Relief	2500-4500	?	N.D./N.D.	Hoorn et al. (1995), Guerrero (1997)
E.C., Colombia, Sabana de Bogotá	Lipid biomarkers	7.6	>1600	2600	62		Anderson et al. 2015
W.C., Central Andes, 16° - 33°30'S	Crustal deformation	~25			25-50		Jordan et al. (1997)
E.C., Altiplano	Crustal deformation	~25			30		Lamb and Hoke (1997)
Altiplano, El Molino Formation	Marine facies	60-73	<0	4000	0	N.D./ ±200##	Sempere et al. (1997)
forearc, Moquegua Formation	Marine facies	25	<0	1100	0	N.D./ ±200##	Sébrier et al. (1988)
Subandes, Anta Formation	Marine facies	14-15	<0	<1000	0	N.D./ ±100##	Jordan and Alonso (1987)
Subandes, Yecua Formation	Marine facies	8-10	<0	<1000	0	N.D./ ±100##	Marshall et al. (1993)
Altiplano, Chucal	Paleobotany; nearest-living-relative method	25-19	1000	4200	24	±200/ ±1500	Munoz and Charrier (1996)
Altiplano, Corocoro	Paleobotany; nearest-living-relative method	mid Miocene	2000	4000	50	N.D./ ±2000	Singewald and Berry (1922)
E.C., Potosi	Paleobotany; nearest-living-relative method	20.8-13.8	2800	4300	65	N.D./ ±2000	Berry (1939)

E.C., Potosi	Paleobotany; foliar-physiognomic method	20.8-13.8	0-1320	4300	0-31	±800[§§]/ ±1200	Gregory-Wodzicki et al. (1998)
Altiplano, Jakokkota	Paleobotany; foliar-physiognomic method	10.66 ± 0.6	590-1610	3940	15-41	±800[§§]/ ±1200	Gregory-Wodzicki et al. (1998)
W.C.	Erosion rates	~15	1000-4500[§§]	~4500	44-67	N.D./N.D.	Alpers and Brimhall (1988)
E.C.	Internal drainage	~15	some	~3800	?	N.D./N.D.	Vandervoort et al. (1995)
forearc, Coastal Cordillera	Landscape development	25(-18?)	0	1100	0	N.D./ ±100[##]	Tosdal et al. (1984)
forearc, Pacific Piedmont	Landscape development	25(-18?)	0	1100-1800	0	N.D./ ±100[##]	Tosdal et al. (1984)
W.C.	Landscape development	25(-18?)	~0	3000	0-33	N.D./ +1000	Tosdal et al. (1984)
E.C.	Landscape development	10	1000-1500	3500	29-43	N.D./ ±1000	Kennan et al. (1997)
E.C., Bolivia, Pislepampa	Paleobotany; nearest-living-relative method	6-7	1200-1400	3600	33-39	±1000	Graham et al. (2001)
E.C., Bolivia, Salla and Puchuni	Stable isotopes (oxygen, carbon)	29-24	0-1500	~4000	0-38	N.D.	Leier (2013)
E.C., Bolivia, Salla and Puchuni	Stable isotopes (oxygen, carbon)	20-15	~2500	~4000	63	N.D.	Leier (2013)
Puna Plateau, Argentina, Salar de Antofalla, Salina del Fraile, and Arizaro Basin	Stable isotopes (deuterium isotope ratios of hydrated volcanic glass)	36	~4000	3600-3900	103-111	N.D.	Canavan et al. (2014)
W.C., Andean plateau, 16 - 26°S	Radiogenic isotopes (Sr, Nd)	23	4200 ±516	4200 ±516	100	N.D.	Scott et al. (2018)

Note: E.C.—Eastern Cordillera, W.C.—Western Cordillera, N.D.—not determined

†%M elev.—percent of modern elevation represented by paleoelevation

§S error—error for paleoelevation stated in original study

#A error—actual error, as suggested by Gregory-Wodzicki (2000)

††Wijninga (1996c) estimated short-term temperature fluctuations of 3°C, and thus a standard error of ±250 m.

§§Although Wijninga (1996c) preferred the interpretation that these sites represent lowland forest, he noted that they might represent Subandean forest. Subandean forests are today found between 1000 and 2300 m, thus errors could be higher.

$$Recalculated using new lapse rate error term [see Gregory-Wodzicki (2000)].

##Error due to sea-level change (Hallam 1992).

3.2.1 The Northern Andes

In the northern Andes of Colombia, discrete phases of tectonic-driven uplift occurred during the Cretaceous-Paleocene (~69-63 Ma), Eocene (46-42 Ma), Late Oligocene (25-22 Ma), Miocene (16-

14 Ma, 10-7 Ma) and Pliocene (3 Ma) to present (Restrepo-Moreno et al. 2019). One of the few areas where paleoelevation estimates are available is the Colombian Eastern Cordillera (Fig. 3.1). The pioneering work in this field comes from Van der Hammen, Werner, and van Dommelen (1973), who, based on palynology, reports a gradual increase in elevation by more than 2 km for the Colombian High Plain of Bogotá from the Pliocene to the earliest Pleistocene. He concludes that the major upheaval occurred during the middle to late Pliocene. Following pollen studies from the same area yield similar results, suggesting that the final uplift of the area took place between 6 and 3 Ma (Hooghiemstra, Wijninga, and Cleef 2006; Wijninga 1996a). The paleoelevation estimates of Hooghiemstra, Wijninga, and Cleef (2006) are based on the progressive disappearance of lowland taxa and the concurrent increase of montane taxa (e.g. *Myrica, Gunnera, Bocconia, Daphnopsis, Monnina*) in the pollen record. Wijninga (1996a) states that during the early Pliocene, low lower montane forest to lowland rainforest conditions occurred in the study area based on pollen (e.g. *Astrocaryum, Amanoa, Macrolobium, Mauritia*) and macrofossil (*Sacoglottis* endocarps) composition.

Anderson et al. (2015) propose a more gradual cooling trend since the late Miocene based on a new lipid biomarker proxy and a revised magnetostratigraphic chronology. For Tequendama section, initially dated to be 16 Ma at the base, a new age of 7.6 to 6.1 Ma is proposed based on the new paleomagnetic data. Their results indicate that the high plain of Bogotá had already reached an elevation of ~1600-2000 m by ca. 7.6 Ma (Anderson et al. 2015). A multiproxy study by Anderson et al. (2016) conducted in the southernmost part of the Colombian Eastern Cordillera is in agreement with pollen-based elevation constraints, finding that a substantial orographic barrier was only established around 6-3 Ma. In contrast, Kroonenberg, Bakker, and Van der Wiel (1990) review available geological and geomorphological data (such as fission-track dating and dissected and tilted planation surfaces) for the Colombian Andes and conclude that the most recent uplift phase around 6-4 Ma affected only the northernmost Colombian Andes. Initial uplift activity in the Eastern Cordillera of Colombia during the latest Oligocene was inferred using detrital zircon ages (Horton et al. 2010).

Moving further south, Coltorti and Ollier (2000) state based on geomorphology that the uplift of the Ecuadorean Cordilleras started in the early Pliocene and only during the Pleistocene reached their present elevation. Unfortunately, paleoelevation estimates for the Western Cordillera of the Northern Andes are scarce. Taken together, there is general agreement of final topographic growth in the Eastern Cordillera during the late Miocene to Pliocene, but it remains unclear when uplift started (Mora et al. 2020). The uplift history of the Western Cordillera is even more uncertain due to a lack of data.

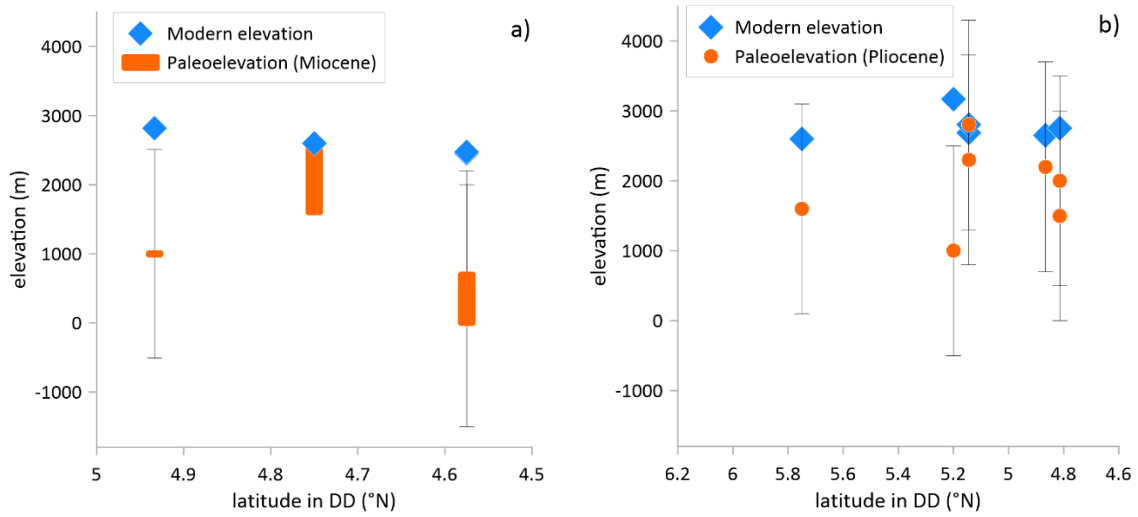

Figure 3.1. Paleoelevation estimates from the Northern Andes (Eastern Cordillera, Colombia) for a) the Miocene (Van der Hammen, Werner, and van Dommelen 1973; Anderson et al. 2015; Wijninga 1996c) and b) the Pliocene (Van der Hammen, Werner, and van Dommelen 1973; Wijninga 1996c; Van der Hammen and Hooghiemstra 1997). Black whiskers indicate the errors of the paleoelevation estimates as suggested by Gregory-Wodzicki (2000). DD: Decimal degrees.

3.2.2 The Central Andes

A review of the quantitative paleoelevation estimates that have been made for the Central Andes suggests that both the Altiplano-Puna and the Eastern Cordillera had attained no more than half of their modern elevation by around 10 Ma (Gregory-Wodzicki 2000). In agreement with that, Graham, Gregory-Wodzicki, and Wright (2001) suggest, based on a palynological assemblage, that about half of the uplift of the Eastern Cordillera of Bolivia was attained only since the Pliocene. Paleotemperature estimates based on fossil-leaf physiognomy in the northern Altiplano and Eastern Cordillera suggest that paleoelevations were less than 2 km by around 10 Ma. At least one discrete pulse of rapid surface uplift of 2.5 ± 1 km occurred between 10 and 6 Ma (Garzione et al. 2008). Early Pliocene paleoelevation reconstructions based on a plant fossil record indicate that, around 4.8 Ma, the northernmost part of the Central Andean Plateau had attained near-modern elevations of ~3800 m (Martinez et al. 2020). In agreement with that, a multiproxy-based paleoelevation study proposed rapid surface uplift of around 2500 m between ~9 and 5.4 Ma, resulting in the modern day elevation of ~ 4.2 km (Kar et al. 2016). Leier et al. (2013) present stable isotope evidence for Oligocene to early Miocene paleoelevations of 0 to 1.5 km, and middle Miocene paleoelevations of 2.5 km for the Eastern Cordillera in Bolivia.

In contrast, Canavan et al. (2014) modeled paleoelevations of the Puna Plateau in Argentina based on stable isotopes of hydrated volcanic glass and found elevations of around 4 km since 36 Ma and limited (less than 1 km) elevation changes since then. In agreement with these results, the Western Cordillera between 16 and 26°S was found to have reached current elevations of around 4.2 km by

23 Ma (Scott et al. 2018). Similar ages for the Western Cordillera of southern Peru are estimated from deuterium isotopes of volcanic glass, indicating surface uplift of 2.2-3.7 km in the early Miocene (19-16 Ma) and modern elevations of 4300 m by 16 Ma (Saylor and Horton 2014). These results suggest that the Western Cordillera and the Puna Plateau rose notably earlier than the Altiplano to the east. However, Garver et al. (2005) provide fission-track ages for the Peruvian Western Cordillera, and state that it is likely that much of the final surface uplift of this area happened in the last 5–6 Myr. For the western flank of the central Andes (northern Chile), geomorphic evidence from river profiles shows that relative surface uplift of at least 1 km occurred after 10 Ma (Hoke et al. 2007). These different uplift estimates for the Central Andean Western Cordillera show once again that the uplift history is not well constrained. More research is necessary as the uplift history differs strongly between the different regions and cannot be generalized.

3.2.3 Discussion and conclusion: Timing of uplift of the Northern and Central Andes

The state of the art regarding the timing of Andean uplift makes it clear that the uplift history needs to be seen in a nuanced light, since it differs substantially between the eastern and western cordilleras and the Interandean plateaus as well as from north to south. The geological record of the Northern Andes is unfortunately incomplete and fragmented due to erosion and poor preservation. Even in those parts where it is complete, not enough information is available (Mora et al. 2020).

A general issue with all paleoaltimetry proxies is that uplift histories are often calculated using modern climate conditions which are not corrected for past climate conditions. Hence, only the direct elevation response (lapse rate) is considered in paleoelevation reconstructions, whereas climate response effects are often neglected in proxy interpretations (Garzione et al. 2017). Paleoaltimetry interpretations based on oxygen isotopes and mass-47 isotopolog compositions together with modern isotope and temperature lapse rates might be biased, because variations in the oxygen isotope composition are not only caused by changes in elevation, but also by regional climate change (increase in precipitation). Reassessment of this relationship through modelling shows that changes in oxygen isotopes are not linear with an increase in elevation. They are rather a response to orographic thresholds which strongly change the regional climate (Insel et al. 2012). However, simulations with an atmospheric general circulation model by Poulsen, Ehlers, and Insel (2010) show that isotopic source and amount effects are influenced by changes in atmospheric circulation and rainfall. Specifically, changes in $\delta^{18}O$ of sedimentary carbonate associated with surface uplift are connected to different summertime circulation changes, such as the formation of the South American Low Level Jet, shift of the Chaco Low, subtropical high and the westerlies, as well as the onset of convective precipitation. High precipitation rates lead to an increase in the $\delta^{18}O$

lapse rate. The experiments of Poulsen, Ehlers, and Insel (2010) show that the mean annual precipitation $\delta^{18}O$ lapse rate doubles with an increase from 50% elevation to modern elevation in the Central Andes. In the Northern Andes, the increase of the $\delta^{18}O$ lapse rate with increasing elevation is not quite as pronounced. These changes of the isotopic lapse rate should be incorporated when uplift estimates based on oxygen isotope paleoaltimetry are made (Poulsen, Ehlers, and Insel 2010). If not accounted for, climate change can yield errors in the interpretation of paleoaltimetric records of hundreds to thousands of meters (Poulsen, Ehlers, and Insel 2010; compare table 3.1; Insel et al. 2012). Some more recent studies attempt to overcome this challenge by accounting for uplift-related climate change (Kar et al. 2016; Garzione et al. 2014) through the incorporation of modelling studies (Ehlers and Poulsen 2009; Insel et al. 2012). However, correcting paleoelevation estimates for climate change is not straightforward either, because land surface temperature reconstructions in northern South America suggest a heterogeneous response to global cooling (Farrera et al. 1999; Pinot et al. 1999; Thompson et al. 1995).

Considering the potentially large errors when climate response effects are ignored in paleoelevation reconstructions, the theory of slow and continuous surface uplift supported by models appears more likely (Barnes and Ehlers 2009; Insel et al. 2012).

Taken together, there seems to be general agreement of final topographic growth in the Northern Andean Eastern Cordillera during the late Miocene to Pliocene, but it remains unclear when uplift started (Mora et al. 2020). The uplift history of the Northern Andean Western Cordillera is even more uncertain due to a lack of data. The Eastern Cordillera of the Central Andes appears to have experienced major uplift during the Miocene to Pliocene. The Puna Plateau might have risen notably earlier. With a presently large range of paleoelevation estimates, the uplift history of the Central Andean Western Cordillera remains ambiguous.

3.3 References

Anderson, V. J., B. K. Horton, J. E. Saylor, A. Mora, E. Tesón, D. O. Breecker, and R. A. Ketcham. 2016. 'Andean topographic growth and basement uplift in southern Colombia: Implications for the evolution of the Magdalena, Orinoco, and Amazon river systems', *Geosphere*, 12: 1235-58.

Anderson, V. J., J. E. Saylor, T. M. Shanahan, and B. K. Horton. 2015. 'Paleoelevation records from lipid biomarkers: Application to the tropical Andes', *Geological Society of America Bulletin*, 127: 1604-16.

Aron, P. G., and C. J. Poulsen. 2018. 'Cenozoic Mountain Building and Climate Evolution.' in C. Hoorn, A. L. Perrigo and A. Antonelli (eds.), *Mountains, Climate and Biodiversity* (Wiley-Blackwell).

Balslev, H. 1988. 'Distribution Patterns of Ecuadorean Plant-Species', *Taxon*, 37: 567-77.

Barnes, J. B., and T. A. Ehlers. 2009. 'End member models for Andean Plateau uplift', *Earth-Science Reviews*, 97: 105-32.

Canavan, R. R., B. Carrapa, M. T. Clementz, J. Quade, P. G. DeCelles, and L. M. Schoenbohm. 2014. 'Early Cenozoic uplift of the Puna Plateau, Central Andes, based on stable isotope paleoaltimetry of hydrated volcanic glass', *Geology*, 42: 447-50.

Coltorti, M., and C. D. Ollier. 2000. 'Geomorphic and tectonic evolution of the Ecuadorian Andes', *Geomorphology*, 32: 1-19.

Ehlers, T. A., and C. J. Poulsen. 2009. 'Influence of Andean uplift on climate and paleoaltimetry estimates', *Earth and Planetary Science Letters*, 281: 238-48.

Farrera, I., S. P. Harrison, I. C. Prentice, G. Ramstein, J. Guiot, P. J. Bartlein, R. Bonnefille, M. Bush, W. Cramer, U. von Grafenstein, K. Holmgren, H. Hooghiemstra, G. Hope, D. Jolly, S.-E. Lauritzen, Y. Ono, S. Pinot, M. Stute, and G. Yu. 1999. 'Tropical climates at the Last Glacial Maximum: a new synthesis of terrestrial palaeoclimate data. I. Vegetation, lake-levels and geochemistry', *Climate Dynamics*, 15: 823-56.

Feng, R., and C. J. Poulsen. 2014. 'Andean elevation control on tropical Pacific climate and ENSO', *Paleoceanography*, 29: 795–809.

Garver, J. I., P. W. Reiners, L. J. Walker, J. M. Ramage, and S. E. Perry. 2005. 'Implications for timing of Andean uplift from thermal resetting of radiation-damaged zircon in the Cordillera Huayhuash, northern Peru', *Journal of Geology*, 113: 117-38.

Garzione, C., D. J. Auerbach, J. Jin-Sook Smith, J. J. Rosario, B. H. Passey, T. E. Jordan, and J. M. Eiler. 2014. 'Clumped isotope evidence for diachronous surface cooling of the Altiplano and pulsed surface uplift of the Central Andes', *Earth and Planetary Science Letters*, 393: 173-81.

Garzione, C. N., G. D. Hoke, J. C. Libarkin, S. Withers, B. MacFadden, J. Eiler, P. Ghosh, and A. Mulch. 2008. 'Rise of the Andes', *Science*, 320: 1304-7.

Garzione, C. N., N. McQuarrie, N. D. Perez, T. A. Ehlers, S. L. Beck, N. Kar, N. Eichelberger, A. D. Chapman, K. M. Ward, M. N. Ducea, R. O. Lease, C. J. Poulsen, L. S. Wagner, J. E. Saylor, G. Zandt, and B. K. Horton. 2017. 'Tectonic Evolution of the Central Andean Plateau and Implications for the Growth of Plateaus', *Annual Review of Earth and Planetary Sciences*, 45: 529-59.

Graham, A., K. M. Gregory-Wodzicki, and K. L. Wright. 2001. 'Studies in neotropical paleobotany. XV. A Mio-Pliocene palynoflora from the Eastern Cordillera, Bolivia: Implications for the uplift history of the Central Andes', *American Journal of Botany*, 88: 1545-57.

Gregory-Wodzicki, K. M. 2000. 'Uplift history of the Central and Northern Andes: A review', *Geological Society of America Bulletin*, 112: 1091-105.

Hallam, A. 1992. *Phanerozoic sea-level changes* (Columbia University Press: New York).

Hoke, G. D., B. L. Isacks, T. E. Jordan, N. Blanco, A. J. Tomlinson, and J. Ramezani. 2007. 'Geomorphic evidence for post-10 Ma uplift of the western flank of the central Andes 18 degrees 30'-22 degrees S', *Tectonics*, 26: 1-17.

Hooghiemstra, H., V. M. Wijninga, and A. M. Cleef. 2006. 'The Paleobotanical Record of Colombia: Implications for Biogeography and Biodiversity', *Annals of the Missouri Botanical Garden*, 93: 297-325.

Hoorn, C., F. P. Wesselingh, H. ter Steege, M. A. Bermudez, A. Mora, J. Sevink, I. Sanmartin, A. Sanchez-Meseguer, C. L. Anderson, J. P. Figueiredo, C. Jaramillo, D. Riff, F. R. Negri, H. Hooghiemstra, J. Lundberg, T. Stadler, T. Sarkinen, and A. Antonelli. 2010. 'Amazonia through time: Andean uplift, climate change, landscape evolution, and biodiversity', *Science*, 330: 927-31.

Horton, B. K., M. Parra, J. E. Saylor, J. Nie, A. Mora, V. Torres, D. F. Stockli, and M.R. Strecker. 2010. 'Resolving uplift of the Northern Andes using detrital zircon age signatures', *GSA Today*, 20: 4-9.

Insel, N., C. J. Poulsen, and T. A. Ehlers. 2009. 'Influence of the Andes Mountains on South American moisture transport, convection, and precipitation', *Climate Dynamics*, 35: 1477-92.

Insel, N., C. J. Poulsen, T. A. Ehlers, and C. Sturm. 2012. 'Response of meteoric $\delta^{18}O$ to surface uplift - Implications for Cenozoic Andean Plateau growth', *Earth and Planetary Science Letters*, 317-318: 262-72.

Kar, N., C. N. Garzione, C. Jaramillo, T. Shanahan, V. Carlotto, A. Pullen, F. Moreno, V. Anderson, E. Moreno, and J. Eiler. 2016. 'Rapid regional surface uplift of the northern Altiplano plateau revealed by multiproxy paleoclimate reconstruction', *Earth and Planetary Science Letters*, 447: 33-47.

Kroonenberg, S. B., J. G. M. Bakker, and A. M. Van der Wiel. 1990. 'Late Cenozoic uplift and paleogeography of the Colombian Andes: constraints on the development of high-andean biota', *Geologie en Mijnbouw*, 69: 279-90.

Leier, A., N. McQuarrie, C. Garzione, and J. Eiler. 2013. 'Stable isotope evidence for multiple pulses of rapid surface uplift in the Central Andes, Bolivia', *Earth and Planetary Science Letters*, 371: 49-58.

Madriñán, S., A. J. Cortes, and J. E. Richardson. 2013. 'Páramo is the world's fastest evolving and coolest biodiversity hotspot', *Frontiers in Genetics*, 4: 1-7.

Martinez, C., C. Jaramillo, A. Correa-Metrio, W. Crepet, J. E. Moreno, A. Aliaga, F. Moreno, M. Ibanez-Mejia, and M. B. Bush. 2020. 'Neogene precipitation, vegetation, and elevation history of the Central Andean Plateau', *Science Advances*, 6: 1-9.

Montgomery, D. R., G. Balco, and S. D. Willett. 2001. 'Climate, tectonics, and the morphology of the Andes', *Geology*, 29: 579-82.

Mora, A., D. Villagómez, M. Parra, V. M. Caballero, R. A. Spikings, B. K. Horton, J. A. Mora-Bohórquez, R. A. Ketcham, and J. P. Arias-Martinez. 2020. 'Late Cretaceous to Cenozoic uplift of the northern Andes: Paleogeographic implications.' in J. Gómez and D. Mateus-Zabala (eds.), *The Geology of Colombia* (Servicio Geológico Colombiano: Bogotá).

Pérez-Escobar, O. A. , A. Zizka, M. A. Bermudez, A. S. Meseguer, F. L. Condamine, C. Hoorn, H. Hooghiemstra, Y. Pu, D. Bogarin, L. M. Boschman, R. T. Pennington, A. Antonelli, and G. Chomicki. 2022. 'The Andes through time: evolution and distribution of Andean floras', *Trends in Plant Science*, 27: 364-78.

Perrigo, A. L., C. Hoorn, and A. Antonelli. 2019. 'Why mountains matter for biodiversity', *Journal of Biogeography*, 00: 1-11.

Pinot, S., G. Ramstein, S. P. Harrison, I. C. Prentice, J. Guiot, M. Stute, and S. Joussaume. 1999. 'Tropical paleoclimates at the Last Glacial Maximum: comparison of Paleoclimate Modeling Intercomparison Project (PMIP) simulations and paleodata', *Climate Dynamics*, 15: 857-74.

Poulsen, C. J., T. A. Ehlers, and N. Insel. 2010. 'Onset of Convective Rainfall During Gradual Late Miocene Rise of the Central Andes', *Science*, 328: 490-93.

Restrepo-Moreno, S. A., D. A. Foster, M. Bernet, K. Min, and S. Noriega. 2019. 'Morphotectonic and Orogenic Development of the Northern Andes of Colombia: A Low-Temperature Thermochronology Perspective.' in F. Cediel and R. P. Shaw (eds.), *Geology and Tectonics of Northwestern South America The Pacific-Caribbean-Andean Junction* (Springer: Switzerland).

Saylor, J. E., and B. K. Horton. 2014. 'Nonuniform surface uplift of the Andean plateau revealed by deuterium isotopes in Miocene volcanic glass from southern Peru', *Earth and Planetary Science Letters*, 387: 120-31.

Schneider, T., T. Bischoff, and G. H. Haug. 2014. 'Migrations and dynamics of the intertropical convergence zone', *Nature*, 513: 45-53.

Scott, E. M., M. B. Allen, C. G. Macpherson, K. J. W. McCaffrey, J. P. Davidson, C. Saville, and M. N. Ducea. 2018. 'Andean surface uplift constrained by radiogenic isotopes of arc lavas', *Nature Communications*, 9: 1-8.

Takahashi, K., and D. S. Battisti. 2007. 'Processes Controlling the Mean Tropical Pacific Precipitation Pattern. Part I: The Andes and the Eastern Pacific ITCZ', *Journal of Climate*, 20: 3434-51.

Thompson, L. G., E. Mosley-Thompson, M. E. Davis, P. N. Lin, K. A. Henderson, J. Cole-Dai, J. F. Bolzan, and K. B. Liu. 1995. 'Late glacial stage and holocene tropical ice core records from huascaran, peru', *Science*, 269: 46-50.

Van der Hammen, T., and H. Hooghiemstra. 1997. 'Chronostratigraphy and Correlation of the Pliocene and Quaternary of Colombia', *Quaternary International*, 40: 81-91.

Van der Hammen, T., J. H. Werner, and H. van Dommelen. 1973. 'Palynological record of the upheaval of the Northern Andes: a study of the Pliocene and Lower Quaternary of the Colombian early evolution of its high-Andean biota', *Review of Palaeobotany and Palynology*, 16: 1-122.

Vera, C., J. Baez, M. Douglas, C. B. Emmanuel, J. Marengo, J. Meitin, M. Nicolini, J. Nogues-Paegle, J. Paegle, O. Penalba, P. Salio, C. Saulo, M. A. Silva Dias, P. Silva Dias, and E. Zipser. 2006. 'The South American Low-Level Jet Experiment', *Bulletin of the American Meteorological Society*, 87: 63-77.

Vuille, M., R.S. Bradley, and F. Keimig. 2000. 'Climate variability in the Andes of Ecuador and its relation to tropical Pacific and Atlantic Sea surface temperature anomalies', *Journal of Climate*, 13: 2520-35.

Wijninga, V. M. 1996a. 'Palynology and paleobotany of the early pliocene section Rio frio 17 (Cordillera Oriental, Colombia): Biostratigraphical and chronostratigraphical implications', *Review of Palaeobotany and Palynology*, 92: 329-50.

Wijninga, V.M. 1996c. 'Palaeobotany and palynology of Neogene sediments from the high plain of Bogotá (Colombia)', University of Amsterdam.

Xie, S. P., and S. G. Philander. 1994. 'A coupled ocean atmosphere model of relevance to the ITCZ in the eastern Pacific', *Tellus*, 46A: 340-50.

Xu, H., Y. Wang, and S. P. Xie. 2004. 'Effects of the Andes on Eastern Pacific Climate: A Regional Atmospheric Model Study', *Journal of Climate*, 17: 589-602.

4 Early Pliocene vegetation and hydrology changes in western equatorial South America

Friederike Grimmer[1], Lydie Dupont[1], Frank Lamy[2], Gerlinde Jung[1], Catalina González[3], Gerold Wefer[1]

[1]MARUM – Center for Marine Environmental Sciences, University of Bremen, Leobener Str. 8, 28359 Bremen, Germany
[2]Alfred-Wegener-Institute for Polar and Marine Research, Am Handelshafen 12, 27570 Bremerhaven, Germany
[3]Department of Biological Sciences, Universidad de los Andes, Cra. 1 #18a-12, Bogotá, Colombia

Published as: Grimmer, F., L. Dupont, F. Lamy, G. Jung, C. Gonzalez, and G. Wefer. 2018. 'Early Pliocene vegetation and hydrology changes in western equatorial South America', *Climate of the Past*, 14: 1739-54.

4.1 Abstract

During the early Pliocene, two major tectonic events triggered a profound reorganization of ocean and atmospheric circulation in the Eastern Equatorial Pacific (EEP), the Caribbean Sea, and on adjacent land masses: the progressive closure of the Central American Seaway (CAS) and the uplift of the northern Andes. These affected amongst others the mean latitudinal position of the Intertropical Convergence Zone (ITCZ). The direction of an ITCZ shift however is still debated, as numeric modelling results and paleoceanographic data indicate shifts in opposite directions. To provide new insights into this debate, an independent hydrological record of western equatorial South America was generated. Vegetation and climate of this area were reconstructed by pollen analysis of 46 samples from marine sediments of ODP Hole 1239A from the EEP comprising the interval between 4.7 and 4.2 Ma. The study site is sensitive to latitudinal ITCZ shifts insofar as a southward (northward) shift would result in increased (decreased) precipitation over Ecuador. The presented pollen record comprises representatives from five ecological groups: lowland rainforest, lower montane forest, upper montane forest, páramo, and broad range taxa. A broad tropical rainforest coverage persisted in the study area throughout the early Pliocene, without significant open vegetation beyond the páramo. Between 4.7 and 4.42 Ma, humidity increases, reaching its peak around 4.42 Ma, and slightly decreasing again afterwards. The stable, permanently humid conditions are rather in agreement with paleoceanographic data indicating a southward shift of the ITCZ, possibly in response to CAS closure. The presence of páramo vegetation indicates that the Ecuadorian Andes had already reached considerable elevation by the early Pliocene. Future studies could extend the hydrological record of the region further back into the late Miocene to see if a more profound atmospheric response to tectonic changes occurred earlier.

4.2 Introduction

The progressive closure of the Central American Seaway (CAS) and the uplift of the northern Andes profoundly reorganized early Pliocene ocean and atmospheric circulation in the Eastern Equatorial Pacific (EEP). The formation of the Isthmus of Panama, and especially the precise temporal constraints of the closure of the Panama Strait, have been subject of numerous studies (Hoorn and Flantua 2015; Steph 2005; Montes et al. 2015; Bartoli et al. 2005; Groeneveld et al. 2014). A recent review based on geological, paleontological, and molecular records narrowed the formation *sensu stricto* down to 2.8 Ma (O'Dea et al. 2016). Temporal constraints on the restriction of the surface water flow through the gateway were established by salinity reconstructions on both sides of the Isthmus (Steph, Tiedemann, Prange, et al. 2006, Fig. 4.1). The salinities first start to diverge around 4.5 Ma. A major step in the seaway closure between 4.7 and 4.2 Ma was also assumed based on the comparison of mass accumulation rates of the carbonate sand-fraction in the Caribbean Sea and the EEP (Haug and Tiedemann 1998).

The closure of the Central American Seaway has been associated with the development of the EEP cold tongue (EEP CT), strengthened upwelling in the EEP, the shoaling of the thermocline, and a mean latitudinal shift of the Intertropical Convergence Zone (ITCZ; (Steph 2005; Steph, Tiedemann, Groeneveld, et al. 2006; Steph, Tiedemann, Prange, et al. 2006; Steph et al. 2010). The direction of a potential shift of the ITCZ is still debated because of a discrepancy between paleoclimate reconstructions based on proxy data and numerical modelling results.

For the late Miocene, a northernmost paleoposition of the ITCZ at about 10–12°N has been proposed (Flohn 1981; Hovan 1995). Subsequently, a southward shift towards 5°N paleolatitude between 5 and 4 Ma is indicated by eolian grain-size distributions in the eastern tropical Pacific (Hovan 1995). Billups et al. (1999) provide additional evidence for a southward shift of the ITCZ between 4.4 and 4.3 Ma. Hence, most proxy data agree about a southward ITCZ shift during the early Pliocene. On the contrary, results from numerical modelling suggest a northward shift of the ITCZ in response to CAS closure (Steph, Tiedemann, Prange, et al. 2006) and Andean uplift (Takahashi and Battisti 2007; Feng and Poulsen 2014).

An independent record of the terrestrial hydrology for the early Pliocene from a study site that is sensitive to latitudinal ITCZ shifts could provide new insights to this debate. Schneider, Bischoff, and Haug (2014) also stress the need of reconstructions of the ITCZ in the early and mid-Pliocene in order to understand how competing effects like an ice-free Northern Hemisphere and a weak EEP CT balanced, and to reduce uncertainties of predictions. Even though changes of ocean–atmosphere linkages related to ENSO (El Niño Southern Oscillation) and ITCZ shifts strongly impact continental precipitation in western equatorial South America, most studies so far have focused on paleoceanographic features such as sea-surface temperatures and ocean stratification.

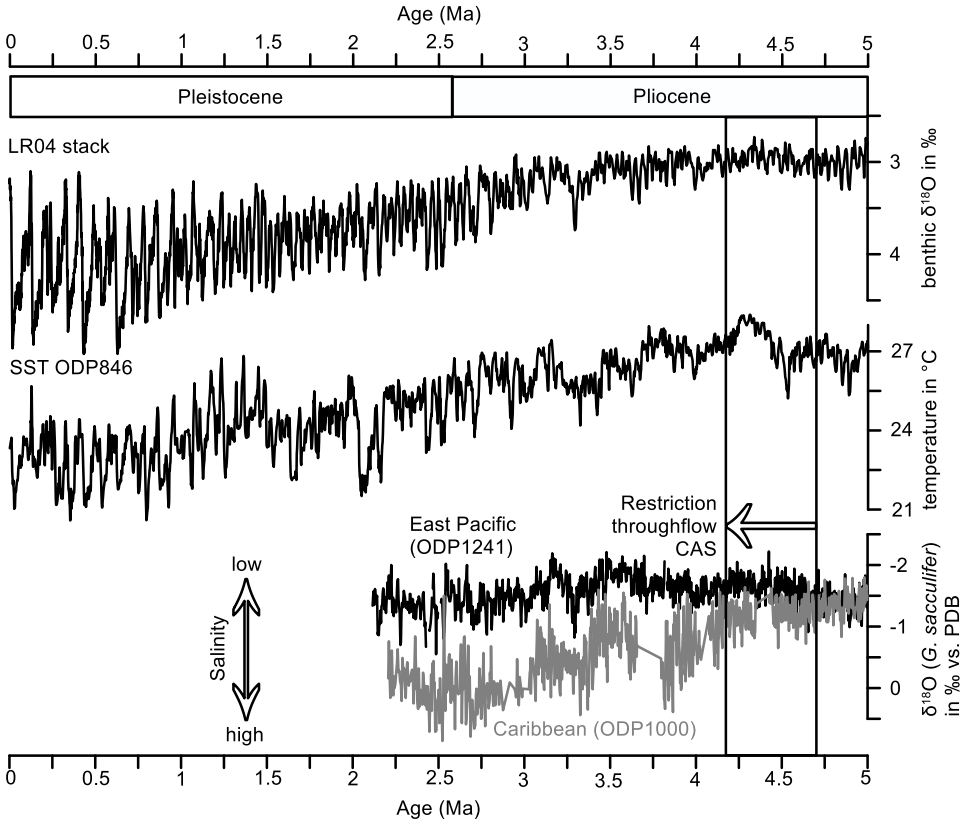

Figure 4.1. LR04 global stack of benthic $\delta^{18}O$ reflecting changes in global ice volume and temperature (Lisiecki and Raymo, 2005). Uk'_{37} sea-surface temperatures (SST) of ODP Site 846 in the Equatorial Pacific Cold Tongue (Lawrence, Liu, and Herbert 2006). $\delta^{18}O$ of the planktonic foraminifer *G. sacculifer* from ODP Site 1000 in the Caribbean and ODP Site 1241 in the East Pacific (Haug, Tiedemann, et al. 2001; Steph 2005; Steph, Tiedemann, Groeneveld, et al. 2006), reflecting changes in sea-surface salinity (see Fig. 4.2 for location of ODP Sites). The box represents the time window analyzed in this study.

The second major tectonic process is the uplift of the northern Andes which strongly altered atmospheric circulation patterns over South America. Three major deformation phases include fan building in the lower Eocene to early Oligocene, compression of Oligocene deposits in the Miocene and Pliocene, and refolding during Pliocene to recent times (Corredor 2003). While the uplift of the Central Andes is well investigated, only few studies deal with the timing of uplift of the northern Andes. Coltorti and Ollier (2000), based on geomorphologic data, conclude that the uplift of the Ecuadorian Andes started in the early Pliocene and continued until the Pleistocene. More recent apatite fission track data indicate that the western Andean Cordillera of Ecuador was rapidly exhumed during the late Miocene (13–9 Ma) (Spikings et al. 2005). Uplift estimates for the Central Andes suggest that the Altiplano had reached less than half of its modern elevation by 10 Ma, with uplift rates increasing from 0.1 mm/yr in the early and middle Miocene to 0.2–0.3 mm/yr to present. For the Eastern Cordillera of Colombia, elevations of less than 40% of the modern values are estimated for the early Pliocene, then increasing rapidly at rates of 0.5–3 mm/yr until modern elevations were reached around 2.7 Ma (Gregory-Wodzicki 2000). Both the tectonic events and the

closure of the Central American Seaway are assumed to have had a large impact on ocean and atmospheric circulation in the eastern Pacific, the Caribbean and on adjacent land masses. Therefore, the reconstruction of continental climate, especially hydrology, will contribute to our understanding of climatic changes in this highly complex area.

To better understand the early Pliocene vegetation and hydrology of western equatorial South America we studied pollen and spores from the early Pliocene section (4.7–4.2 Ma) of the marine sediment record at ODP Site 1239 and compared this record to Holocene samples from the same Site. In addition, we use elemental ratios to estimate variations in fluvial terrestrial input (Ríncon-Martínez et al. 2010).

While other palynological studies of the region have been conducted for the mid-Pliocene to Holocene (Seilles et al. 2016; Hooghiemstra 1984; González, Urrego, and Martínez 2006), only a few palynological records for the early Pliocene exist (Wijninga and Kuhry, 1990; Wijninga, 1996). The record contributes to elucidate how vegetation and climate in this area responded to changes in atmospheric and oceanic circulation, possibly induced by the closure of the Central American Seaway and the uplift of the northern Andes. Therefore, the main objectives of the study are firstly, to investigate long-term vegetation and climatic changes, focusing on hydrology, in western equatorial South America and, secondly, to interpret these changes in relation to climate phenomena influencing the hydrology of the region, especially the mean latitudinal position of the ITCZ and variability related to ENSO. These objectives are approached by the following research questions: 1) What floral and vegetation changes took place in the coastal plain of western equatorial South America and the Ecuadorian Andes from 4.7 to 4.2 Ma? 2) What are the climatic implications of the vegetation change, especially in terms of hydrology? 3) What are the implications for Andean uplift, especially regarding the development of the high Andean páramo vegetation?

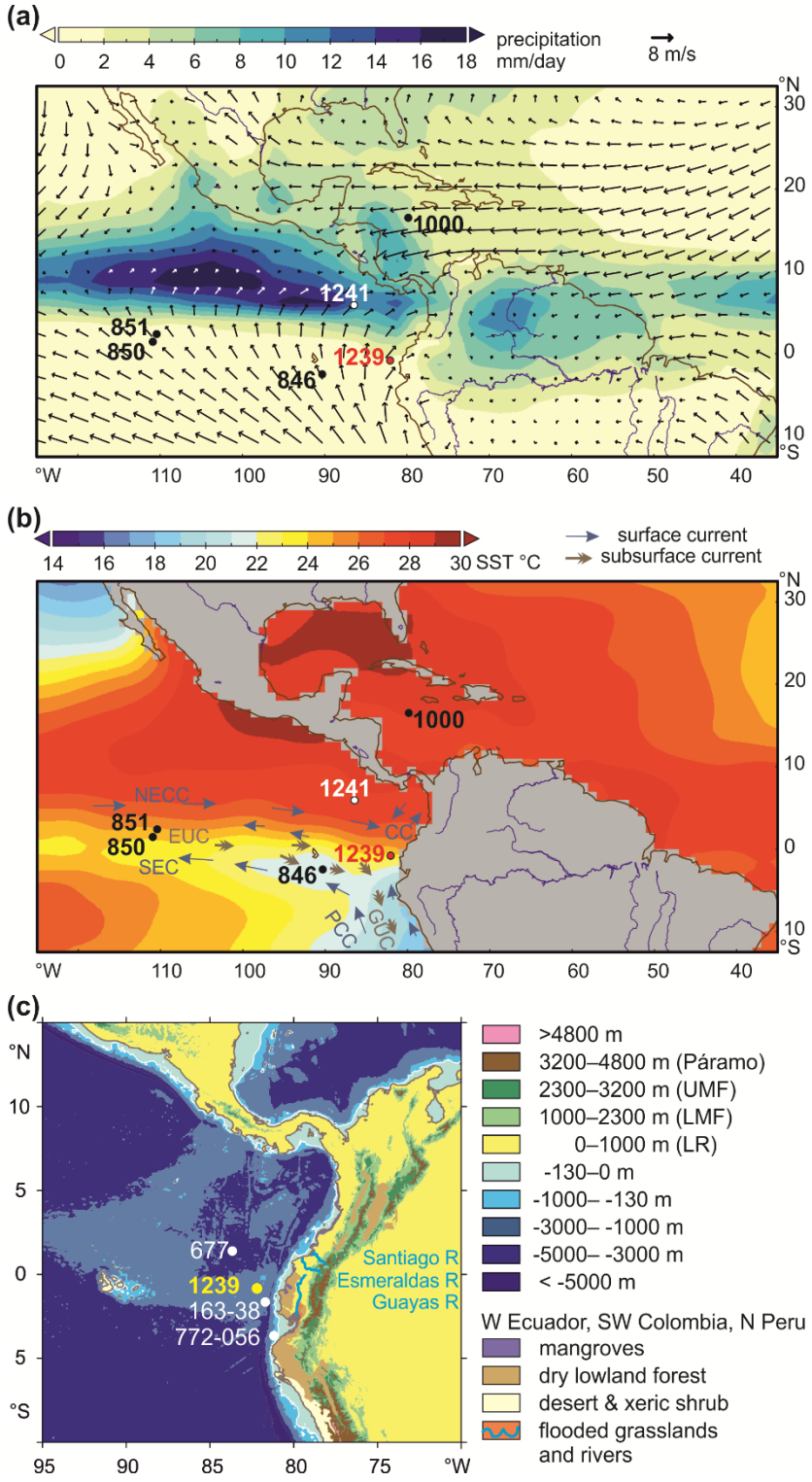

Figure 4.2. Modern climate (boreal summer) and vegetation and core site positions of ODP Sites 677, 846, 850, 851, 1000, 1239, 1241, Trident core TR163-38, and M772-056 mentioned in the text. A. 1981-2010 AD long-term monthly July precipitation in mm/day (CPC Merged Analysis of Precipitation) and .995 sigma level (near surface) wind field (NCEP). July is the middle of the rainy season in northern South America, when the ITCZ is at its northern boreal summer position. Salinity estimates for the Caribbean indicate a position of the ITCZ further north during the Pliocene. Direction of wind is not favorable for wind transport of pollen and spores to ODP Site 1239. B. Long-term monthly July sea-surface temperatures (NODC), surface and subsurface currents of the eastern equatorial Pacific (Mix et al. 2003). NECC, North Equatorial Countercurrent; SEC, South Equatorial Current; PCC, Peru-Chile Current (continuation of the Humboldt Current); CC, Coastal Current; EUC, Equatorial Undercurrent; GUC, Gunther Undercurrent. C.

Contours, bathymetry (ETOPO1), main rivers in Ecuador, and vegetation. Transport of pollen and spores in the ocean over the Peru-Chile Trench, which is very narrow east of the Carnegie Ridge, probably takes place in nepheloid layers. Páramo vegetation is found between 3200 and 4800 m, upper montane Andean forest (UMF) grows between 1000 and 2300 m, sub-Andean lower montane forest (LMF) between 1000 and 2300 m, and lowland forest (LR) below 1000m. The distribution of desert and xeric shrubs in northern Peru, drier broad-leaved forest, flooded grasslands, and mangroves in Ecuador and Colombia is denoted in different colors (see legend, WWF). Source areas of pollen and spores in sediments of ODP Site 1239 are sought in western Ecuador, northwestern Peru, and southwestern Colombia (see text). Abbreviated web sources and retrieval dates are listed under references.

4.3 Modern setting

4.3.1 Climate and ocean circulation

The climate of western equatorial South America is complex and heterogeneous, as it is not only controlled by large-scale tropical climate phenomena such as the ITCZ and ENSO, but is also strongly influenced by small-scale climate patterns caused by the diverse Andean topography (Niemann, Brunschön, and Behling 2010; Marchant et al. 2001). The annual cycle of precipitation in northwestern South America is controlled by insolation changes. During boreal summer when insolation is strongest in the Northern Hemisphere, the ITCZ is located at its northernmost position around 9°–10° N (Vuille, Bradley, and Keimig 2000). Approaching austral summer, the ITCZ moves southward across the equator. Within the range of the ITCZ, annual precipitation patterns are generally characterized by two minima and two maxima. The coastal areas of southern Ecuador where the ITCZ has its southernmost excursion show an annual precipitation pattern with one maximum during austral summer and a pronounced dry season during austral winter (Bendix and Lauer 1992).

This general circulation pattern is modified by ENSO at interannual time-scales. During warm El Niño events, the lowlands of Ecuador experience abundant precipitation whereas the northwestern Ecuadorian Andes experience drought (Vuille, Bradley, and Keimig 2000). Regional climate patterns are also modified by the topography of the Andes which pose an effective barrier for the large-scale atmospheric circulation. While precipitation patterns east of the Andes are driven by moisture-laden easterly trade winds originating over the tropical Atlantic and the Amazon basin, the coastal areas and the western Andean slopes are dominated by air masses originating in the Pacific (Vuille, Bradley, and Keimig 2000, Fig. 4.2). The warm annual El Niño current which flows southward along the Colombian Pacific coast warms the air masses along the coast. This moist air brings over 6000 mm yearly precipitation to the northern coastal plain. In contrast, the coastal areas of southernmost Ecuador and northern Peru are under the influence of the Peru-Chile Current, which is a continuation of the cold Humboldt Current transporting cold and nutrient rich waters and giving rise to a long strip of coastal desert (Balslev 1988). The westwards flow of the cold surface waters of the EEP CT to the western Pacific via the South Equatorial Current (SEC) is

driven by the Walker Circulation. Warm waters return eastwards via the North Equatorial Countercurrent (NECC, see Fig. 4.2). An abrupt transition between the cold SEC and the warm NECC is the Equatorial Front (EF, Pak and Zaneveld 1974).

4.3.2 Geography, vegetation and pollen transport

Ecuador is geographically divided into three main regions: the coastal plain with several rivers draining into the Pacific, the Andes, and the eastern lowlands which constitute the western margin of the Amazon Basin. The mountains form two parallel cordilleras which are separated by the Interandean Valley. The diverse vegetation is the result of the combined effects of elevation and precipitation. In the coastal plain there is an abrupt shift from tropical lowland rainforests in the north to a desert dominated by annual xerophytic herbs in the south. This shift reflects the dependence of the vegetation on precipitation which ranges from 100 to 6000 mm per year on the coastal plain. The western slopes of the Andes are covered by montane forest, which is partly interrupted by drier valleys in southern Ecuador (Balslev 1988).

Along the coast, mangrove stands occur in the salt- and brackish-water tidal zone of river estuaries and bays. They are formed by two species of *Rhizophora* (*R. harrisonii* and *R. mangle*), and to a lesser extent *Avicennia, Laguncularia*, and *Conocarpus* are present (Twilley et al. 2001). The lowland rainforest is characterized by the dominant plant families Fabaceae, Rubiaceae, Arecaceae, Annonaceae, Melastomataceae, Sapotaceae, and Clusiaceae in terms of species richness. In the understory, Rubiaceae, Araceae, and Piperaceae form the predominant elements (Gentry 1986). In the lower montane forest, *Cyathea*, Meliaceae (e.g. *Ruagea*), Fabaceae (e.g. *Dussia*), Melastomataceae (e.g. *Meriania, Phainantha*), Rubiaceae (e.g. *Cinchona*), Proteaceae (e.g. *Roupala*), Lauraceae (e.g. *Nectandra*), and Pteridaceae (e.g. *Pterozonium*) are common elements. Upper montane forests are dominated *by Myrsine, Ilex, Weinmannia, Clusia, Schefflera, Myrcianthes, Hedyosmum*, and *Oreopanax* (Jørgensen and León-Yánez 1999). Above ca. 3200 m, trees become sparse and eventually the vegetation turns into páramo. The páramo is a unique ecosystem of the high altitudes of the northern Andes of South America and of southern Central America, located between the continuous forest line and the permanent snowline at about 3000–5000 m (Luteyn 1999). The grass páramo is formed by tussock grasses, mainly *Calamagrostis* and *Festuca*. These are complemented by shrubs of *Diplostephium, Hypericum*, and *Pentacalia*, and forest patches of *Polylepis*. The shrub páramo consists of cushion plants like *Azorella, Plantago*, and *Werneria*, and shrubs like *Loricaria* and *Chuquiraga*. The vegetation of the desert páramo is scarce. Some common taxa are *Nototriche, Draba*, and *Culcitium* (Sklenár and Jorgensen 1999).

Rincon-Martínez et al. (2010) showed that the terrigenous sediment supply at ODP Site 1239 during Pleistocene interglacials is mainly fluvial and input of terrestrial material drops to low

amounts during the drier glacial stages. Consequently, transport of pollen and spores to the ocean is also mainly fluvial (González et al., 2010). High rates of orographic precipitation characterize the western part of equatorial South America. These heavy rains quickly wash out any pollen that might be in the air and result in large discharge by the Ecuadorian Rivers (Fig. 4.2). Esmeraldas and Santiago Rivers mainly drain the northern coastal plain of Ecuador, and the southern coastal plain is drained by several smaller rivers, which end in the Guayas River (Balslev 1988). Moreover, the predominantly westerly winds (Fig. 4.2) are not favorable for eolian pollen dispersal to the ocean. Nevertheless, some transport by SE trade winds is possible and should be taken into account.
After reaching the ocean, pollen and spores might pass the Peru-Chile Trench – which is quite narrow along the Carnegie Ridge – by means of nepheloid layers at subsurface depths. Some northward transport from the Bay of Guayaquil by the Coastal Current (Fig. 4.2) is likely. However, the Peru-Chile Current flows too far from the coast to have strong influence on pollen and spore dispersal. We consider western Ecuador, northernmost Peru and southwestern Colombia the main source areas of pollen and spores in sediments of ODP Site 1239.

4.3.3 Drilling site

ODP Site 1239 is located at 0°40.32'S, 82°4.86'W, about 120 km offshore Ecuador in a water depth of 1414m, near the eastern crest of Carnegie Ridge and just next to a downward slope into the Peru-Chile Trench (Shipboard Scientific Party 2003). Its location is close to the Equatorial Front (Fig. 4.2) which separates the warm and low-salinity waters of Panama Basin from the cooler and high-salinity surface waters of the EEP CT. The region of Site 1239 reveals a thick sediment cover, with dominant sediments in the region being foraminifer-bearing diatom nannofossil ooze (Shipboard Scientific Party 2003). A tectonic backtrack path on the Nazca plate (Pisias 1995) reveals a paleoposition of Site 1239 about 150–200 km further westward (away from the continent) and slightly southward relative to South America at 4–5 Ma compared to the present day position (Shipboard Scientific Party 2003). Due to its proximity to the Ecuadorian coast, Site 1239 is suitable to record changes in fluvial runoff, related to variations of precipitation in northwestern South America. Most of the material is discharged by the Guayas River and Esmeraldas River (Rincón-Martínez et al. 2010).

Table 4.1. List of identified pollen and spore taxa in marine ODP Holes 1239A (Pliocene samples) and 1239B (core top samples, taxa in grey occurred only in core top samples) and grouping according to their main ecological affinity (Marchant et al. 2002; Flantua et al. 2014).

Páramo	Upper montane forest	Lower montane forest	Lowland rainforest	Broad range taxa	Humid indicators
Polylepis/ Acaena	Podocarpaceae	Urticaceae/ Moraceae	*Wettinia*	Poaceae	Cyperaceae
Jamesonia/ Eriosorus	*Hedyosmum*	*Erythrina*	*Socratea*	Cyperaceae	*Ranunculus*
Huperzia	*Clethra*	*Alchornea*	Polypodiaceae	Tubuliflorae (Asteraceae)	*Hedyosmum*
Ranunculus	*Morella*	*Styloceras T*	*Pityrogramma/ Pteris altissima T*	Amaranthaceae	*Ilex*
Draba	Acanthaceae	Malpighiaceae		Rosaceae	*Pachira*
Sisyrinchium	Melastomataceae	Cyatheaceae		*Ambrosia/ Xanthium*	*Morella*
Cystopteris diaphana T	*Daphnopsis*	*Vernonia T*		Ericaceae	Malpighiaceae
	Bocconia	*Pteris grandifolia T*		*Artemisia*	Cyatheaceae
	Myrsine	*Pteris podophylla T*		*Ilex*	*Selaginella*
	Lophosoria	*Saccoloma elegans T*		*Thevetia*	*Pityrogramma/ Pteris altissima T*
	Elaphoglossum	*Thelypteris*		*Salacia*	*Hymenophyllum T*
	Hypolepis hostilis T	*Ctenitis subincisa T*		Bromeliaceae	*Thelypteris*
	Grammitis			Malvaceae	*Ctenitis subincisa T*
	Dodonaea viscosa			Euphorbiaceae	*Alnus*
	Alnus			*Liliaceae*	*Cystopteris diaphana T*
				Lycopodiaceae excl. *Huperzia*	
				Selaginella	
				Hymenophyllum T	
				Calandrinia	

4.4 Methods

A total of 65 samples of 10 cm^3 volume have been analyzed. For the interval between 301 and 334 mbsf (4.7 and 4.2 Ma), 46 sediment samples were taken at 67 cm intervals on average from ODP Hole 1239A (cores 33X5-37X1). Seventeen samples were taken more or less regularly distributed over the rest of the upper 450 m of Hole A (until 6 Ma). Additionally, two core top samples were taken from ODP Hole 1239B as modern analogues. Standard analytical methods were used to

process the samples, including decalcification with HCl (~10%) and removal of silicates with HF (~40%). Two tablets of exotic *Lycopodium* spores (batch #177,745 containing 18584 ± 829 spores per tablet) were added to the samples during the decalcification step for calculation of pollen concentrations (grains/cm³). After neutralization with KOH (40%) and washing, the samples were sieved with ultrasound over an 8µm screen to remove smaller particles. Samples were mounted in glycerin and a minimum of 100 pollen/spore grains (178 on average, Fig. S1) were counted in each sample using a Zeiss Axioskop and 400x and 1000x (oil immersion) magnification.

For pollen identification, the Neotropical Pollen Database (Bush and Weng 2007), a reference collection for Neotropical species held at the Department of Palynology and Climate Dynamics in Göttingen, and related literature (Colinvaux, De Oliveira, and Moreno Patino 1999; Murillo and Bless 1974, 1978; Hooghiemstra 1984; Roubik and Moreno P. 1991) were used. Pollen types were grouped according to their main ecological affinity (Marchant et al. 2002; Flantua et al. 2014). The zonation of the diagrams was based on constrained cluster analysis by sum-of-squares (CONISS) of the pollen percentage curves, using the square root transformation method (Edwards & Cavalli–Sforza's chord distance) implemented in TILIA (Grimm 1991, Supplementary Figure). Percentages are based on the pollen sum, which includes all pollen and fern spore types including unidentifiable ones. Confidence intervals were calculated after Maher (1972). An initial age model for Site 1239 was established based on biostratigraphic information (Shipboard Scientific Party 2003). The age model was refined by matching the benthic stable isotope records from Site 1239 with those from Site 1241 by visual identification of isotope stages (Tiedemann et al. 2007). Site 1241 has an orbitally tuned age model. Thus, this procedure resulted in an indirectly orbitally tuned age model for Site 1239, spanning the interval from 5 to 2.7 Ma (Tiedemann et al. 2007, Fig. S2). A coring gap of ca. 5 meters exists between cores 35X (347 mcd) and 36X (352 mcd) of Hole 1239A (Tiedemann et al. 2007; Table AT3).

Elemental concentrations (total elemental counts) of Fe and K were measured in high resolution (every 2 cm) using an Avaatech™ X-Ray Fluorescence (XRF) Core Scanner at the Alfred-Wegener-Institute, Bremerhaven, with correction for dead time. Both Holes A and B of ODP Site 1239 were sampled. A nondestructive measuring technique was applied, allowing rapid semi-quantitative geochemical analysis of sediment cores (Richter et al. 2006). Several studies comparing XRF core scanner data to geochemical measurements on discrete samples showed that major elements can be precisely measured with the scanner in a non-destructive way (e.g. Tjallingii et al. 2007).

4.5 Results

Five groups were established with pollen taxa grouped according to their main ecological affinity (Table 4.1). The groups páramo, upper montane forest, lower montane forest, and lowland

rainforest represent vegetation belts with different altitudinal ranges (Hooghiemstra 1984; Van der Hammen 1974b). To track changes of humidity, an additional group named "Indicators of humid conditions" was established. This group includes those taxa that permanently need humid conditions to grow. Changes of the pollen percentages of the ecological groups for the Pliocene interval and the core top samples are shown in Figs. 3 and 5. Pollen percentages of single taxa are shown in Fig. S1.

To put the results of the detailed early Pliocene section into context of long-term changes, we plot a selection together with the results of a coarse resolution pilot study in Fig. 4.3. Percentages of humidity indicators hint to slightly drier conditions at the beginning of the Pliocene. A trend towards higher palynomorph concentrations is found for the period from 6 to 2 Ma. Grass pollen percentages remain low indicating mainly closed forest at altitudes below the páramo. Representation of lowland rainforest was low around 4.7 Ma, increased by 4.5 Ma, declined again to low levels around 3.5 Ma, and rose to remain at higher levels during the Pleistocene. Continuous presence of pollen and spores from the páramo indicates that the Ecuadorian Andes had reached high altitudes before the Pliocene.

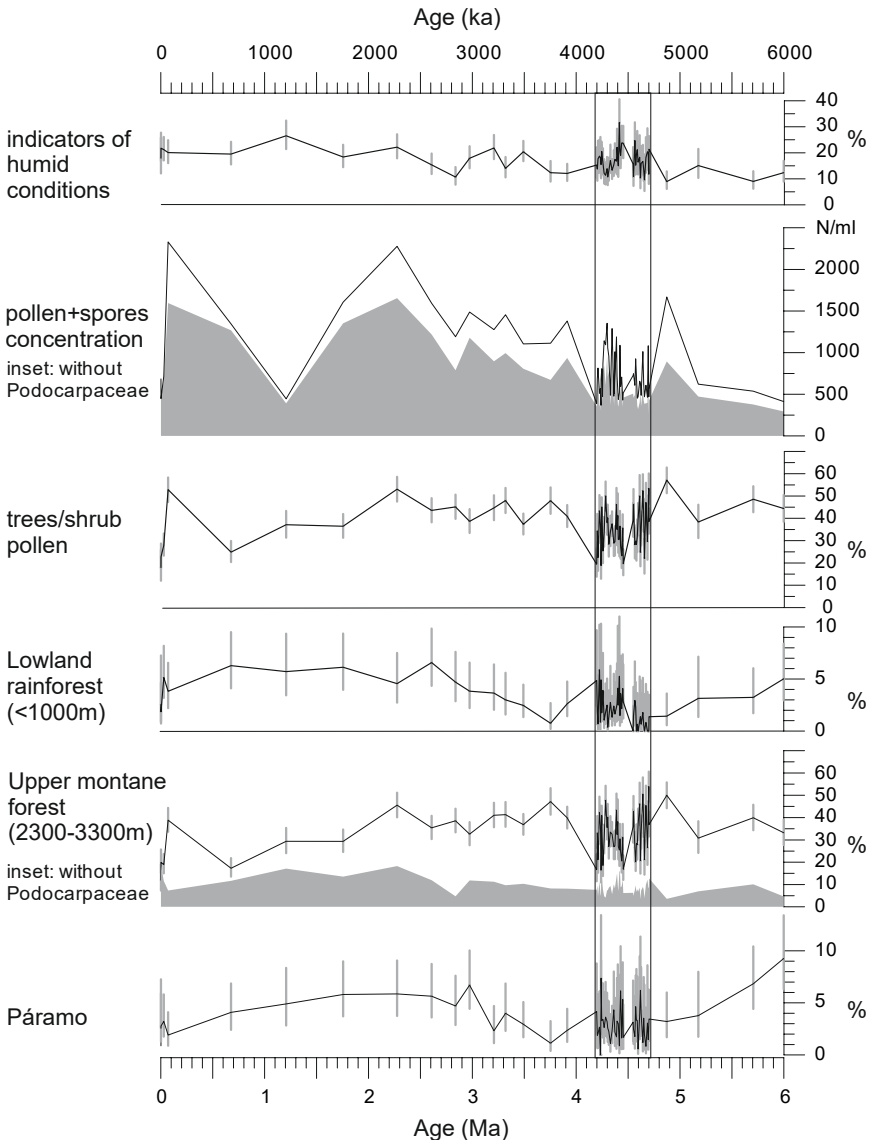

Figure 4.3. Pliocene and Pleistocene palynomorph percentages (based on the total of pollen and spores) of ODP Hole 1239A for three vegetation belts, humidity indicators, grass pollen and pollen and spore concentration per ml. 95% confidence intervals as grey bars after Maher (1972). Age model for the last 5 Ma after Tiedemann et al. (2007) and for 6 to 5 Ma after Mix et al. (2003).

4.5.1 Description of the early Pliocene pollen record

In the early Pliocene samples, 141 different palynomorph types were recognized, including 77 pollen and 64 fern spore types. A high percentage of tree and shrub pollen (46–88%) is present throughout the interval, compared to low percentages of herbs and grass pollen (0–25%; Fig. 4.4). In most of the vegetation belts, one or two pollen or spore taxa are overrepresented. The lowland rainforest is mainly represented by Polypodiaceae, the lower montane forest is controlled by Cyatheaceae, and the upper montane forest is strongly influenced by Podocarpaceae and *Hedyosmum*. In the páramo, the percentages of the pollen taxa are more evenly balanced. Of the total sum, the Andean forest pollen makes by far the largest percentage, with the upper montane

forest ranging between 17 and 54% and the lower montane forest between 5 and 19%. The páramo is represented with 0 to 10% and the lowland rainforest with 0 to 6%. The remaining fraction has a wide or unknown ecological range.

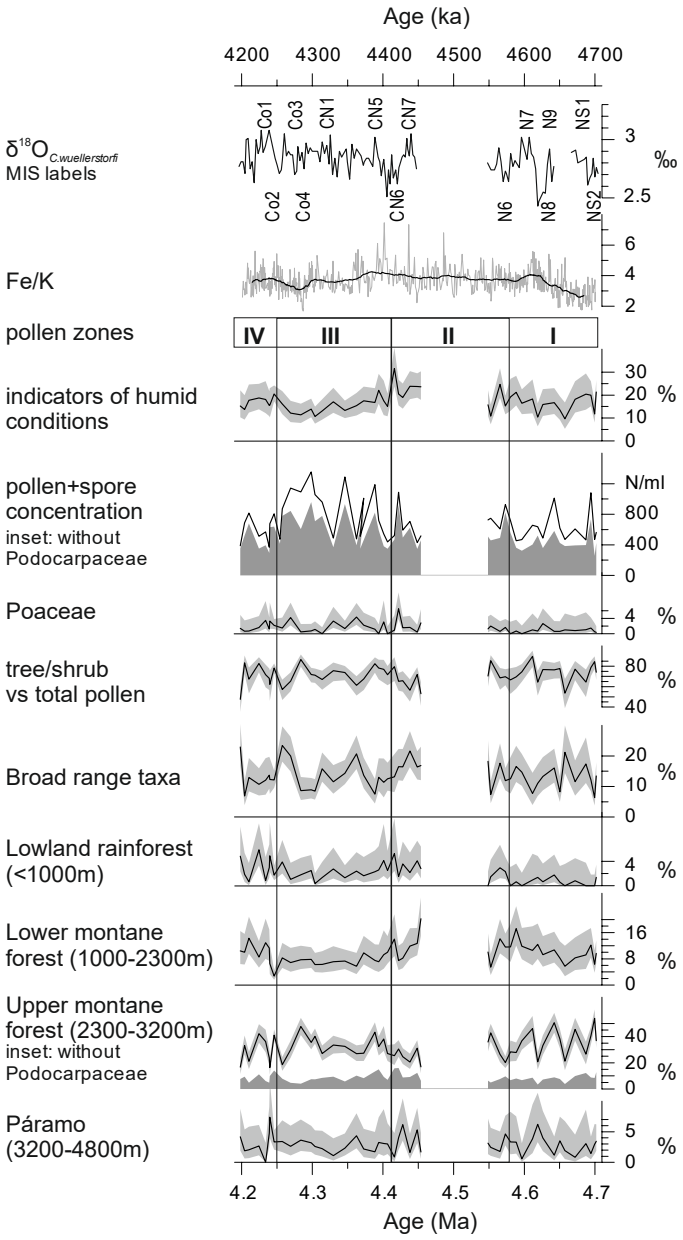

Figure 4.4. Palynomorph percentages of ODP Hole 1239A for the four vegetation belts and other groups from 4.7 to 4.2 Ma. Grey shading represents the 95% confidence intervals (after Maher 1972). Vertical black lines delimit the pollen zones. At the top stable oxygen isotopes of the benthic foraminifer *C. wuellerstorfi* (Tiedemann et al., 2007) of ODP Hole 1239A, marine isotope stages (MIS), and elemental ratios of Fe/K from Holes 1239A and 1239B. Ages are from Tiedemann et al. (2007). A coring gap is present in Hole 1239A between 4.45 and 4.55 Ma.

The pollen record of ODP Hole 1239A was divided into four main pollen zones based on constrained cluster analysis (Fig. 4.4 and Fig. S1). Pollen zone I (333.4–325.2 mbsf: 4.70–4.58 Ma,

14 samples) has low pollen and spores concentrations. It is characterized by low pollen percentages of lowland rainforest, increases in pollen values of lower montane forest, the percentage of fern spores, and the Fe/K ratio. The pollen concentrations of broad range taxa, upper montane forest, páramo, and indicators of humid conditions go through frequent fluctuations. Coastal desert herbs (Amaranthaceae) are well represented (Fig. S1). Percentages of Poaceae pollen are low.

In pollen zone II (324.8–316.4 mbsf: 4.46–4.42 Ma, 10 samples), the pollen and spores concentration is similar to pollen zone I. The lowland rainforest pollen, indicators of humid conditions, and the Fe/K ratio reach their maximum. Fern spores also reach their first maximum. Percentages of lower montane forest and páramo are high, whereas the percentage of upper montane forest is low at this time due to a strong decline of Podocarpaceae pollen. The representation of broad range taxa diminish in the interval above the gap, the decrease being mainly controlled by *Selaginella*, Cyperaceae, *Ambrosia/Xanthium*, and Amaranthaceae. Pollen zone II encloses a coring gap of almost 100 ka.

Pollen zone III (315.5–305.4 mbsf: 4.41–4.26 Ma, 14 samples) shows a stepwise increase of the pollen and spores concentration with its maximum at 4.3 Ma. The concentration is strongly controlled by Podocarpaceae pollen which account for up to 44% in this zone. The pollen of lowland rainforest, lower montane forest, páramo, indicators of humid conditions, and Fe/K show lower values than in zone II. Broad range taxa show some larger fluctuations. The upper montane forest pollen has its maximum extent of this zone (48%) at 4.28 Ma due to the high percentage of Podocarpaceae. If the Podocarpaceae pollen are excluded from the upper montane forest, the representation of this vegetation belt shows the same pattern of decline as that of the lower montane forest and lowland rainforest.

In pollen zone IV (304.7–301.3 mbsf: 4.25–4.12 Ma, 8 samples), the pollen and spores concentration decreases sharply after 4.24 Ma. The pollen percentage of lower montane forest increases. The percentage of fern spores is at its maximum in this zone. Percentages of páramo, upper montane forest, broad range taxa, indicators of humid conditions, and the Fe/K ratio remain similar as in zone III. The percentage of lowland rainforest pollen goes through frequent and large fluctuations.

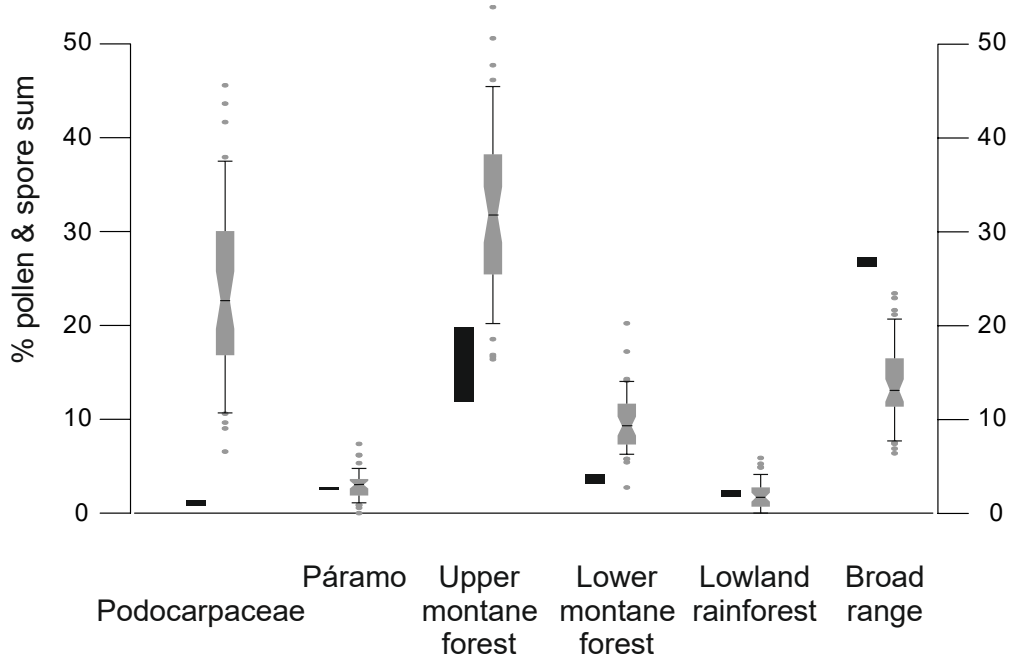

Figure 4.5. Comparison of the palynomorph percentages (based on total pollen and spores) of Podocarpaceae and the different vegetation belts between 2 Holocene samples (black) and Pliocene samples between 4.7-4.2 Ma (box-whisker plots).

4.5.2 Modern vs. Pliocene pollen assemblages

Two samples from the top of ODP Hole 1239B have been analyzed to facilitate a comparison of the recent palynological signal with modern vegetation (Fig. 4.5 and Fig. S1). Although there is no detailed age control on these surface/subsurface samples, a Holocene age can be assigned based on the benthic oxygen isotope record (Rincón-Martínez et al. 2010). Fifty-one different palynomorph types were recognized, including 29 pollen and 22 fern spore types.

The samples are characterized by low pollen and spore concentrations of 685 and 465 grains/cm^3, respectively. Indicators of humid conditions show intermediate values. Herbs and grass pollen are very abundant with 20–26%, but tree and shrub pollen decreased to 35–46% compared to the early Pliocene interval. Broad range taxa reach their maximum abundance with 26–27%. Lowland rainforest and páramo pollen have similar representations as in the Pliocene, whereas the lower and upper montane forest pollen reach their lowest percentages. When compared to the Pliocene pollen composition, some floristic differences are seen. During the Holocene *Podocarpus* is replaced by *Alnus* as the most abundant upper montane forest tree, although *Podocarpus* was still abundant during the glacial (González et al. 2010). Another notable difference is the presence of *Rhizophora* pollen in one of the core top samples, whereas it is completely absent in the early Pliocene interval.

4.5.3 Description of the páramo

The pollen spectrum from the páramo at ODP Site 1239 includes three different taxa which are mainly confined to the páramo: the pollen type *Polylepis/Acaena*, and the fern spores *Huperzia* and *Jamesonia/Eriosorus* (Fig. 4.6). Other taxa, which are characteristic of páramos but cannot be exclusively attributed to this ecosystem, were not included in the páramo sum (e.g. Asteraceae, Poaceae, Ericaceae). The record shows the continuous presence of páramo vegetation since at least 6 Ma. The summed páramo pollen constitutes up to 9% of the total pollen and spore sum, with the highest fraction found at the beginning of the record (6 Ma), and the lowest fractions around 4.23 and 4.59 Ma, at ca. 3.75 Ma and during the late Pleistocene (Figs. 4 and 6).

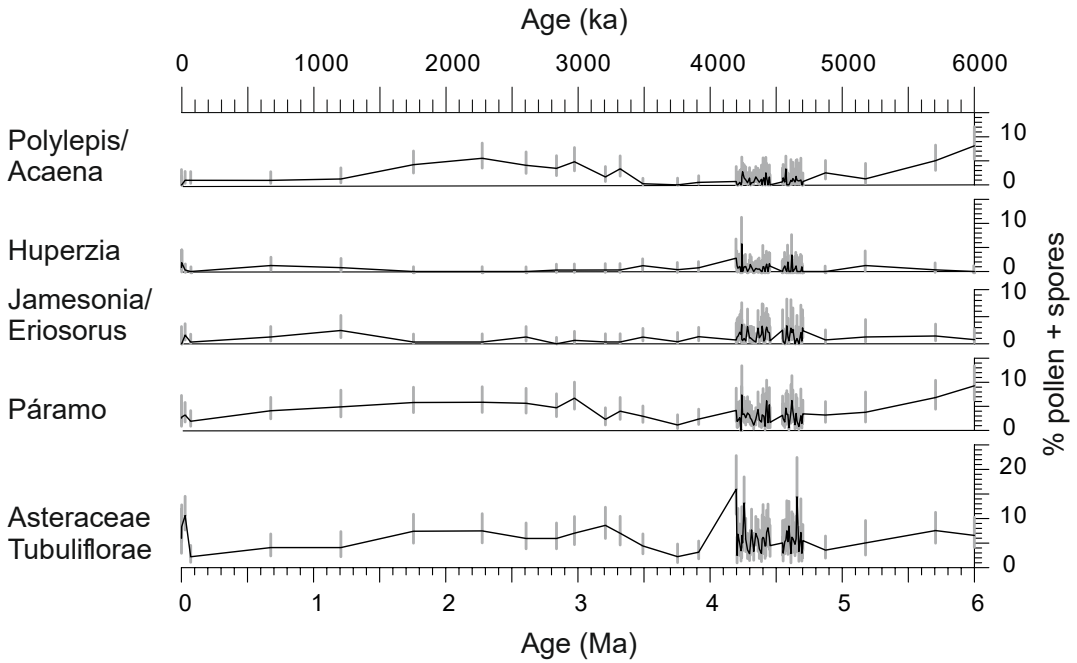

Figure 4.6. Palynomorph percentages of páramo indicators and Asteraceae Tubuliflorae (excluding *Ambrosia/Xanthium* T) of the past 6 Ma indicating the presence of páramo vegetation at least since the late Miocene. 95% confidence intervals (grey bars) after Maher (1972). Ages after Tiedemann et al. (2007) and Mix et al (2003).

4.6 Discussion

4.6.1 Fe/K as a tracer for changes in fluvial runoff

The Fe/K ratio has been shown to be a suitable tracer to distinguish between terrigenous input of slightly weathered material from drier regions and highly weathered material from humid tropical latitudes. Sediments from deeply chemically weathered terrains have higher iron concentrations compared to the more mobile potassium (Mulitza et al. 2008). Before paleoclimatic interpretations can be made based on elemental ratios, other processes which possibly influence the distribution of Fe/K in marine sediments should be examined, like changes of the topography of Andean river

drainage basins, the input of mafic rock material, or diagenetic Fe remobilization (Govin et al. 2012). For northeastern South America it was shown that during the middle Miocene, uplift of the Eastern Andean Cordillera led to changes in the drainage direction of the Orinoco and Magdalena rivers and to the formation of the Amazon River (Hoorn et al. 1995; Hoorn et al. 2010). If a similar temporal history of uplift and changing drainage patterns is assumed for the western Andean Cordillera, the large-scale patterns of the present topography and river drainage basins should have been in place by the early Pliocene. Therefore, the main direction of fluvial transport of Fe should have been similar to today. Diagenetic alteration was shown not to affect Fe concentrations at Site 1239 (Rincón-Martínez 2013). The Fe/K ratio therefore seems to be an adequate tracer of fluvial input at this study site. The trend of Fe/K is similar to the pattern of humidity inferred from the pollen spectrum, showing the highest values around 4.46 Ma, thus supporting the hydrological interpretation of the pollen record.

4.6.2 The Holocene as modern reference

In order to better understand the source areas and transport ways of pollen grains to the sediments, we make a comparison of the results of our two Holocene samples (Fig. S1) with that of another pollen record retrieved from the Carnegie Ridge southeast of ODP Site 1239 (TR 163-38, Fig. 4.2) reflecting rainfall and humidity variation of the late Pleistocene (González et al. 2006). Holocene samples of Site 1239 gave similar results showing extensive open vegetation (indicated by pollen of Poaceae, Cyperaceae, Asteraceae) and maximum relative abundance of fern spores although concentration is low (González et al., 2006). As also indicated by the elemental ratios, fluvial transport of pollen predominates in this area (González et al., 2006; Ríncon-Martínez, 2013). This is understandable, as both ocean currents and wind field do not favor transport from Ecuador to Site 1239 (Fig. 4.2).

Despite the expansion of open vegetation, González, Urrego, and Martínez (2006) interpreted this record to reflect permanently humid conditions, with disturbance processes caused by human occupation and more intense fluvial dynamics. The relatively high percentage of indicators of humid conditions in our core top samples compared to pollen zones III and IV in the early Pliocene would be in agreement with this interpretation. The core top samples from ODP hole 1239B and the most recent part of core TR 163-38 are taken as a basis for the hydrological interpretation of the Pliocene pollen record.

4.6.3 Climatic implications of vegetation change

The presented marine palynological record provides new information on floristic and vegetation changes occurring along diverse ecological and climatic gradients through the early Pliocene. The

consistently high percentage of tree and shrub pollen, compared to a low percentage of herbs and grass pollen (< 25%) suggests the predominance of forests and the nearly absence of open grasslands (apart from páramo) during the early Pliocene. Moreover, the very low percentage of dry indicators (Amaranthaceae) suggests the absence of persisting drought conditions and supports the idea of a rather stable and humid climate that favored a closed forest cover. This is in good accordance with Pliocene climate models suggesting warmer and wetter conditions on most continents, which led to expansions of tropical forests and savannas at the expense of deserts, for instance in Africa (Salzmann et al. 2011). During the early Pliocene, no profound changes in the vegetation occur. All altitudinal vegetation belts are already present, with varying ratios, and only pollen percentages of lowland rainforest rise from almost absent to 6%.

Shifts in the vegetation are driven by various parameters such as temperature, precipitation, CO_2, radiation, and any combination thereof. However, a hint to which parameter has strongest influence on the vegetation might be given by the pattern of expansion and retreat of different vegetation belts. Hooghiemstra and Ran (1994) indicate that if temperature were the dominant driver of vegetation change, altitudinal shifting of vegetation belts would lead to increase in the representation of one at the cost of another. We hardly see such a pattern in our record with the possible exception in zone III where the trends between pollen percentages of páramo and those of upper montane forest (without Podocarpaceae) are reversed (Section 4.3.2; Fig. 4.8). However, the more general pattern indicates parallel changes in the representation of the forest belts suggesting that not temperature but humidity had the stronger effect on the Pliocene vegetation of Ecuador.

4.6.4 Development of the coastal vegetation

Early Pliocene pollen zones I and IV show an expansion of coastal desert herbs (Amaranthaceae, Fig. S1), which coincides with low sea-surface temperatures at ODP Site 846 in the EEP, suggesting an influence of the Peru-Chile Current (continuation of the Humboldt Current) on the coastal vegetation of southern Ecuador. Remarkably, the lowland rainforest and the coastal desert herbs follow a similar trend. This seems odd at the first glance, but a possible mechanism to explain this pattern would invoke effects of El Niño, the warm phase of ENSO. The main transport agent for pollen in this region are rivers, but in the coastal desert area of southern Ecuador and northern Peru, fluvial discharge rates are low (Milliman and Farnsworth 2011). Therefore, pollen might be retained on land until an El Niño event causes severe flooding in the coastal areas (Rodbell et al. 1999) and episodically fills the rivers which transport the pollen to the ocean. Such possible effects of El Niño seem to be strongest in pollen zones I and IV where pollen percentages of the lowland rainforest and coastal desert herbs, but also the upper montane forest, fluctuate most strongly. The

lowland rainforest of the coastal plain of Ecuador and western Colombia is within the present-day range of the ITCZ, and expanded from 4.7 Ma onwards possibly due to a southward displacement of the mean latitude of the ITCZ (Figs. 3 and 4).

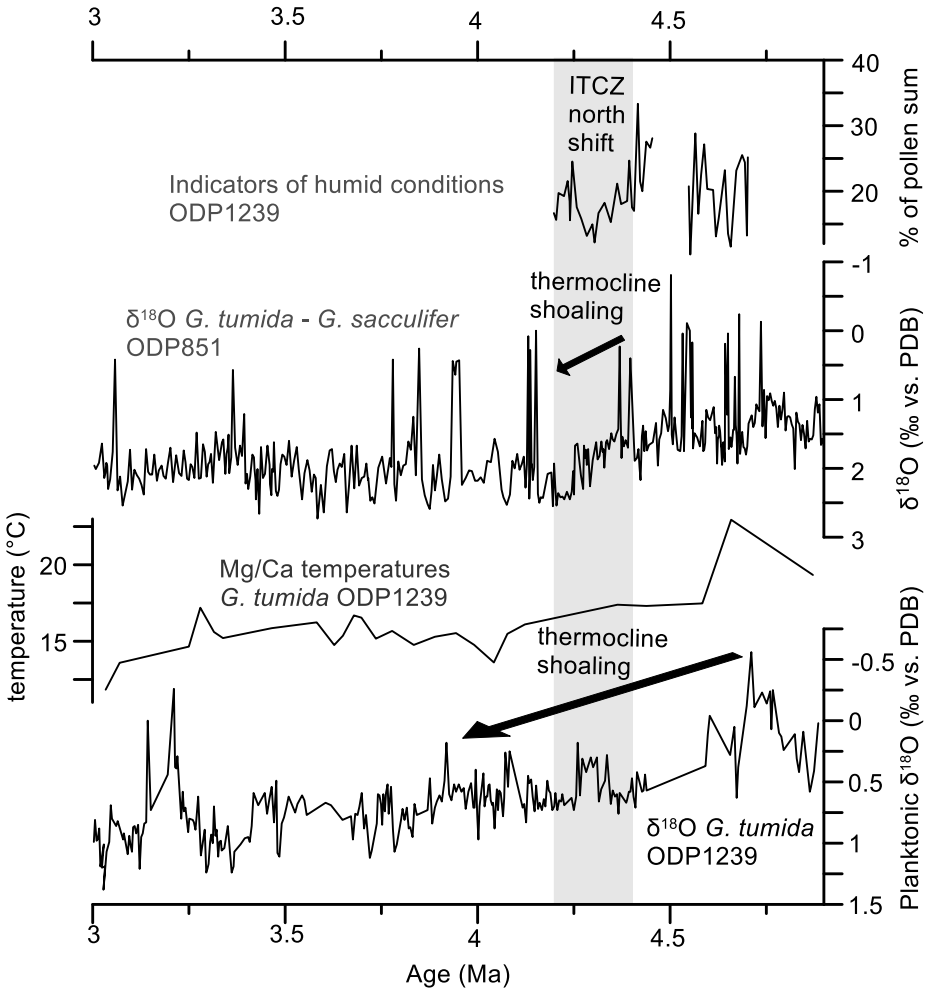

Figure 4.7. Percentages of indicators of humid conditions (ODP Site 1239, this study), *G. tumida* – *G. sacculifer* difference in $\delta^{18}O$ from ODP Site 851 in the eastern equatorial Pacific (Cannariato and Ravelo 1997), and *G. tumida* Mg/Ca temperatures and $\delta^{18}O$ from ODP Site 1239 (Steph 2005; Steph et al. 2010). Grey shading marks the period of thermocline shoaling at ODP Site 851 and ITCZ north shift.

4.6.5 Development of the montane vegetation

Podocarpaceae strongly dominate the pollen spectrum in general. However, the trend in pollen percentages of Podocarpaceae divert from that of the other pollen taxa, which may be explained by additional transport of Podocarpaceae pollen by wind. The high pollen production of Podocarpaceae and their specialized morphology (Regal 1982) facilitate their eolian transport. In contrast, pollen from most other taxa is predominantly fluvially transported (González, Urrego, and Martínez 2006), therefore exhibiting a different pattern where high pollen concentrations correspond to high fluvial discharge in the source area.

Eolian transport of Podocarpaceae explains the high pollen concentrations in pollen zone III, which occur despite less humid conditions compared to pollen zones II and IV. The increased eolian transport at 4.63 Ma and between 4.4 and 4.25 Ma is proposed here to be the result of an intensification of the easterly trade winds. Increase in trade wind strength at 4.4 Ma would be in line with a shift in the locus of maximum opal accumulation rates in the ocean associated with a shift in nutrient availability from ODP Site 850 to ODP Site 846 nearer to the continent (positions shown in Fig. 4.2) (Farrell et al., 1995). Dynamic modelling indicates that stronger easterlies would cause shoaling of the EEP thermocline (Zhang et al. 2012), which took place between 4.8 and 4.0 Ma (Fig. 4.7; Steph et al., 2006a). Related to this process, a critical step of easterly trade wind intensification, indicated by increased eolian transport of Podocarpaceae pollen, occurred between 4.4 and 4.25 Ma.

Comparing the pollen percentages of páramo and upper montane forest, Fig. 4.8 indicates that UMF maxima coincide with páramo minima and SST maxima at ODP Site 846 (Lawrence et al., 2006). This might be explained by a shift of the upper montane forest to higher altitudes at the cost of the area occupied by páramo vegetation as a result of higher atmospheric temperatures and/or increased orographic precipitation in the western Andean Cordillera caused by higher sea-surface temperatures and increased evaporation.

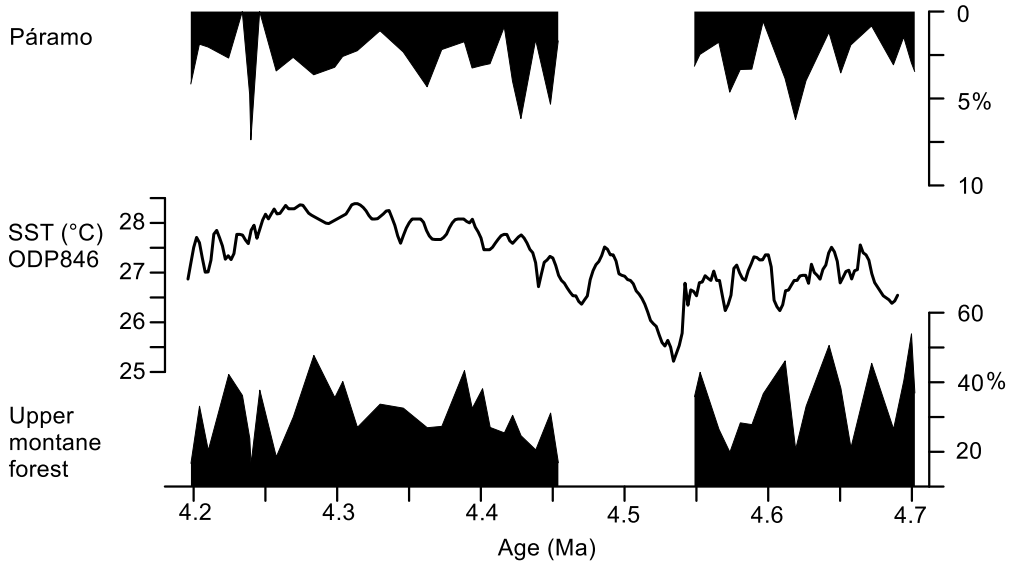

Figure 4.8. Pollen percentages of upper montane forest and páramo, and UK'37 sea-surface temperatures (SST) of ODP site 846 in the eastern equatorial Pacific (Lawrence, Liu, and Herbert 2006).

4.6.6 Development of the páramo and implications for Andean uplift

In order to use the existence of páramo vegetation as an indicator for Andean elevation, the altitudinal restriction of the páramo taxa to environments above the forest line is a prerequisite.

Although no taxa restricted to páramo were identified in the marine samples, or rather, they could not be identified due to the lack of genus-level morphological distinction (especially *Espeletia* from the Asteraceae and some Poaceae, e.g. *Festuca*), several taxa are mainly confined to high Andean environments. Dwarf trees of *Polylepis* typically form patches above the forest line and its natural altitudinal range is thought to occur between a lower limit which forms the transition to other forest types and up to 5000 m in Bolivia (Kessler 2002). *Huperzia* occurs in montane forests as epiphytes and with terrestrial growth form in the páramo (Sklenár, Dusková, and Balslev 2011). *Jamesonia* and *Eriosorus* are both found in cool and wet highlands, with most species being found between 2200 and 5000 m (Sánchez-Baracaldo 2004). Asteraceae are not restricted to the páramo, but their occurrence in the montane forest and in the lowland rainforest of the Pacific coast is scarce (Behling, Hooghiemstra, and Negret 1998). With a contribution of up to 16% of the pollen sum, their source area can be attributed mainly to the páramo. Additionally, the fluctuations are similar to the other páramo taxa (Fig. 4.6), which is another indication for their common source area.

The pollen record shows a continuous existence of páramo vegetation. During the warm Pliocene, the upper montane forest is assumed to have extended to similar or even higher altitudes as today. Despite this upward expansion of the upper montane forest, the páramo was still present, which implies that the western Cordillera of the Ecuadorian Andes had already gone through substantial uplift by that time. Furthermore, the pollen record has a large montane signature, which would not be the case if the Andes had reached less than half of their modern height by the early Pliocene (Coltorti and Ollier 2000). The upper montane forest which constitutes up to 60% of the pollen sum shows that montane habitats with the corresponding altitudinal belts were already existent. These findings suggest an earlier development of the high Andean páramo ecosystem than previously inferred from palynological studies of the eastern Cordillera in Colombia (Van der Hammen, Werner, and van Dommelen 1973; Hooghiemstra, Wijninga, and Cleef 2006). This might also be an indication that the uplift history of the western Cordillera of Ecuador is temporally more closely related to the uplift of the Central Andes where a major phase of uplift occurred between 10 and 6 Ma (Garzione et al. 2008).

In another recent palynological study, the arrival of palynomorphs from the páramo in sediments of the Amazon Fan has been documented since 5.4 Ma (Hoorn et al. 2017). Since the Amazon has its westernmost source in Peru, this signal might be related to the uplift of the Central Andes. These new records agree with paleoclimatic studies showing that modern type precipitation patterns have likely been in place since the middle Miocene (Kaandorp, Wesselingh, and Vonhof 2006; Barnes et al. 2012; Hoorn et al. 2010), which would have required a significant orographic barrier. High

Andean mountains acting as a climate divide might thus go as far back as the Mid-Miocene. However, earliest evidence for a páramo vegetation is now set at latest Miocene.

4.6.7 Comparing models and proxy data

Several studies have suggested the existence of a "permanent El Niño" during the Pliocene (e.g. Wara, Ravelo, and Delaney 2005; Fedorov et al. 2006). El Niño events are characterized by a shift in the Walker circulation, resulting in exceptionally heavy precipitation particularly over the lowlands of central and southern Ecuador (Bendix and Bendix 2006) and simultaneous below-average rainfall over the northwestern slopes of the Andes (Vuille, Bradley, and Keimig 2000). A permanent El Niño-like climate state during the early Pliocene would thus have involved permanently humid conditions with high rates of precipitation and fluvial discharge in the lowlands. Such a climate would have favored the persistence of a broad rain forest coverage and precluded the development of the desert that exists in coastal southern Ecuador today. The presented pollen record indeed indicates very humid conditions and the only indicator of dry vegetation is a small percentage of Amaranthaceae pollen. The predicted pattern of expansion of lowland rainforest at the cost of Andean forest during permanent El Niño is not reflected in the pollen record.

The hypothesis of a permanent El Niño climate state involving a reduced zonal Pacific sea-surface temperature gradient has recently been questioned as sea-surface temperature reconstructions differ substantially depending on the method. Zhang, Pagani, and Liu (2014) claim that a zonal temperature gradient of ca. 3°C existed since the late Miocene and even intensified during the Pliocene. Our pollen record instead indicates an influence of periodic El Niño-related variations on the coastal and montane vegetation, especially between 4.7 and 4.55 Ma and between 4.26 and 4.2 Ma, recorded by strong fluctuations in the pollen percentages of coastal and montane vegetation. Our record does not show increased representation of one vegetation belt at the cost of another indicating that altitudinal shifts were not extensive and moisture availability might have been an important driver of Pliocene vegetation change. Changes in humidity could be caused by a latitudinal displacement of the ITCZ. A southward displacement of the ITCZ over both Atlantic and Pacific has been proposed as a response to stronger zonal temperature and pressure gradients which developed after the restriction of the Central American Seaway and/or a weakening of Southern Hemisphere temperature gradients (Billups et al. 1999). The timing of the southward shift was narrowed down to 4.4 to 4.3 Ma in this study, based on $\delta^{18}O$ records of planktonic foraminifera. The pollen record suggests a slightly different timing, with a gradual southwards displacement of the ITCZ between 4.7 Ma and 4.42 Ma when the southernmost position was reached. A less humid phase, indicated by a decrease of humid indicators, lowland rainforest pollen, lower montane forest pollen, and the Fe/K ratio, followed between 4.42 and 4.26 Ma where the

ITCZ presumably had a slightly more northern position. This phase coincides with the shoaling of the thermocline at ODP Site 851 in the eastern equatorial Pacific (Cannariato and Ravelo 1997, Fig. 4.6). A southward displacement of the ITCZ during the early Pliocene would also be in accordance with eolian deposition patterns in the EEP which show a latitudinal shift in eolian grain-size and eolian flux between 6 and 4 Ma (Hovan 1995). The rather small and slow changes in humidity imply that the ITCZ shift was a gradual process, rather than the response to a single threshold. Just like the Central American Seaway was restricted and reopened several times before its definitive closure at around 2.8 Ma (O'Dea et al. 2016), the atmospheric circulation might have adapted gradually in several small steps to these tectonic changes.

Numerical models suggesting a northward shift of the ITCZ in response to the closure of the Central American Seaway or the uplift of the northern Andes do not necessarily disagree with an early Pliocene southward shift inferred from proxy data. Both events occurred gradually over several millions of years and despite recent advances in constraining these events, the timing of major phases in the uplift histories are still debated. In the case of the Central American Seaway, the timing of surface water restriction based on diverging salinities in the Caribbean and Pacific Ocean, respectively, is well constrained and numerous global oceanographic changes have been associated with it. Possibly these oceanic reorganizations did not directly trigger modifications of the atmospheric circulation (Kaandorp et al., 2006; Hoorn et al., 2010), but critical periods of uplift influencing atmospheric circulation might have occurred earlier. On the other hand, the respective model sensitivity experiments generally only consider isolated changes in single boundary conditions (e.g. closed or open Central American Seaway). Therefore, the effect of those (i.e. a northward shift of the ITCZ) might counteract the general trend of a southward shift since the late Miocene due to a decrease in the hemispheric temperature gradient (e.g. Pettke, Halliday, and Rea 2002). Additionally, global coupled models exhibit uncertainties in the representation of ocean–atmosphere feedback and cloud–radiation feedbacks, which are especially strong in the study region (i.e. showing a double ITCZ and an extensive EEP cold tongue (Li and Xie 2014)). This is problematic also in the light of the high sensitivity of the ITCZ position to slight shifts in the atmospheric energy balance (Schneider, Bischoff, and Haug 2014). Another aspect to consider is that whereas proxy records record the transient response of the climate system over a limited period of time, the mentioned model simulations rather follow the overall equilibrium response than reproducing a stepwise process of environmental changes.

Concerning the uplift of the northern Andes, there is still a large uncertainty about the time when the Cordilleras reached their current elevation. Moreover, phases of major uplift might have strongly differed regionally. Paleobotanists (e.g. Hooghiemstra, Wijninga, and Cleef 2006; Hoorn et al. 2010; Van der Hammen, Werner, and van Dommelen 1973) and some tectonic geologists

(e.g. Mora et al. 2008) argued for a rapid rise of the Eastern Cordillera since 4–6 Ma, while others conclude that this is rather unlikely implying an earlier uplift based on biomarker-based paleotemperatures (e.g. Anderson et al. 2015; Mora-Páez et al. 2016). Possibly the Pliocene oceanic reorganizations did not directly trigger modifications of the atmospheric circulation, which probably was more or less in place (Kaandorp et al., 2006; Hoorn et al., 2010). Critical periods of uplift influencing atmospheric circulation might have occurred earlier (see also above). The estimates for uplift of the western Cordillera in Ecuador differ even more strongly, and range from rapid exhumation around 13 and 9 Ma based on thermochronology (Spikings et al. 2005) to a recent uplift during the Pliocene and Pleistocene (Coltorti and Ollier 2000). Our pollen record from the páramo shows that the Ecuadorian Andes must have already reached close to modern elevations by the early Pliocene in line with inferences of Hoorn et al. (2017) and Bermúdez et al. (2015). If an early Andean uplift is assumed, the atmospheric response predicted by the model would have occurred earlier, which would also be in agreement with proxy data indicating a northern position of the ITCZ during the late Miocene (Hovan 1995).

Overall, even if the timing and identification of major steps in the shoaling and restriction of the Central American Seaway or in the uplift of the northern Andes are resolved, the critical threshold for profound changes in atmospheric circulation and climate may have occurred at any time during the tectonic processes. Within the analyzed time window, large changes in atmospheric circulation which have been proposed as a response to the closure of the Central American Seaway (Ravelo et al. 2004) are absent.

4.7 Conclusions

1) Between 4.7 and 4.2 Ma, a permanently humid climate with broad rainforest coverage existed in western equatorial South America. No evidence was found for a permanent El Niño-like climate state, but strong fluctuations in the vegetation between 4.7 and 4.55 Ma and between 4.26 and 4.2 Ma indicate strong periodic El Niño variability at this time. Hydrological changes between 4.55 and 4.26 Ma are attributed to gradual shifts of the Intertropical Convergence Zone which reached its southernmost position around 4.42 Ma and shifted slightly north afterwards.
2) The most prominent shift recorded during the early Pliocene is an increase in the representation of the lowland rainforest around 4.5 Ma.
3) Between 4.41 and 4.26 Ma, an increased eolian influx of Podocarpaceae pollen indicates an increased strength of the easterly trade winds, which is presumably related to the shoaling of the EEP thermocline.

4) Results from proxy data and numerical modelling studies regarding the position of the ITCZ during the early Pliocene are not necessarily contradictory. Considering the temporal uncertainties regarding major steps of CAS closure and uplift of the northern Andes, the proposed northward shift of the ITCZ in response to these events might have occurred much earlier (e.g. during the middle to late Miocene).
5) The continuous presence of páramo vegetation since 6 Ma implies that the Ecuadorian Andes had already reached an elevation suitable for the development of vegetation above the upper forest line by the latest Miocene. We present new paleobotanical evidence indicating an earlier development of páramo vegetation than previously suggested by terrestrial paleobotanical records.

Data availability

The underlying research data are stored in PANGAEA as datasets PANGAEA.884280, PANGAEA.891294 and PANGAEA.884153, which are combined in PANGAEA.884285 <https://doi.pangaea.de/10.1594/PANGAEA.884285>.

Author contribution

L. Dupont and F. Grimmer conceived the idea, and L. Dupont, F. Grimmer and F. Lamy carried out the analyses. F. Grimmer prepared the manuscript with contributions from all co-authors.

Acknowledgements

We thank Carina Hoorn, Jun Tian, Henry Hooghiemstra & Suzette Flantua and an anonymous referee for their insightful comments on the original manuscript. This project was funded by the Deutsche Forschungsgemeinschaft (DFG) through the TROPSAP project (DU221/6) and via the DFG Research Center / Cluster of Excellence "The Ocean in the Earth System — MARUM". The first author thanks GLOMAR – Bremen International Graduate School for Marine Sciences, University of Bremen, Germany, for support. The IODP Gulf Coast Repository (GCR) we acknowledge for their assistance in providing the core samples.

4.8 References

Anderson, V. J., Saylor, J. E., Shanahan, T. M., and Horton, B. K.: Paleoelevation records from lipid biomarkers: Application to the tropical Andes, Geological Society of America Bulletin, 127, 1604-1616, 2015.

Balslev, H.: Distribution Patterns of Ecuadorean Plant-Species, Taxon, 37, 567-577, 1988.

Barnes, J. B., Ehlers, T. A., Insel, N., McQuarrie, N., and Poulsen, C. J.: Linking orography, climate, and exhumation across the central Andes, Geology, 40, 1135-1138, 2012.

Bartoli, G., Sarnthein, M., Weinelt, M., Erlenkeuser, H., Garbe-Schönberg, D., and Lea, D. W.: Final closure of Panama and the onset of northern hemisphere glaciation, Earth and Planetary Science Letters, 237, 33-44, 2005.

Behling, H., Hooghiemstra, H., and Negret, A. J.: Holocene history of the Choco Rain Forest from Laguna Piusbi, Southern Pacific Lowlands of Colombia, Quaternary Research, 50, 300-308, 1998.

Bendix, A. and Bendix, J.: Heavy rainfall episodes in Ecuador during El Nino events and associated regional atmospheric circulation and SST patterns, Advances in Geosciences, 6, 43-49, 2006.

Bendix, J. and Lauer, W.: Die Niederschlagsjahreszeiten in Ecuador und ihre klimadynamische Interpretation, Erdkunde, 46, 118-134, 1992.

Billups, K., Ravelo, A. C., Zachos, J. C., and Norris, R. D.: Link between oceanic heat transport, thermohaline circulation, and the Intertropical Convergence Zone in the early Pliocene Atlantic, Geology, 24, 319-322, 1999.

Bush, M. B. and Weng, C.: Introducing a new (freeware) tool for palynology, Journal of Biogeography, 34, 377-380, 2007.

Cannariato, K. G. and Ravelo, A. C.: Pliocene-Pleistocene evolution of eastern tropical Pacific surface water circulation and thermocline depth, Paleoceanography, 12, 805-820, 1997.

Colinvaux, P., De Oliveira, P. E., and Moreno Patino, J. E.: Amazon Pollen Manual and Atlas, Harwood Academic Publishers, Amsterdam, 1999.

Coltorti, M. and Ollier, C. D.: Geomorphic and tectonic Evolution of the Ecuadorian Andes, Geomorphology, 32, 1-19, 2000.

Corredor, F.: Eastward extent of the Late Eocene-Early Oligocene onset of deformation across the northern Andes: constraints from the northern portion of the Eastern Cordillera fold belt, Colombia, Journal of South American Earth Sciences, 16, 445-457, 2003.

CPC Merged Analysis of Precipitation: https://www.esrl.noaa.gov/psd/data/gridded/data.ncep.reanalysis.derived.html, last access: February 2008.

ETOPO1: https://maps.ngdc.noaa.gov/viewers/wcs-client/, last access: June 2018.

Fedorov, A. V., Dekens, P. S., McCarthy, M., Ravelo, A. C., deMenocal, P. B., Barreiro, M., Pacanowski, R. C., and Philander, S. G.: The Pliocene paradox (mechanisms for a permanent El Nino), Science, 312, 1485-1489, 2006.

Feng and Poulsen, C. J.: Andean elevation control on tropical Pacific climate and ENSO, Paleoceanography, 29, 795–809, 2014.

Flantua, S., Hooghiemstra, H., Van Boxel, J. H., Cabrera, M., González-Carranza, Z., and González-Arango, C.: Connectivity dynamics since the last glacial maximum in the northern Andes: a pollen-driven framework to assess potential migration. In: Paleobotany

and Biogeography: A Festschrift for Alan Graham in His 80th Year, W. D. Stevens, O. M. M., P. H. Raven (Ed.), Missouri Botanical Garden Press, St. Louis, 2014.

Flohn, H.: A hemispheric circulation asymmetry during Late Tertiary, Geologische Rundschau, 70, 725-736, 1981.

Garzione, C. N., Hoke, G. D., Libarkin, J. C., Withers, S., MacFadden, B., Eiler, J., Ghosh, P., and Mulch, A.: Rise of the Andes, Science, 320, 1304-1307, 2008.

Gentry, A. H.: Species richness and floristic composition of Chocó region plant communities, Caldasia, 15, 71-91, 1986.

González, C., Urrego, L. E., and Martínez, J. I.: Late Quaternary vegetation and climate change in the Panama Basin: Palynological evidence from marine cores ODP 677B and TR 163-38, Palaeogeography, Palaeoclimatology, Palaeoecology, 234, 62-80, 2006.

Govin, A., Holzwarth, U., Heslop, D., Ford Keeling, L., Zabel, M., Mulitza, S., Collins, J. A., and Chiessi, C. M.: Distribution of major elements in Atlantic surface sediments (36°N-49°S): Imprint of terrigenous input and continental weathering, Geochemistry, Geophysics, Geosystems, 13, 2012.

Gregory-Wodzicki, K. M.: Uplift history of the Central and Northern Andes: A review, Geological Society of America Bulletin, 112, 1091-1105, 2000.

Grimm, E.: Tilia and Tiliagraph. Illinois State Museum, Springfield, 1991.

Groeneveld, J., Hathorne, E. C., Steinke, S., DeBey, H., Mackensen, A., and Tiedemann, R.: Glacial induced closure of the Panamanian Gateway during Marine Isotope Stages (MIS) 95–100, Earth and Planetary Science Letters, 404, 296-306, 2014.

Haug, G. H. and Tiedemann, R.: Effect of the formation of the Isthmus of Panama on Atlantic Ocean thermohaline circulation, Nature, 393, 673-676, 1998.

Haug, G. H., Tiedemann, R., Zahn, R., and Ravelo, A. C.: Role of Panama uplift on oceanic freshwater balance, Geology, 29, 207-210, 2001.

Hooghiemstra, H.: Vegetational and Climatic History of the High Plain of Bogotá, Colombia: A Continuous Record of the Last 3.5 Million Years, A.R. Gantner Verlag K.G., Vaduz, 1984.

Hooghiemstra, H., Wijninga, V. M., and Cleef, A. M.: The Paleobotanical Record of Colombia: Implications for Biogeography and Biodiversity, Annals of the Missouri Botanical Garden, 93, 297-325, 2006.

Hoorn, C.: Andean tectonics as a cause for changing drainage patterns in Miocene northern South America, Geology, 23, 237-240, 1995.

Hoorn, C., Bogotá-A., G. R., Romero-Baez, M., Lammertsma, E. I., Flantua, S., Dantas, E. L., Dino, R., do Carmo, D. A., and Chemale Jr, F.: The Amazon at sea: Onset and stages of the Amazon River from a marine record, with special reference to Neogene plant turnover in the drainage basin, Global and Planetary Change, 153, 51-65, 2017.

Hoorn, C. and Flantua, S.: An early start for the Panama land bridge, Science, 348, 186-187, 2015.

Hoorn, C., Wesselingh, F. P., ter Steege, H., Bermudez, M. A., Mora, A., Sevink, J., Sanmartin, I., Sanchez-Meseguer, A., Anderson, C. L., Figueiredo, J. P., Jaramillo, C., Riff, D., Negri, F. R., Hooghiemstra, H., Lundberg, J., Stadler, T., Sarkinen, T., and Antonelli, A.: Amazonia through time: Andean uplift, climate change, landscape evolution, and biodiversity, Science, 330, 927-931, 2010.

Hovan, S. A.: Late Cenozoic Atmospheric Circulation Intensity and climatic history recorded by eolian deposition in the eastern equatorial pacific ocean, Leg 138, Proceedings of the Ocean Drilling Program, Scientific Results, 138, 615-625, 1995.

Jørgensen, P. M. and León-Yánez, S.: Catalogue of the vascular plants of Ecuador = Catálogo de las plantas vasculares del Ecuador, Missouri Botanical Garden Press, St. Louis, Missouri, 1999.

Kaandorp, R. J. G., Wesselingh, F. P., and Vonhof, H. B.: Ecological implications from geochemical records of Miocene Western Amazonian bivalves, Journal of South American Earth Sciences, 21, 54-74, 2006.

Kessler, M.: The "Polylepis problem": Where do we stand?, Ecotropica, 8, 97-110, 2002.

Lawrence, K. T., Liu, Z., and Herbert, T. D.: Evolution of the eastern tropical Pacific through Plio-Pleistocene glaciation, Science, 312, 79-83, 2006.

Li, G. and Xie, S. P.: Tropical Biases in CMIP5 Multimodel Ensemble: The Excessive Equatorial Pacific Cold Tongue and Double ITCZ Problems, Journal of Climate, 27, 1765-1780, 2014.

Luteyn, J. L.: Páramos, Memoirs of The New York Botanical Garden, 1999.

Maher, L. J.: Nomograms for computing 0.95 confidence limits of pollen data, Review of Palaeobotany and Palynology, 13, 85-93, 1972.

Marchant, R., Almeida, L., Behling, H., Berrio, J. C., Bush, M., Cleef, A., Duivenvoorden, J., Kappelle, M., De Oliveira, P., Teixeira de Oliveira-Filho, A., Lozano-Garcia, S., Hooghiemstra, H., Ledru, M.-P., Ludlow-Wiechers, B., Markgraf, V., Mancini, V., Paez, M., Prieto, A., Rangel, O., and Salgado-Labouriau, M.: Distribution and ecology of parent taxa of pollen lodged within the Latin American Pollen Database, Review of Palaeobotany and Palynology, 121, 1-75, 2002.

Marchant, R., Behling, H., Berrio, J. C., Cleef, A., Duuivenvoorden, J., Hooghiemstra, H., Kuhry, P., Melief, B., Van Geel, B., Van der Hammen, T., Van Reenen, G., and Wille, M.: Mid- to Late-Holocene pollen-based biome reconstructions for Colombia, Quaternary Science Reviews, 20, 1289-1308, 2001.

Milliman, J. D. and Farnsworth, K. L.: River discharge to the coastal ocean: a global synthesis, Cambridge University Press, Cambridge; New York, 2011.

Mix, A., Tiedemann, R., and Blum, P.: Proceedings of the Ocean Drilling Program, Initial Reports, 202, 2003.

Montes, C., Cardona, A., Jaramillo, C., Pardo, A., Silva, J. C., Valencia, V., Ayala, C., Pérez-Angel, L. C., Rondriguez-Parra, L. A., Ramirez, V., and Nino, H.: Middle Miocene closure of the Central American Seaway, Paleoceanography, 348, 226-229, 2015.

Mora-Páez, H., Mencin, D. J., Molnar, P., Diederix, H., Cardona-Piedrahita, L., Peláez-Gaviria, J.-R., and Corchuelo-Cuervo, Y.: GPS velocities and the construction of the Eastern Cordillera of the Colombian Andes, Geophysical Research Letters, 43, 8407-8416, 2016.

Mora, A., Parra, M., Strecker, M. R., Sobel, E. R., Hooghiemstra, H., Torres, V., and Jaramillo, J. V.: Climatic forcing of asymmetric orogenic evolution in the Eastern Cordillera of Colombia, GSA Bulletin, 120, 930-949, 2008.

Mulitza, S., Prange, M., Stuut, J. B., Zabel, M., von Dobeneck, T., Itambi, A. C., Nizou, J., Schulz, M., and Wefer, G.: Sahel megadroughts triggered by glacial slowdowns of Atlantic meridional overturning, Paleoceanography, 23, 2008.

Murillo, M. T. and Bless, M. J. M.: Spores of recent Colombian Pteridophyta. I. Trilete Spores, Review of Palaeobotany and Palynology, 18, 223-269, 1974.

Murillo, M. T. and Bless, M. J. M.: Spores of recent Colombian Pteridophyta. II. Monolete Spores, Review of Palaeobotany and Palynology, 25, 319-365, 1978.

NCEP reanalysis data provided by the NOAA/OAR/ESRL PSD, B., Colorado, USA,: http://www.esrl.noaa.gov/psd/data/gridded/data.ncep.reanalysis.derived.html last access: January 2010.

Niemann, H., Brunschön, C., and Behling, H.: Vegetation/modern pollen rain relationship along an altitudinal transect between 1920 and 3185ma.s.l. in the Podocarpus National Park region, southeastern Ecuadorian Andes, Review of Palaeobotany and Palynology, 159, 69-80, 2010.

NODC (Levitus) World Ocean Atlas: http://www.esrl.noaa.gov/psd/data/gridded/data.nodc.woa94.html, last access: March 2010, 1994.

O'Dea, A., Lessios, A. H., Coates, A. G., Eytan, R. I., Restrepo-Moreno, S. A., Cione, A. L., Collins, L. S., de Queiroz, A., Farris, D. W., Norris, R. D., Stallard, R. F., Woodburne, M. O., Aguilera, O., Aubry, M.-P., Berggren, W. A., Budd, A. F., Cozzuol, M. A., Coppard, S. E., Duque-Caro, H., Finnegan, S., Gasparini, G. M., Grossman, E. L., Johnson, K. G., Keigwin, L. D., Knowlton, N., Leigh, E. G., Leonard-Pingel, J. S., Marko, P. B., Pyenson, N. D., Rachello-Dolmen, P. G., Soibelzon, E., Soibelzon, L., Todd, J. A., Vermeij, G. J., and Jackson, J. B. C.: Formation of the Isthmus of Panama, Science Advances, 2, 2016.

Pak, H. and Zaneveld, J. R.: Equatorial Front in the Eastern Pacific Ocean, J Phys Oceanogr, 4, 570-578, 1974.

Pettke, T., Halliday, A. N., and Rea, D. K.: Cenozoic evolution of Asian climate and sources of Pacific seawater Pb and Nd derived from eolian dust of sediment core LL44-GPC3, Paleoceanography, 17, 2002.

Pisias, N.: Paleoceanography of the eastern equatorial Pacific during the Neogene: Synthesis of Leg 138 drilling results, Proceedings of the Ocean Drilling Program, Scientific Results, 138, 5-21, 1995.

Ravelo, A. C., Andreasen, D. H., Lyle, M. W., Lyle, A. O., and Wara, M. W.: Regional climate shifts caused by gradual global cooling in the Pliocene epoch, Nature, 429, 2004.

Regal, P. J.: Pollination by Wind and Animals: Ecology of Geographic Patterns, Annual Review of Ecology and Systematics, 13, 497-524, 1982.

Richter, T. O., van der Gaast, S., Koster, B., Vaars, A., Gieles, R., de Stigter, H. C., de Haas, H., and van Weering, T. C. E.: The Avaatech XRF Core Scanner: Technical description and applications to NE Atlantic sediments. In: New Techniques in Sediment Core Analysis, Rothwell, R. G. (Ed.), Geological Society, London, Special Publications, 2006.

Rincón-Martínez, D.: Eastern Pacific background state and tropical South American climate history during the last 3 million years, 2013. Fachbereich Geowissenschaften, Universität Bremen, Bremen, 2013.

Rincón-Martínez, D., Lamy, F., Contreras, S., Leduc, G., Bard, E., Saukel, C., Blanz, T., Mackensen, A., and Tiedemann, R.: More humid interglacials in Ecuador during the past 500 kyr linked to latitudinal shifts of the equatorial front and the Intertropical Convergence Zone in the eastern tropical Pacific, Paleoceanography, 25, 2010.

Rodbell, D. T., Seltzer, G. O., Anderson, D. M., Abbott, M. B., Enfield, D. B., and Newman, J. H.: An ~15,000-year record of El Nino-driven alluviation in southwestern Ecuador, Science, 283, 516-520, 1999.

Roubik, D. W. and Moreno, P.: Pollen and spores of Barro Colorado Island, Monographs in systematic botany from the Missouri Botanical Garden, 36, 1991.

Salzmann, U., Williams, M., Haywood, A. M., Johnson, A. L. A., Kender, S., and Zalasiewicz, J.: Climate and environment of a Pliocene warm world, Palaeogeography, Palaeoclimatology, Palaeoecology, 309, 1-8, 2011.

Sánchez-Baracaldo, P.: Phylogenetics and biogeography of the neotropical fern genera Jamesonia and Eriosorus (Pteridaceae), American Journal of Botany, 91, 274-284, 2004.

Schneider, T., Bischoff, T., and Haug, G. H.: Migrations and dynamics of the intertropical convergence zone, Nature, 513, 45-53, 2014.

Seilles, B., Goni, M. F. S., Ledru, M. P., Urrego, D. H., Martinez, P., Hanquiez, V., and Schneider, R.: Holocene land-sea climatic links on the equatorial Pacific coast (Bay of Guayaquil, Ecuador), The Holocene, 26, 567-577, 2016.

Sklenár, P., Dusková, E., and Balslev, H.: Tropical and Temperate: Evolutionary History of Páramo Flora, Bot Rev, 77, 71-108, 2011.

Sklenár, P. and Jorgensen, P. M.: Distribution patterns of Páramo Plants in Ecuador, Journal of Biogeography, 26, 681-691, 1999.

Spikings, R. A., Winkler, W., Hughes, R. A., and Handler, R.: Thermochronology of allochthonous terranes in Ecuador: Unravelling the accretionary and post-accretionary history of the Northern Andes, Tectonophysics, 399, 195-220, 2005.

Steph, S.: Pliocene stratigraphy and the impact of Panama uplift on changes in Caribbean and tropical east Pacific upper ocean stratification, 2005. Mathematisch-Naturwissenschaftliche Fakultät, Christian-Albrechts-Universität Kiel, Kiel, 2005.

Steph, S., Tiedemann, R., Groeneveld, J., Sturm, A., and Nürnberg, D.: Pliocene Changes in Tropical East Pacific Upper Ocean Stratification: Response to Tropical Gateways?, Proceedings of the Ocean Drilling Program, Scientific Results, 202, 2006a.

Steph, S., Tiedemann, R., Prange, M., Groeneveld, J., Nurnberg, D., Reuning, L., Schulz, M., and Haug, G. H.: Changes in Caribbean surface hydrography during the Pliocene shoaling of the Central American Seaway, Paleoceanography, 21, 2006b.

Steph, S., Tiedemann, R., Prange, M., Groeneveld, J., Schulz, M., Timmermann, A., Nürnberg, D., Rühlemann, C., Saukel, C., and Haug, G. H.: Early Pliocene increase in thermohaline overturning: A precondition for the development of the modern equatorial Pacific cold tongue, Paleoceanography, 25, 2010.

Takahashi, K. and Battisti, D. S.: Processes Controlling the Mean Tropical Pacific Precipitation Pattern. Part I: The Andes and the Eastern Pacific ITCZ, Journal of Climate, 20, 3434-3451, 2007.

Tiedemann, R., Sturm, A., Steph, S., Lund, S. P., and Stoner, J. S.: Astronomically calibrated timescales from 6 to 2.5 Ma and benthic isotope stratigraphies, sites 1236, 1237, 1239, and 1241, Proceedings of the Ocean Drilling Program, Scientific Results, 202, 2007.

Tjallingii, R., Röhl, U., Kölling, M., and Bickert, T.: Influence of the water content on X-ray fluorescence core-scanning measurements in soft marine sediments, Geochemistry, Geophysics, Geosystems, 8, 2007.

Twilley, R. R., Cárdenas, W., Rivera-Monroy, V. H., Espinoza, J., Suescum, R., Armijos, M. M., and Solórzano, L.: The Gulf of Guayaquil and the Guayas River Estuary, Ecuador. In: Coastal Marine Ecosystems of Latin America, Seeliger, U. and Kjerfve, B. (Eds.), Springer, Heidelberg, 2001.

Van der Hammen, T.: The Pleistocene Changes of Vegetation and Climate in Tropical South America, Journal of Biogeography, 1, 3-26, 1974.

Van der Hammen, T., Werner, J. H., and van Dommelen, H.: Palynological record of the upheaval of the Northern Andes: a study of the Pliocene and Lower Quaternary of the Colombian early evolution of its high-Andean biota, Review of Palaeobotany and Palynology, 16, 1-122, 1973.

Vuille, M., Bradley, R. S., and Keimig, F.: Climate variability in the Andes of Ecuador and its relation to tropical Pacific and Atlantic Sea surface temperature anomalies, Journal of Climate, 13, 2520-2535, 2000.

Wara, M. W., Ravelo, A. C., and Delaney, M. L.: Permanent El Nino-like conditions during the Pliocene warm period, Science, 309, 758-761, 2005.

World Wildlife Fund (WWF): https://www.worldwildlife.org/ecoregions/ last access: October 2017.

Zhang, X., Prange, M., Steph, S., Butzin, M., Krebs, U., Lunt, D. J., Nisancioglu, K. H., Park, W., Schmittner, A., Schneider, B., and Schulz, M.: Changes in equatorial Pacific thermocline depth in response to Panamanian seaway closure: Insights from a multi-model study, Earth and Planetary Science Letters, 2012. 76-84, 2012.

Zhang, Y. G., Pagani, M., and Liu, Z.: A 12-million-year temperature history of the tropical Pacific Ocean, Science, 344, 84-87, 2014.

5 Piacenzian environmental change and the onset of cool and dry conditions in tropical South America

Friederike Grimmer[1], Lydie Dupont[1], Gerlinde Jung[1], and Gerold Wefer[1]

[1]MARUM – Center for Marine Environmental Sciences, University of Bremen, Leobener Str. 8, 28359 Bremen, Germany

Published as: Grimmer, F., L. M. Dupont, G. D. Jung, and G. Wefer. 2020. 'Piacenzian Environmental Change and the Onset of Cool and Dry Conditions in Tropical South America', *Paleoceanography and Paleoclimatology*, 35. https://doi.org/10.1029/2020PA004060

5.1 Abstract

The Piacenzian (3.60 – 2.58 Ma) covers the last stage of the Neogene just before the Earth's climate turned from relatively stable warm conditions to the cooler climate with high amplitude glacial-interglacial oscillations of the Pleistocene. Even during this period early fluctuations towards cooler conditions occurred and sea surface temperature (SST) reconstructions show stepwise increasing gradients. The zonal Pacific SST gradient which indicates the strength of the Walker Circulation appears to have increased in two steps starting in the Piacenzian. We investigated vegetation and climate change in western equatorial South America under influence of the Walker Circulation and to detect signs for the onset of cooling in the tropics. We studied vegetation changes in western Ecuador using palynological analysis of 88 sediment samples from marine Ocean Drilling Program Site 1239 dated between 3.9 and 2.7 Ma. A general trend towards more open vegetation is observed. The climate changes towards cooler conditions, which is manifested by a lowering of the forest line from 3.3 Ma on. Increase of Amaranthaceae pollen after 3.1 Ma suggests drier conditions along the coast. A comparison with mid-Piacenzian warm period (mPWP) modeling shows that data and models agree regarding a drier coastal climate during the mPWP. The isochronous occurrence of environmental changes in the presented record, i.e. cooling and coastal drying, with the first major pulse of ice-rafted debris and cooling temperatures in the Northern Hemisphere (between 3.28 and 3.31 Ma) suggests that these changes might have been a precursor of the intensification of Northern Hemisphere glaciation.

5.2 Plain language summary

Around 3.6 to 2.6 million years ago was a time in Earth's history when many conditions were similar to today like the arrangement of the continents, vegetation, and greenhouse gas concentrations. However, the Arctic was not yet covered by ice sheets and the global climate was warmer, making this time period well suited to study the drivers and mechanisms of warm climates.

Towards the end of this period, global climate started to cool which is known mainly from Northern Hemisphere climate reconstructions. We wanted to find out if cooling and drying conditions found in other records also occurred in the South American tropics. Fossil pollen assemblages preserved in marine sediments can tell us which plants grew in our study area (broadly western Ecuador). Since plants have different (known) climatic requirements, we can reconstruct past rainfall and temperatures as well. We find cooling and drying of Neotropical climate, possibly linked to the period preceding the intensification of the Northern Hemisphere glaciations. However, the observed pattern of climatic change does not favor a strengthening of the atmospheric circulation at that time, as proposed in earlier studies. Studying past climates can help us to better understand and constrain present and future climate developments.

5.3 Introduction

Warm climate states in Earth's history are the target of many studies due to their potential to serve as an analogue for future climate change. The Piacenzian (3.60 – 2.58 Ma) is of particular interest because it is the most recent period of sustained warmth when most geological boundary conditions were similar to today, including the configuration of the continents, atmospheric CO_2 concentration, and flora and fauna (Haywood, Dowsett, and Dolan 2016; Dowsett, Barron, and Poore 1996). Piacenzian mean global temperatures were substantially higher than pre-industrial temperatures. While the tropics were similar to today, high-latitude air temperatures were ~7 °C warmer at 70° S and ~10 °C warmer at 80° N (Rickaby and Halloran 2005; Contoux, Ramstein, and Jost 2012). As early as 3.6 Ma, a gradual increase in mean global ice volume began leading ultimately to the Northern Hemisphere glaciation (Mudelsee and Raymo 2005).

The climate in western tropical South America is strongly influenced by sea surface temperatures (SST) of the Pacific and the central Pacific SST gradient. SST records show a development of the Eastern Equatorial Pacific (EEP) cold tongue at least as early as 3.6 – 3.5 Ma (Steph et al. 2010; Lawrence, Liu, and Herbert 2006). Between ~ 3.6 and 3.2 Ma, the zonal SST gradient between the western Pacific warm pool and the EEP cold tongue markedly increased (between Ocean Drilling Program (ODP) Site 806 and ODP Site 846; Fig. 5.1). After 3.2 Ma, eastern and western Pacific SSTs approached each other again until ~ 2.3 Ma (Fedorov et al. 2015). The increased zonal SST gradient would have strengthened the Walker circulation implying that during the (early) Pliocene a weaker Walker Circulation resulted in more and stronger El-Niño conditions (Wara, Ravelo, and Delaney 2005), a state also called El Padre (Ford et al. 2015). A strengthened Walker Circulation would become manifest in western Ecuadorean climate not only in the decadal variability but also in the long-term changes. Less precipitation over western Ecuador is expected when the strengthening of the Walker Circulation causes the average latitudinal position of the Intertropical

Convergence Zone (ITCZ) to shift northwards (Perez-Angel and Molnar 2017). At 2.6 Ma also the meridional SST gradient increased with the intensification of the Northern Hemisphere ice sheets (Brierley et al. 2009; Fig. 5.1).

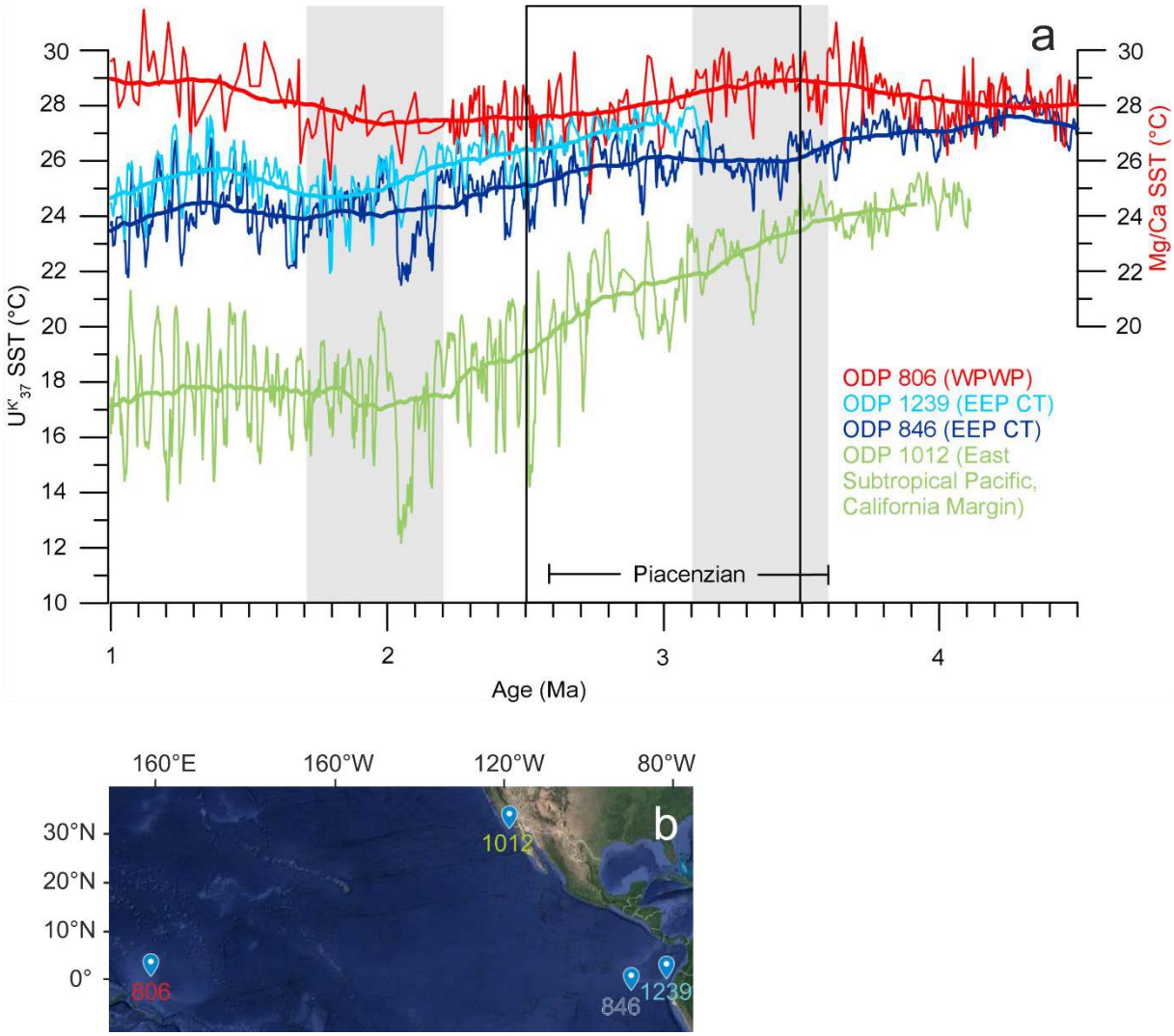

Figure 5.1. a) Pacific sea surface temperature reconstructions from 4.5 to 1 Ma (Brierley et al. 2009; Etourneau et al. 2010; Lawrence, Liu, and Herbert 2006; Wara, Ravelo, and Delaney 2005). Long-term trends are displayed as 400 ka running means for ODP Sites 846, 1239, and 1012, and as 600 ka running mean for ODP Site 806, respectively. The zonal gradient increased in two steps between 3.6 Ma and 1.7 Ma (grey shading) and the meridional gradient increased from 3.5 to 2.5 Ma (black box). WPWP = Western Pacific Warm Pool, EEP CT = Eastern Equatorial Pacific Cold Tongue. b) Locations of ODP Sites shown in panel a.

A need for paleoclimate and paleovegetation records especially from South America of the mid-Piacenzian has been indicated by the PRISM4 group (Dowsett et al. 2016) to improve global land surface reconstructions. The mid-Piacenzian warm period (mPWP) is a target modeling interval for understanding mechanisms and feedbacks that sustained such a warm climate. Several studies

are available modeling mPWP climate (Contoux, Ramstein, and Jost 2012), the atmospheric Hadley and Walker circulations (Kamae, Ueda, and Kitoh 2011), and the orbitally-forced interglacial climate variability and vegetation response (Prescott et al. 2014; Prescott et al. 2018). While several proxy records document vegetation change and gradual cooling of high latitude climate in the Northern Hemisphere after ~ 3.5 Ma (e. g. Andreev et al. 2014; Brigham-Grette et al. 2013; Demske, Mohr, and Oberhansli 2002; Panitz et al. 2016), reconstructions of Pliocene vegetation and terrestrial climate in the low latitudes are rare (e. g. Dupont 2006; Vallé et al. 2014; Hooghiemstra and Ran 1994a). Several pollen studies from Colombia exist for the mid-Pliocene (Wijninga and Kuhry 1990; Wijninga 1996b; Van der Hammen, Werner, and van Dommelen 1973; Hooghiemstra 1989; Hooghiemstra, Wijninga, and Cleef 2006). However, these records cover mainly the Andes and not the lowlands, which also should be considered inferring changes in atmospheric circulation. While precipitation is the critical climatic factor in the lowlands (Vuille, Bradley, and Keimig 2000), the altitudinal vegetation belts in the Andes are also strongly temperature-dependent (Hooghiemstra and Ran 1994a). Therefore, a pollen record covering both the coastal areas and the mountains could provide new insights into vegetation and climatic changes in western equatorial South America.

Vegetation and climate in this region are strongly influenced by the heterogeneous Andean topography. The timing of uplift in the area, however, is not yet fully resolved. Geologic activity in the Western Andean Cordillera of Ecuador occurred as early as late Miocene times (Spikings et al. 2005), but geomorphologic data suggests that surface uplift only started in the early Pliocene and did not cease until the Pleistocene (Coltorti and Ollier 2000). Two recent palynological studies from the Ecuadorian and central Andes recorded pollen typical of high altitude páramo vegetation in late Miocene sediments, suggesting the presence of elevations above the upper forest line at least since then (Hoorn et al. 2017; Grimmer et al. 2018).

Here we present a new record of Piacenzian vegetation and climate changes in western equatorial South America based on palynological analysis of sediments from ODP Site 1239 in the eastern equatorial Pacific. The aims of this study are (1) to investigate floral and vegetation changes, (2) to infer climatic changes from the response of the vegetation, and (3) to assess if and how the onset of global cooling is manifested in the study area. We compared our results with published climate modelling of the mid-Piacenzian warm period.

5.3.1 Modern vegetation

The study region comprises western equatorial South America from southern Colombia to northern Peru and from the Pacific coast to the western Andean Cordillera. In this mountainous area the vegetation is arranged in belts, from the lowland along the coast to the high-altitude

páramo (Van der Hammen 1985). In the coastal lowlands, tropical moist or dry broadleaf forest is found depending on the amount of precipitation received in the area (Fig. 5.2). Typical elements of the lowland vegetation are Arecaceae (e.g. *Mauritia*), Fabaceae, and Rubiaceae, complemented by Araceae and Piperaceae in the understory (Gentry 1986). The moist broadleaf forest occupies most of the Andean Cordilleras up to an altitude of about 3200 m where trees become sparse. In the lower montane forest, which is found between 1000 and 2300 m, *Acalypha, Alchornea* and *Cecropia* are common genera. Frequent taxa of the upper montane forest (2300 to 3200 m) are *Alnus, Hedyosmum, Ilex, Myrica, Podocarpus* and *Weinmannia*. The upper forest line may be composed of Asteraceae, Ericaceae, and *Polylepis* (Rosaceae). The high elevation areas above the upper forest line are covered by montane grasslands and shrublands called páramo (Fig. 5.2a), which is typically formed by Poaceae and species of *Espeletia* (Asteraceae) amongst others (Van der Hammen 1985). Knowledge of modern pollen-vegetation relationships is helpful for the interpretation of fossil pollen records (Niemann, Brunschön, and Behling 2010). A recent pollen rain study from southwest Ecuador shows that lake sediment surface samples capture the regional vegetation, with anemophilous taxa such as Podocarpaceae being overrepresented (Hagemans et al. 2019). Caryophyllaceae and *Puya* are examples of taxa which are underrepresented in the pollen rain compared to their abundance in the vegetation. This study further confirms the usefulness of *Hedyosmum* and Podocarpaceae as indicators for upper montane forest (Hagemans et al. 2019).

5.3.2 Modern climate and ocean circulation

Rainfall is the most important climate factor in the lowlands. The variability in precipitation also impacts the vegetation in the mountains, but the altitudinal vegetation zones are mainly defined by temperature. The mean annual temperature at 1500 m is 20°C (with absolute minimum and maximum temperatures of 5 and 30°C, respectively). At 3000 m, the mean annual temperature drops to 8°C (with a range from -4 to 22°C; Pourrut 1995).

The general precipitation pattern is determined by the seasonal position of the ITCZ. Its southernmost position on the western South American coast is at about 4° S. Accordingly, precipitation is low in the coastal area further south (Fig. 5.2b). At the precipitation equator (3-5° N), the annual precipitation has two maxima in April and October and two minima in January and July. Away from the precipitation equator, the Northern Hemisphere type of precipitation has one long dry season between October and March, while the Southern Hemisphere type is bimodal with one long dry season from April to September and a shorter one during austral summer. However, this pattern is strongly modified along the Ecuadorean coast, where a unimodal pattern with one rainy season during austral summer and a dry season in winter prevails (Bendix and Lauer 1992; Fig. 5.2b). The climate in this region is influenced by the cold Peru Current being the northern

extension of the Humboldt-Current (Pourrut 1995). In the northern coastal area, the dominating westerly winds transport warm air from the Pacific which is heated by the seasonal southward directed warm Niño-Current (Bendix and Lauer 1992).

The North and South Equatorial Currents flow westward between 10° and 25° N and 0° and 20° S, respectively (Brown et al. 2001). This flow is driven by the trade winds and causes the piling up of warm waters in the western Pacific (Pourrut 1995). These currents are counterbalanced by the North Equatorial Counter Current flowing eastward between 4° and 10° N and the weaker South Equatorial Counter Current between 5° and 10° S (Brown et al. 2001). For a more detailed description of the oceanographic setting of ODP Site 1239, please refer to Grimmer et al. (2018).

5.3.3 Sediment and pollen transport

Because of the prevailing westerly winds, the main pollen fraction is presumably transported to the ocean by rivers rather than by wind. Rincón-Martínez et al. (2010) showed that terrigenous sediment transport to ODP Site 1239 is increased during humid interglacials and is therefore controlled by continental rainfall. Fluvial transport of pollen to the ocean depends on precipitation which is generally high within the range of the ITCZ. Secondarily, transport within the ocean depends on the direction of ocean currents. Terrigenous sediment supply at ODP Site 1239 is sourced at the delta systems of the Guayas (southern Ecuador) and/or Esmeraldas and Cayapas river (northern Ecuador; Rincón-Martínez 2013). These rivers or rather their tributaries originate in the western flanks of the Western Andean Cordillera (U.S. Army Corps of Engineers 1998). Their catchment area which is assumed to be the main pollen source area is depicted in Figure 2. Although most of the sediment is deposited in the Ecuador Trench after reaching the ocean, the eastern part of the Carnegie Ridge still receives a moderate load (Pazmiño Manrique 2005).

The evolution of the catchment area towards its modern configuration is closely linked to Andean uplift. From the Eastern Peruvian Andes it is known that Andean-Amazonian drainage patterns started to establish as early as late Cretaceous to early Paleocene times (Hurtado et al. 2018). If a similar uplift history is assumed for the Western Cordillera of Ecuador, the modern catchment area might have been in place long before Pliocene times.

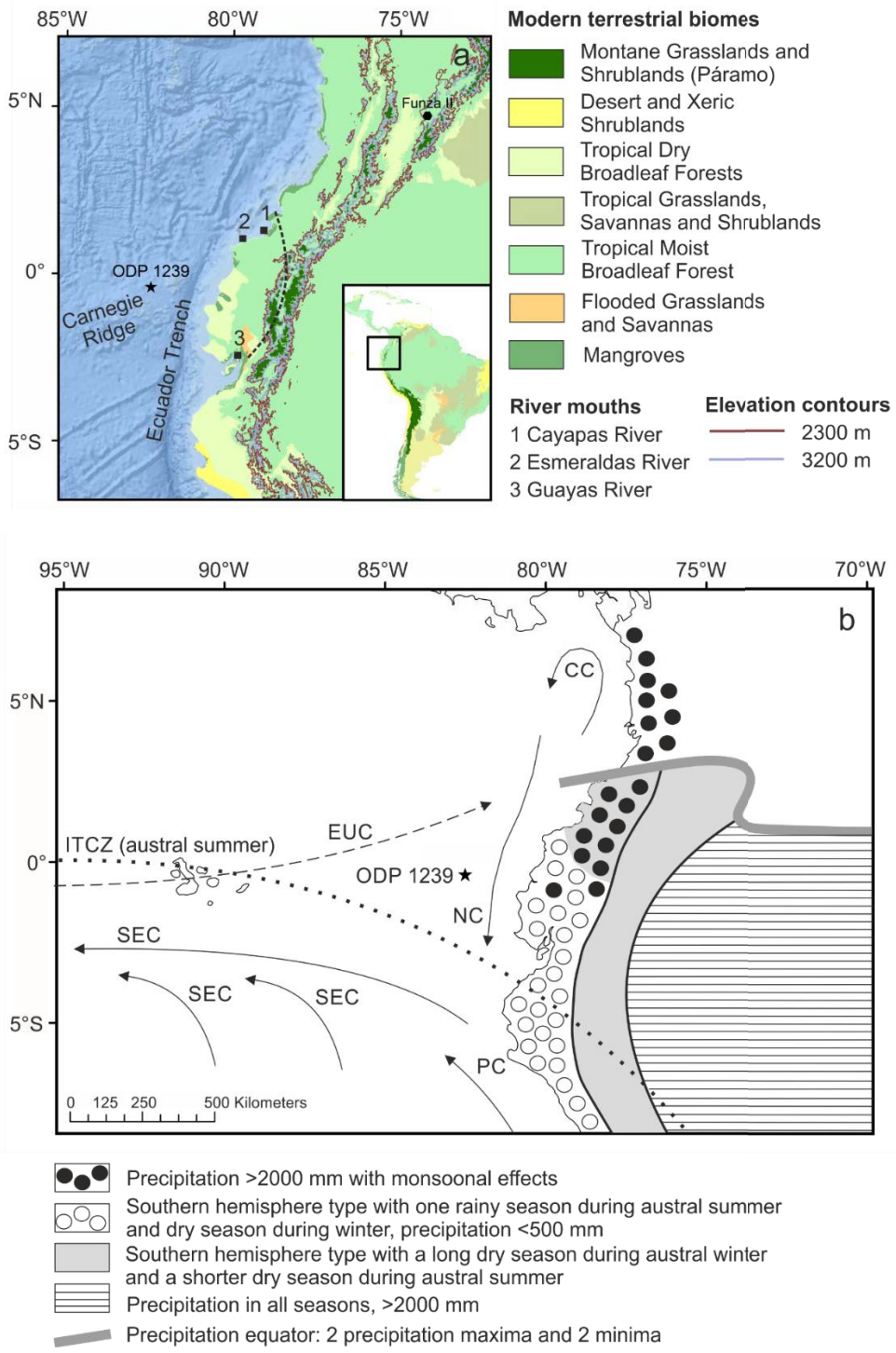

Figure 5.2. Map of the study site. a) Present day vegetation types of western equatorial South America (World Wildlife Fund (WWF)), elevation contours delimiting the lower boundaries of the upper montane forest at 2300 m and the páramo at 3200 m (U.S. Geological Survey's Center for Earth Resources Observation and Science, 1996), river mouths of Ecuador's largest rivers, catchment area marked with a dashed half circle indicates the potential pollen source area, bathymetry of the Eastern Equatorial Pacific and location of Ocean Drilling Program (ODP) Site 1239. b) Precipitation regimes of western equatorial South America (modified after Bendix and Lauer 1992), southernmost limit of the Intertropical Convergence Zone (ITCZ) during austral summer (dotted line), and main ocean currents (modified after Kessler 2006). CC= Colombia Current, EUC= Equatorial Undercurrent, NC= Niño Current, PC= Peru Current, SEC= South Equatorial Current.

5.4 Methods

For the interval between 253 and 139 mbsf (3.6 and 2.7 Ma), 84 sediment samples of 10 cm^3 were taken at 137 cm intervals on average from ODP Hole 1239A (cores 28X5–16H2). Four additional samples were taken between 3.9 and 3.6 Ma. Processing of the samples was done according to standard analytical methods (Faegri and Iversen 1989), including decalcification with HCl (~ 10 %) and removal of silicates with HF (~ 40 %). Two tablets of *Lycopodium* spores (batch no. 177745 containing 18584 ± 829 spores per tablet) were added to each sample during decalcification for calculation of pollen concentrations (Stockmarr 1971). After neutralization with KOH (40 %) and washing, the samples were sieved in an ultrasonic bath over an 8 µm screen to remove smaller particles. Samples were mounted in glycerol, and a minimum of 130 pollen grains and spores (280 on average) were counted in each sample with a Zeiss Axioskop at 400× and 1000× (oil immersion) magnification. Because of variable pollen and spore counts most percentage curves have been plotted with 95% confidence intervals, which size depends on the calculation sum. The Neotropical Pollen Database (Bush and Weng 2007) and related literature (Hooghiemstra 1984; Murillo and Bless 1974, 1978; Roubik and Moreno P. 1991) were used for pollen identification. Pollen types were grouped according to their ecologic preferences (Flantua et al. 2014; Marchant et al. 2002). The zonation was based on constrained incremental sum-of-squares cluster analysis (CONISS) of the pollen percentage curves, applying the square root transformation method (Edwards & Cavalli–Sforza's chord distance) implemented in TILIA (Grimm 1991). Percentages are based on the pollen sum, including all pollen and fern spore types and unidentifiable ones. Reworked pollen was absent from the analyzed core interval. High biological productivity at ODP Site 1239 reduces the oxygen content in the sediments (Shipboard Scientific Party 2003). Therefore, the preservation of palynomorphs is enhanced.

Confidence intervals for pollen percentages and pollen concentrations were calculated after the method of Maher (1972) and Maher (1981), respectively. The initial age model of ODP Site 1239 was based on biostratigraphic information (Shipboard Scientific Party 2003). It was improved by correlating the benthic stable isotope records from Site 1239 with those from nearby ODP Site 1241 by visual identification of isotope stages (Tiedemann et al. 2007). Because Site 1241 has an orbitally tuned age model, this procedure resulted in an indirectly orbitally tuned age model for Site 1239, spanning the interval from 5 to 2.7 Ma (Tiedemann et al. 2007).

5.5 Results

Grouping of the identified pollen taxa according to their main ecological affinity resulted in five groups: páramo, upper montane forest, lower montane forest, lowland rainforest, and broad range taxa (Table 5.1). Taxa with single occurrences were excluded from the interpretation. The temporal

resolution of the record is 10.8 ka on average in the interval from 3.6 to 2.7 Ma. The pollen concentration in this interval ranges from 580 to 2959 grains/cm^3 (average: 1364 grains/cm^3). Most numerous are Podocarpaceae pollen grains with values between 9 and 47%. The cluster analysis performed on the relative abundances yielded a division into four pollen zones (PiaI - PiaIV; Fig. 5.3) which are described in the following section.

Table 5.1. Identified Pollen and Spore Taxa in Marine ODP Core 1239.

Vegetation type	Pollen Taxa	Spore Taxa
Páramo	*Orthrosanthus, Polylepis/Acaena, Puya, Ranunculus, Sisyrinchium, Valeriana triphylla T*	*Jamesonia/Eriosorus, Huperzia*
Upper montane forest (UMF)	Acanthaceae, *Bocconia, Clethra, Daphnopsis, Dodonaea viscosa, Hedyosmum,* Melastomataceae, *Morella, Myrsine,* Podocarpaceae	***Elaphoglossum**, Lophosoria quadripinnata, Grammitis, Hypolepis hostilis T*
Lower montane forest (LMF)	*Alchornea, Croton, Erythrina,* Malpighiaceae, *Passiflora, Styloceras T*, Urticaceae/Moraceae, *Vernonia T*	*Ctenitis subincisa*, Cyatheaceae excl. *Cyathea horrida, Pteris grandifolia T, Pteris podophylla T, Thelypteris*
Lowland rainforest (LR)	*Cordia lanata T, Socratea, Wettinia*	*Pityrogramma-Pteris altissima T, Pityrogramma*, Polypodiaceae
Broad range taxa	Amaranthaceae, *Ambrosia/Xanthium,* Anacardiaceae T, Apocynaceae, ***Artemisia**, Bomarea*, Bromeliaceae, *Calandrinia*, Caryophyllaceae, Cyperaceae, **Ericaceae**, Euphorbiaceae T, *Ilex*, Liguliflorae (Asteraceae), Liliaceae, Malvaceae, *Monnina*, Myrtaceae, Nyctaginaceae, **Poaceae**, *Polygonum (Persicaria T)*, Proteaceae, Rosaceae, *Salacia, Thevetia, Tournefortia*, **Tubuliflorae (Asteraceae)**	*Anemia T, Anthoceros, Cystopteris-Hypolepis, Hymenophyllum trichophyllum*, Lycopodiaceae excl. *Huperzia*, *Saccoloma elegans T, Schizaea pennula, Selaginella*

Note. Grouping was done according to their main ecological affinity (Flantua et al. 2014; Marchant et al. 2002). T = type. Pioneer taxa are printed in bold.

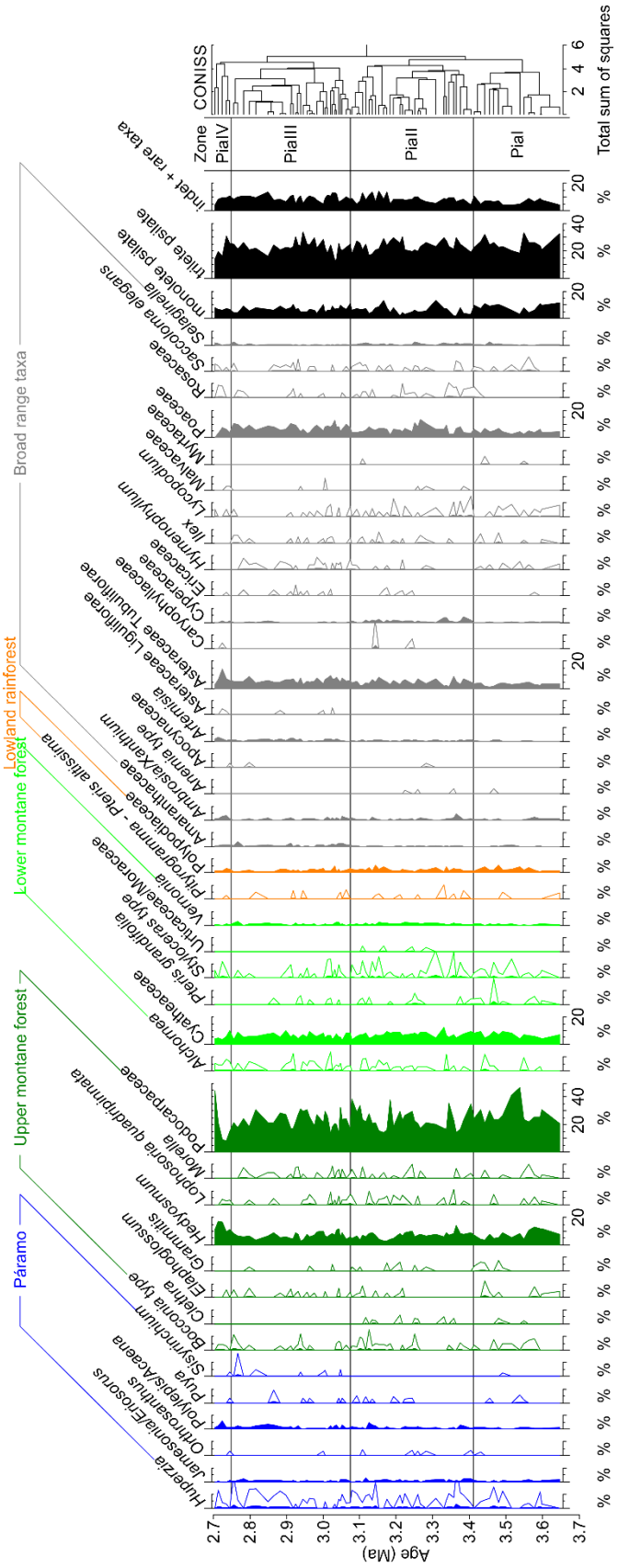

Figure 5.3. Relative abundances (colored areas) of pollen and spores that occurred in more than two samples and grouping according to altitudinal preference. Colored lines represent 10x exaggeration curves. Pollen zones (PiaI - PiaIV) are based on constrained cluster analysis.

5.5.1 Floristic and vegetation changes from 3.9 to 2.7 Ma

Pollen Zone PiaI (15 samples; 256.30-235.86 mbsf; 3.65-3.41 Ma): The average pollen and spores concentration is on a fairly high level (mean: 1288 grains/cm^3). Pollen percentages of broad range taxa (Poaceae, Tubuliflorae, Amaranthaceae, Ericaceae, Cyperaceae, *Artemisia*) are on a low level (10% on average). The abundance of most lower-montane forest pollen increases (the sum increases from ~7 to ~10%). The lowland rainforest taxa show a similar trend. Podocarpaceae pollen, dominating the upper montane forest taxa, has a relative abundance around 30%. From 3.9 Ma on, *Grammitis* spores (upper montane forest) occur in the record. From 3.5 Ma on, pollen of *Sisyrinchium*, *Orthrosanthus* (páramo) and *Hymenophyllum* (broad range) appears in the record. *Puya* pollen appears as a new páramo genus from 3.75 Ma on. The representation of páramo is rather low in this interval (sum páramo pollen 2% on average; Fig. 5.3).

Pollen Zone PiaII (30 samples; 234.60-187.71 mbsf; 3.40-3.08 Ma): The pollen and spores concentration increases substantially and reaches its maximum at 3.13 Ma with 2960 grains per cm^3. Percentages of broad range taxa increase compared to Pollen Zone PiaI (~16%; e.g. *Artemisia*, Rosaceae, Cyperaceae). In this group, Caryophyllaceae pollen first appear in the record around 3.24 Ma. The representation of the lower montane forest maintains high (~10%, mainly due to *Vernonia*, Cyatheaceae, and *Styloceras*). *Clethra* (upper montane forest) pollen disappears after ~ 3.1 Ma. The abundance of upper montane forest pollen declines slightly (from 36 to 32%) and the abundance of páramo increases slightly (from 2 to 3%) compared to Pollen zone PiaI, while pollen percentages of pioneer plants like *Elaphoglossum*, Poaceae, Asteraceae (Tubuliflorae, *Artemisia*), and Ericaceae also rise (from ~8 to ~11%; Fig. 5.3).

Pollen Zone PiaIII (31 samples; 186.77-147.46 mbsf; 3.07-2.76 Ma): The pollen and spores concentration is low throughout this interval (1104 grains/cm^3 on average). The abundance of tree/shrub pollen further declines whereas the abundance of herbs/grass pollen and broad range taxa (18% on average; e.g. *Artemisia*) increases. The relative abundance of lower montane forest pollen decreases slightly compared to Pollen zone PiaII (from 10 to 8%). The abundances of upper montane forest and páramo pollen remain constant. Amaranthaceae pollen increases substantially in abundance (from 0.3 to 0.9% compared to PiaIII; Fig. 5.4). Pollen of pioneer plants like *Elaphoglossum*, Poaceae, *Artemisia*, and Ericaceae continue to be prevalent (Fig. 5.3, 5.5).

Pollen Zone PiaIV (5 samples; 145.70-138.75 mbsf; 2.74-2.70 Ma): The pollen and spores concentration remains low in this zone (1106 grains/cm^3 on average). After a long downward trend, the abundance of tree/shrub pollen increases again, which is mainly due to an increase of the upper montane forest taxa *Hedyosmum* and Podocarpaceae. Herbs and grass pollen decrease accordingly. *Hedyosmum* pollen has its highest relative abundance in this zone (17%). All Asteraceae pollen (*Artemisia*, *Ambrosia*/*Xanthium*, Tubuliflorae) have high relative abundances in this zone.

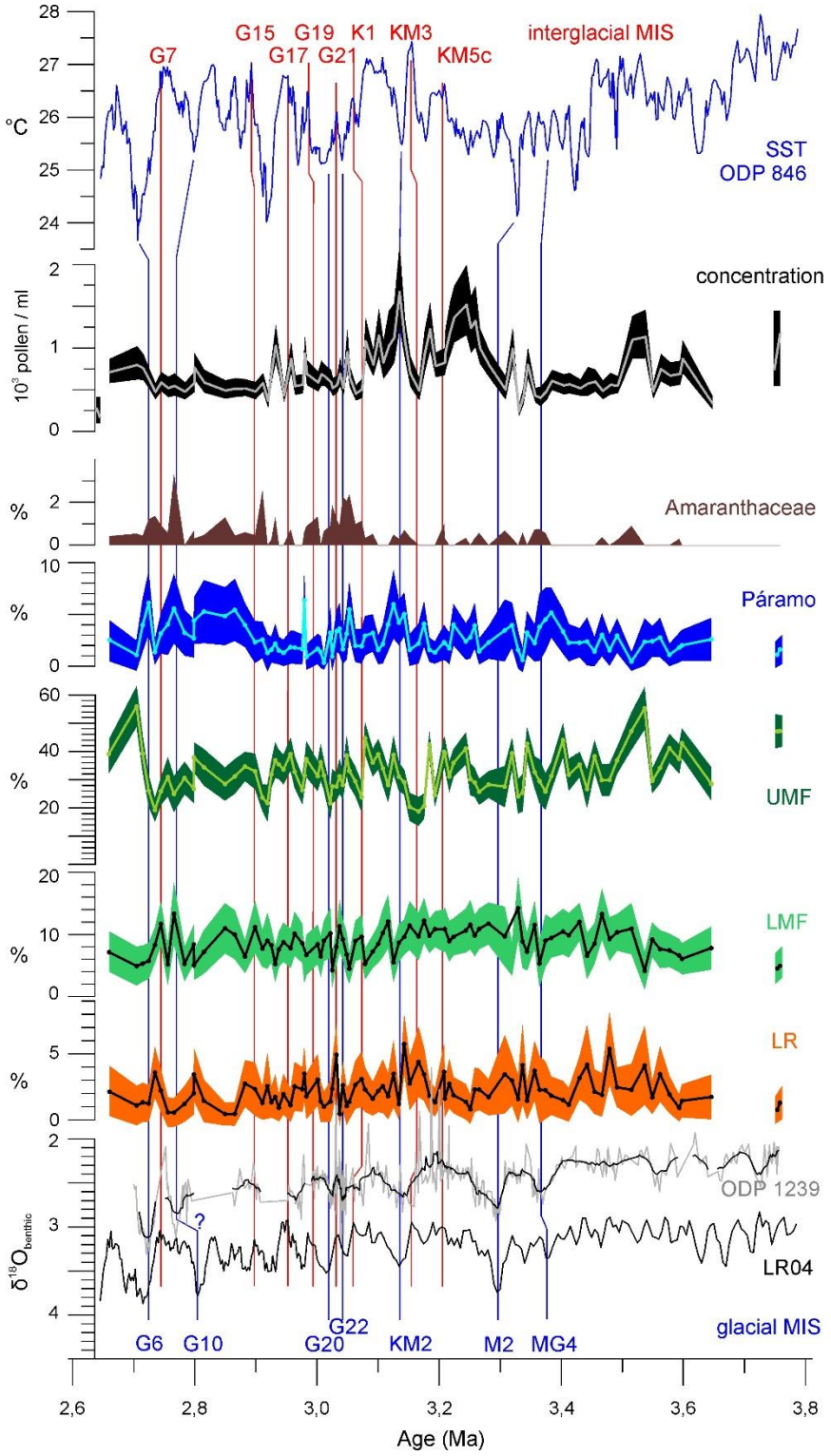

Figure 5.4. Palynomorph percentages of ODP Hole 1239A for Amaranthaceae and the four vegetation belts (lowland rainforest=LR, lower montane forest=LMF, upper montane forest=UMF, páramo) from 3.8 to 2.7 Ma. Colored shading represents the 95% confidence intervals (after Maher 1972). Glacial and interglacial marine isotope stages (MIS) are shown in blue and red, respectively. At the top the $U^{k'}_{37}$ sea surface temperatures (SST) of ODP Site 846 (Lawrence, Liu, and Herbert 2006) are shown. At the bottom the LR04 global stack of benthic $\delta^{18}O$ reflecting changes in global ice volume and temperature (Lisiecki and Raymo 2005), and stable oxygen isotopes of the benthic foraminifer *C. wuellerstorfi* (Tiedemann et al. 2007) of ODP Hole 1239A are presented. Ages are from Tiedemann et al. (2007).

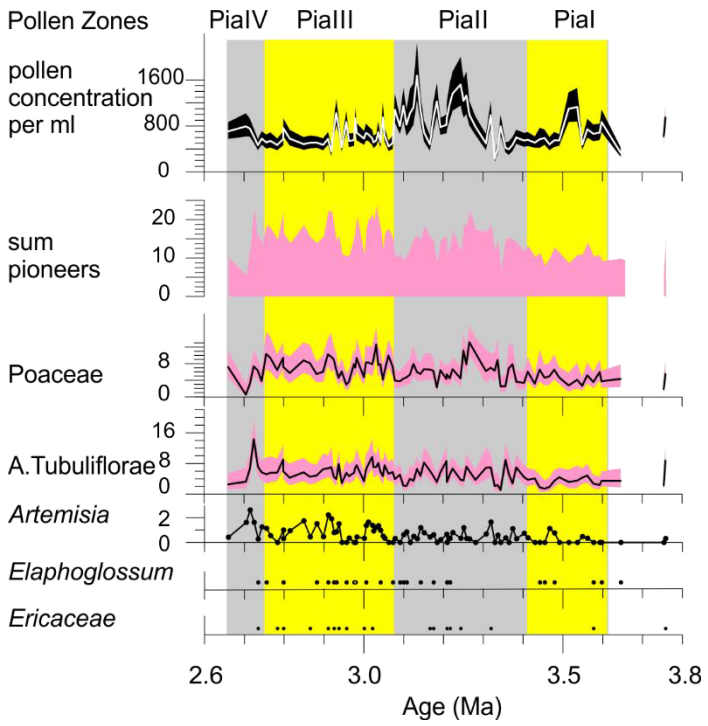

Figure 5.5. Pollen and spores concentration, sum of the pioneer taxa, and relative abundances of the individual pioneer taxa, for the interval from 3.8 to 2.6 Ma. Grey and yellow background delimits the pollen zones.

5.6 Discussion

5.6.1 On opening up of the canopy, erosion, and pioneer taxa

Between ~ 3.3 and 3.05 Ma, the pollen and spores concentration doubles compared to the preceding interval (Fig. 5.4). The two possible mechanisms for this increase are a change of the amount of transported pollen (e.g. through changing climatic conditions resulting in a shift of the pollen source area), or a change of the amount of produced pollen (higher production could be caused by changes in the vegetation cover, especially by an expansion of anemophilous taxa). To disentangle the two mechanisms, we compared the pollen concentrations of selected taxa to their relative abundances (Fig. 5.6) to establish how far relative and absolute abundance run parallel. For instance, the relative abundances of Asteraceae Tubuliflorae, Podocarpaceae, *Hedyosmum* pollen, and Cyatheaceae spores did not increase when their pollen concentration increased between 3.3 and 3.0 Ma. This points toward a general shift of the amount of transported pollen grains. On the other hand, the pollen records of Poaceae, Cyperaceae, Amaranthaceae, Polypodiaceae, *Selaginella*, and *Polylepis/Acaena* show an increase in concentration simultaneously with an increase in relative abundance (Fig. 5.6). This pattern probably indicates an increase of the amount of produced pollen/spores due to an expansion of the range of source plants that are larger pollen producers. Most of those taxa are common in open habitats (*Polylepis/Acaena*, Poaceae, and Cyperaceae in the páramo, Amaranthaceae in coastal deserts and shrubland) which are generally more prone to

erosion and provide a greater contact surface for wind. This might be an additional reason for higher pollen concentrations of these taxa. Increased sedimentation rates at ODP Site 1239 between 3.3 and 3.0 Ma of 14 to 17 cm/ka (compared to 10 to 13 cm/ka before and after that; Tiedemann et al. 2007) together with the increased pollen concentration support the argument of a change in the amount of transported pollen; hence, we infer a general shift of the pollen transport around 3.3 Ma accompanied by a shift in the vegetation favoring taxa which produce large amounts of pollen.

What could have caused the shift in pollen transport? Increased precipitation as the direct effect of high SST is unlikely because high pollen concentration does not line up with high SSTs (Fig. 5.4). On a global scale erosion rates increased since 3-4 Ma due to elevated climate instability, in which periods of mass wasting alternated with periods of enhanced transport (Herman & Champagnac, 2016; Peizhen et al., 2001). Regionally, tectonic movements related to a late step of northern Andean uplift might have reshaped the drainage basin to include regions with higher precipitation. Gregory-Wodzicki (2000) suggest that the Colombian Andes were only at 40% of their modern elevation by 4 Ma and reached modern values around 2.7 Ma. Mora et al. (2008) state that the Eastern Cordillera of Colombia reached a critical elevation as an orographic barrier between ~ 6 and 3 Ma. Following mountain uplift, precipitation in the mountain regions would generally have been higher at the luv side of the mountains (and lower downwind – in the shade of the mountains). These regions would have been increasingly susceptible to erosion and higher runoff would have enhanced pollen transport. As this would be a permanent change of the topography and drainage basin, the question remains why the pollen concentration decreased again after ca. 3.1 Ma.

Pioneer plants like *Elaphoglossum*, Poaceae, Asteraceae (mainly Tubuliflorae, *Artemisia*), and Ericaceae (Lozano, Bussmann, and Küppers 2007) start expanding from ca. 3.4 Ma on (Fig. 5.5). After the period of increased erosion and pollen transport, they expand further from ~ 3.1 Ma on. These pioneers presumably colonized the newly created open habitats. After 2.75 Ma, the montane forest trees *Hedyosmum* and Podocarpaceae recapture the open patches formerly occupied by herbs and grasses.

Our findings overall agree well with the pollen record Funza II from the high plain of Bogotá (Hooghiemstra and Ran 1994a), which is one of the few records of vegetation and climate change in the northern Andes covering parts of the late Pliocene. It overlaps with our record over the time interval from 3.2 Ma to 2.7 Ma. The upper montane forest in Funza II was more open compared to the Middle and Upper Pleistocene. Although our record does not extend to the Pleistocene, we also observe a decrease of tree/shrub pollen and an increase of herbs and grass pollen as well as broad range taxa in the time interval from 3.6 to 2.7 Ma, indicating more open conditions. Funza

II further shows that azonal forests were irregularly formed by pioneers like *Dodonaea* and other taxa like *Ilex*. This would be in agreement with our observation of an increased abundance of *Ilex* (Fig. 5.3).

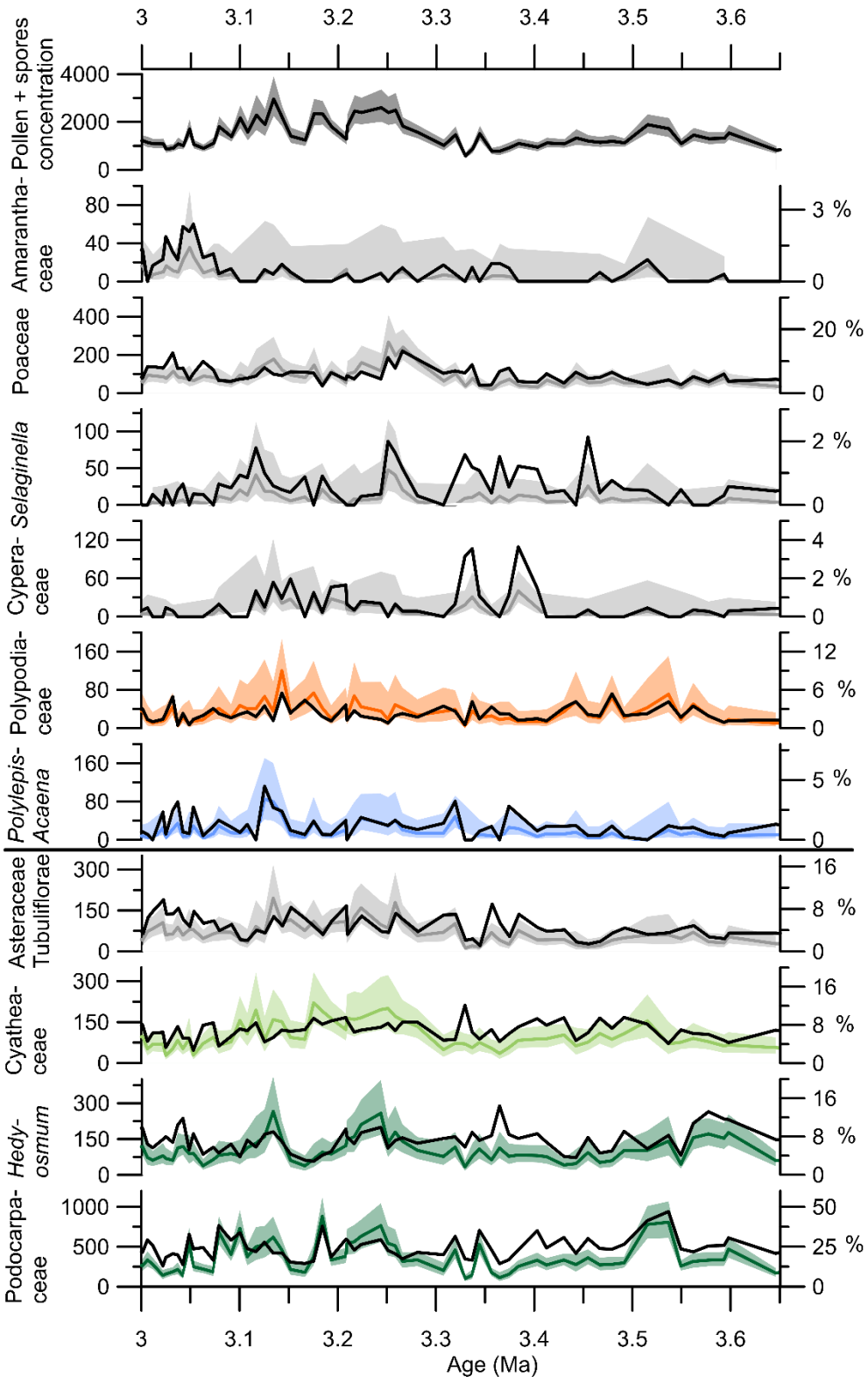

Figure 5.6. Relative abundances (black lines) and concentrations (colored lines) with 95% confidence intervals (shaded areas) of selected taxa for the Piacenzian (3.65-3.0 Ma). Colors denote affiliations to the different ecological groups (blue = páramo, dark green = UMF, light green = LMF, orange = LR, grey = broad range).

5.6.2 Developments in the páramo and the upper forest line

Between 3.91 and 3.42 Ma, a regionally warm climate is expressed in our record. High temperatures during this interval are reflected in an upward expansion of the upper montane forest, indicated by an increased abundance of upper montane forest pollen (e.g. Podocarpaceae) and a decline of páramo pollen. The study area is predominantly covered by closed forests with only few patches of open vegetation beyond the páramo. This is expressed by the highest abundance of tree and shrub pollen of the analyzed period, as well as a low representation of broad range taxa, a group consisting predominantly of herbs.

While the páramo at our study site was floristically very stable in the early Pliocene (4.7-4.2 Ma; Grimmer et al. 2018), new taxa (*Sisyrinchium, Orthrosanthus, Puya*) appear from 3.75 Ma onwards (Fig. 5.7). This development probably reflects the dynamic nature of this relatively newly established ecosystem and has also been described by Van der Hammen, Werner, and van Dommelen (1973) for the central part of the Colombian Eastern Cordillera. The early Pliocene composition of the páramo (4.7-4.2 Ma) has a clear neotropical signature with *Jamesonia/Eriosorus, Huperzia* and *Polylepis/Acaena* having immigrated to the páramo from lower elevation habitats of the neotropics and subsequently adapted to new environmental conditions (Sklenár, Dusková, and Balslev 2011). In contrast, the taxa which appear in the record after 3.75 Ma predominantly immigrated to the area from other floristic realms: *Sisyrinchium* originally occurred in temperate and cool regions of both hemispheres and *Orthrosanthus* had a south temperate distribution (Sklenár, Dusková, and Balslev 2011). This suggests that the high-elevation ecosystem was first colonized by taxa from proximate habitats of the neotropics and thereafter, with the progressive formation of the Isthmus of Panama, taxa from more distant locations gradually arrived.

Around 3.5 Ma, a transition occurred from warm climatic conditions with a relatively high upper forest line (high abundance of UMF) to colder climatic conditions with a lower forest line (decreased abundance of UMF and increased abundance of páramo vegetation). At the same time, the sea surface temperature at ODP Site 846 decreased (compare Fig. 5.4). Additional to the true páramo taxa, the abundance of some broad range taxa which are assumed to have their main occurrence in the páramo (Tubuliflorae, Poaceae, Ericaceae) also increased. This is another indication of colder climatic conditions with a lowered forest line. This trend continues through pollen zones PiaII and PiaIII. Páramo pollen has maximum abundances during MG4, M2, and KM2 (Fig. 5.4). This local cooling trend thus starts well before the M2 glacial, which is the first large excursion of the LR04 stack (~ 3.3 Ma; Lisiecki and Raymo 2005).

Two taxa which grow predominantly at the upper forest line are *Polylepis/Acaena* and *Morella* (formerly Myrica; Kessler 2002; Marchant et al. 2002). The oscillations of *Polylepis/Acaena* are generally opposite to those of the upper montane forest. During warm phases, when the upper

montane forest extends to higher altitudes, the abundance of *Polylepis/Acaena* is low and vice versa. *Morella* already appears sporadically in the earliest Pliocene samples and has frequent occurrences from 3.6 Ma onward (Fig. 5.3). This record probably reflects the establishment of *Morella* in the area. Andriessen et al. (1993) dated the immigration of *Morella* to the high plain of Bogotá at 3.7 – 2.7 Ma. Van der Hammen and Hooghiemstra (1997) mention *Morella's* first appearance before 4 Ma, which is in agreement with our record. The Funza II record (Hooghiemstra and Ran 1994a) shows that the transitional zone between the upper montane forest and the páramo was abundantly covered with *Morella*. It is not known whether *Morella* immigrated to South America only after the establishment of the Panamanian Land Bridge (Gentry 1982) or if South America was colonized earlier by long-distance dispersal independent of tectonic processes. Taking into account recent advances in dating the closure of the Central American Seaway (e.g. O'Dea et al. 2016) and results of molecular studies showing that the South American species of *Morella* went through rapid diversification around 4 Ma (Herbert 2005), it seems more likely that *Morella* reached the northern Andes via long-distance dispersal before 4 Ma and established rapidly on the high-altitude open grounds created by Andean uplift.

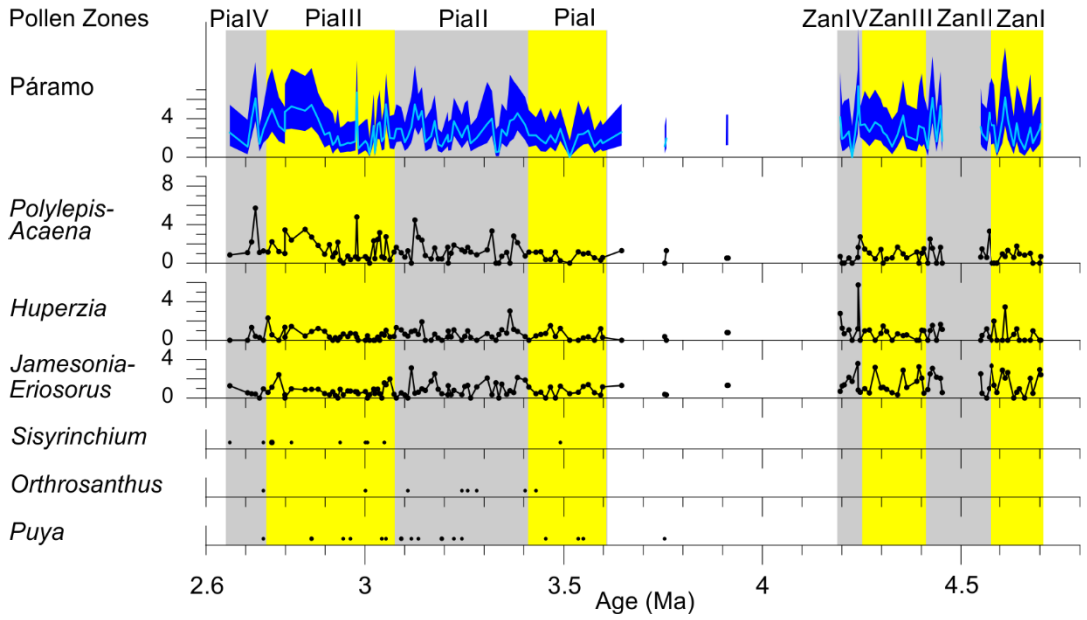

Figure 5.7. Páramo sum with 95% confidence intervals shown as blue shading, and relative abundances of the most prevalent páramo taxa for the time window 4.7-2.6 Ma (4.7-4.2 Ma is from Grimmer et al. (2018)). Grey and yellow background delimits the pollen zones.

5.6.3 Glacial-interglacial variability and comparison with mid-Piacenzian warm period (mPWP) modeling

Comparing the pollen record to marine isotope stages (MIS) can yield information about the response of the vegetation to glacial-interglacial climatic variability. When looking at the changing extent of the vegetation belts during glacials and interglacials, it becomes apparent that páramo pollen has maxima during most glacials while lowland rainforest pollen shows glacial minima (Fig. 5.4). Obviously, the expansion and contraction of vegetation belts with the glacial/interglacial climatic oscillations affects all vegetation belts down to the lowland rainforest, and is not limited to the páramo and upper montane forest. A similar glacial/interglacial vegetation response was found in a late Quaternary pollen record from the Panama Basin (González, Urrego, and Martínez 2006).

Another observation is that minima in pollen concentration occur during interglacial MIS, while there is no such clear relation between glacial peaks and pollen concentration (Fig. 5.4). The dry indicators, on the other hand, show maxima during some glacials (G6, G10, G22, MG4). This is interesting because the pollen record does not indicate a clear pattern of dry glacials vs. humid interglacials as shown in a multiproxy record of terrigenous input of the late Pleistocene by Rincón-Martínez et al. (2010). Thus, this pattern of cold/dry and warm/wet oscillations presumably did not exist in the late Pliocene and must have developed later. The dynamics of the late Quaternary Equatorial Front-ITCZ system with its large meridional SST gradient during glacials presumably operated differently in the late Pliocene.

Regarding data-model comparison, mainly mid-Piacenzian interglacials have been modelled (Prescott et al. 2018; Prescott et al. 2014), but some general conclusions can be drawn for the mPWP. Compared to modern conditions, temperatures are higher in the western Andes and lower in the Eastern part of the Andes in the model of Contoux, Ramstein, and Jost (2012) which is due to changes in topography. Although the Pliocene Andean forest is not analogous to the modern assemblage due to immigration of Northern Hemisphere taxa, our record shows that the relative abundance of upper montane forest pollen was twice as high in the mPWP compared to the Holocene (Fig. 5.8). This would be in agreement with higher temperatures in the western Andes and an elevated upper forest line.

In the models, precipitation over the tropical Pacific Ocean is lower compared to modern which is explained by a slowing down of the Walker Circulation due to a reduced zonal SST gradient which induces a broadening of the ITCZ (Contoux, Ramstein, and Jost 2012; Chandan and Peltier 2017). Prescott et al. (2014) also mention a possible ITCZ shift related to the altered pole to equator temperature gradient. These findings agree with our interpretation of a drier climate in coastal Ecuador during the mPWP.

Two recent modeling studies (Prescott et al. 2018; Prescott et al. 2014) investigated climate variability in and around four different interglacials of the mid-Piacenzian warm period (MIS G17, K1, KM3 and KM5c) as well as vegetation response to orbital forcing. Comparing model outputs to the palynological record can identify areas of data-model mismatch and validate model performance. The models generally show that in our study area, the simulated changes regarding climate parameters (temperature, precipitation) and vegetation due to orbital forcing are small (in contrast to, e.g. central and eastern Asia). Concerning the mean annual surface air temperature (SAT), interglacial K1 has slightly higher variability in our study area compared to KM5c. For the seasonal SAT change, the variability during K1 is even larger (Prescott et al. 2014). Surface temperature variability would be reflected in our record mainly through changes in the relative abundances of páramo and upper montane forest pollen, indicating vertical movements of the upper forest line. When comparing the representation of páramo and UMF around the two interglacials (two samples before and two samples after the peak), we find that the variability in both interglacials is similar. Simulations conducted for KM5c between 3189 ka and 3197 ka all demonstrate a significant terrestrial warming over South America of up to 1°C (Prescott et al. 2014). This is in agreement with the pollen record exhibiting relatively low abundance of páramo pollen compared to a high abundance of UMF pollen.

When comparing the modelled development of predicted plant functional types, they remain constant over all four interglacials with around 85-95% broad leaf forest and 5-15% grass (Prescott et al. 2018). This shows that the trend of opening up that we see in the pollen record is not reflected in the model predictions. A reason for mismatch might be that smaller changes within the range of 10% are not shown in the model. Furthermore, plant functional types cannot be directly compared to pollen abundances because of differences in pollen production rates across plant types (Prescott et al. 2018).

The models run with prescribed or dynamic vegetation both show higher annual SATs during all interglacials compared to control run KM5c (Prescott et al. 2018). These lower mean annual temperatures during KM5c relative to the other modelled interglacials are not in agreement with our observations of a high abundance of upper montane forest and a low abundance of páramo pollen (high upper forest line) during KM5c (Fig. 5.4). A data-model mismatch could indicate that orbital forcing at this time was not the dominant contribution to climate change, but other factors influencing the vegetation were more important. This could be local or regional (sub-gridscale) features not captured by the model due to the coarse model resolution, or variations in pCO_2, or feedbacks such as aerosol cycles etc. which were not included in the model (Prescott et al. 2018). Interestingly, the model HadCM3 with dynamic vegetation predicts higher precipitation over Colombia and lower precipitation over coastal Ecuador and the eastern equatorial Pacific compared

to control run KM5c for interglacial G17 (Prescott et al. 2018). At the same time, our pollen record shows an increase of Amaranthaceae pollen from coastal Ecuador while the montane forest is still well represented and the pollen concentration is moderately high. This could be related to a northward shift/broadening of the ITCZ, as described in the following section.

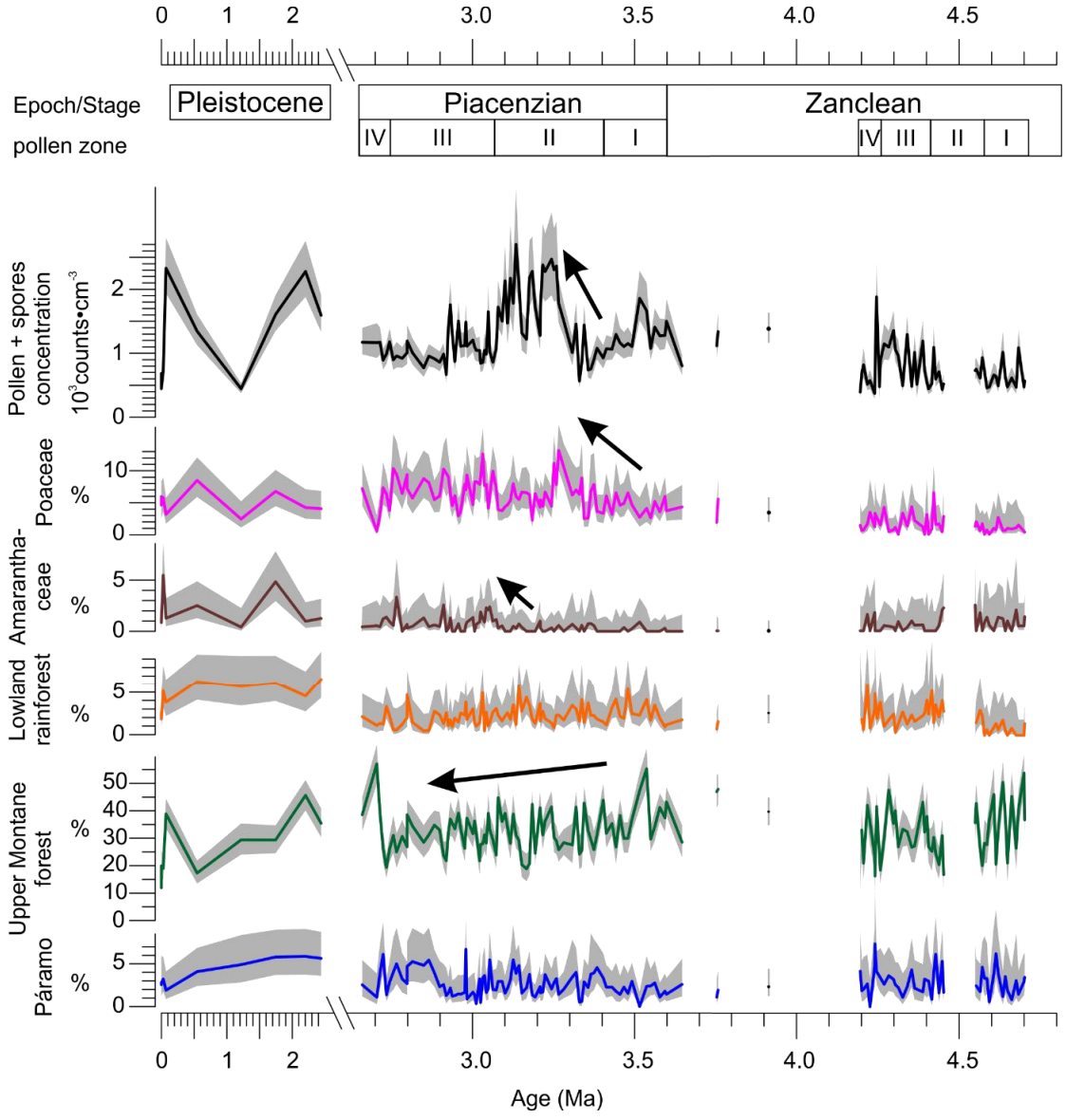

Figure 5.8. Long-term vegetation development of selected groups and taxa in western equatorial South America from 0 to 4.7 Ma (data from 4.7-4.2 Ma are from Grimmer et al. (2018)). Note the break of the x-axis between 2.5 and 2.7 Ma.

5.6.4 Trends in vegetation and climate

One of the most obvious trends in this record is the increase of pollen of Amaranthaceae, starting around 3.1 Ma and suggesting an expansion of the coastal desert area. Dry vegetation might have replaced parts of the lowland rainforest which diminished slightly during this period (Fig. 5.4, 5.8).

There is generally less pollen of trees and shrubs and more of herbs and grasses, but humidity in the mountains is still available as shown by the representation of several montane tree and tree-fern taxa, which are humidity-dependent (e.g. *Hedyosmum, Morella*, Cyatheaceae). Additionally, the representation of the lower and upper montane forest is rather stable. This suggests that the mountains still received enough rainfall, while the desert area of southern Ecuador expanded. Such a precipitation pattern is typical for La Niña conditions (Vuille, Bradley, and Keimig 2000). However, the zonal sea surface temperature gradient in the equatorial Pacific between 3.1 and 2.7 Ma is rather small (Wara, Ravelo, and Delaney 2005; compare Fig. 5.1; Lawrence, Liu, and Herbert 2006), which would not support La Niña conditions and a strong Walker Circulation accordingly. This seeming contradiction migth be explained by model simulations for the mid-Pliocene warm period that find a precipitation decrease over the tropical Pacific explained by a broadening of the ITCZ due to a weakened Walker Circulation and a smaller zonal sea surface temperature gradient (Contoux, Ramstein, and Jost 2012). This pattern would be in agreement with the observed hydrological changes in the study area and the reconstructed zonal sea surface temperature gradient. The model of Chandan and Peltier (2017) shows higher precipitation over the Ecuadorean Andes and an area of lower precipitation over the coastal Pacific for the mPWP compared to modern, which is also in accordance with our record.

The environmental changes in Ecuador after 3.3 Ma took place at around the same time as the first major pulse of ice-rafted debris during M2 (Kleiven et al. 2002) and might be a precursor of global climate changes leading to the intensification of the Northern Hemisphere glaciation at the start of the Pleistocene. In that case, it would parallel temperature decline in the Northern Hemisphere as recorded for northern Norway (Panitz et al. 2016), in Lake Baikal in central Asia (Demske et al., 2002), and Lake El'gygytgyn in northern Siberia (Brigham-Grette et al. 2013, Andreev et al. 2014). Drying coastal climate in Ecuador after 3.1 Ma would have preceded global changes associated with the increase of the Northern Hemisphere glaciation such as strengthening of the NE trade winds at ~2.7 Ma as recorded offshore of West Africa (Vallé et al. 2014), in Chinese Loess sediments (Yang and Ding 2010), and for North America (Naafs et al. 2012), as well as aridification of Central Asia after 2.6 Ma (Cai et al. 2012; Wu et al. 2007).

5.7 Conclusions/Outlook

This study aimed to (1) investigate vegetation change in western equatorial South America during the Piazencian, (2) to infer climatic changes from the response of the vegetation, and (3) assess if and how the onset of global cooling is manifested in the study area.

The climate in western equatorial South America was stable and warm from ~ 3.9 to 3.3 Ma, when a lowered forest line showed first evidence of cooling. After 3.75 Ma, floristic changes occurred in

the páramo due to immigration of taxa from distant locations. A doubling of the pollen and spores concentration occurred between ~ 3.3 and 3.05 Ma, caused by a general shift of the pollen transport accompanied by a shift in the vegetation favoring taxa which produce large numbers of pollen. The increased pollen transport may have been an effect of increased erosion rates due to tectonic processes and/or climate change (e.g. increased precipitation). After 3.1 Ma, the open habitats created by erosion were colonized by pioneer plants.

Shifts of the upper forest line after 3.5 Ma indicate temperature fluctuations towards cooler conditions. After 3.1 Ma, an increase of Amaranthaceae pollen suggests an expansion of the coastal desert area while the montane forests still received abundant rainfall. This pattern is most likely caused by a precipitation decrease over the coastal areas which can be explained by a broadening of the ITCZ due to a weakened Walker Circulation. This explanation is in agreement with sea surface temperature reconstructions (Lawrence, Liu, and Herbert 2006; Wara, Ravelo, and Delaney 2005; Etourneau et al. 2010) and modeling results for the mid-Pliocene warm period (Contoux, Ramstein, and Jost 2012).

The isochronous occurrence of environmental changes in the present record with the first major pulse of ice-rafted debris as well as cooling temperatures in the Northern Hemisphere suggests that these changes might be a precursor of the intensification of Northern Hemisphere glaciation.

We hope that this study will be a valuable contribution to improving global land surface reconstructions. Future work should focus on an extension of the record into the Pleistocene, which could give more insights into the timing of the strengthening of the Walker Circulation. Further modeling studies could shed light on the role of the tropics in the onset of NHG.

Acknowledgments

We thank Maike Stoltmann for assistance with sample preparation. We acknowledge the IODP Gulf Coast Repository (GCR) for their assistance in providing the core samples. We are grateful for receiving a research grant from the Deutsche Forschungsgemeinschaft (DFG) for the TROPSAP project(DU221/6). Our thanks also go to three anonymous reviewers, who provided useful comments and suggestions that helped to improve the paper.

Data availability

The underlying research data are stored in PANGAEA as data set (https://doi.org/10.1594/PANGAEA.921208).

5.8 References

Andreev, A. A., Tarasov, P. E., Wennrich, V., Raschke, E., Herzschuh, U., Nowaczyk, N. R., . . . Melles, M. (2014). Late Pliocene and Early Pleistocene vegetation history of northeastern Russian Arctic inferred from the Lake El'gygytgyn pollen record. *Climate of the Past, 10*(3), 1017-1039. doi:10.5194/cp-10-1017-2014

Andriessen, P. A. M., Helmens, K. F., Hooghiemstra, H., Riezebos, P. A., & Van der Hammen, T. (1993). Absolute Chronology of the Pliocene-Quaternary Sediment Sequence of the Bogota Area, Colombia. *Quaternary Science Reviews, 12*(7), 483-501. doi:10.1016/0277-3791(93)90066-U

Bendix, J., & Lauer, W. (1992). Die Niederschlagsjahreszeiten in Ecuador und ihre klimadynamische Interpretation. *Erdkunde, 46*, 118-134.

Brierley, C. M., Fedorov, A. V., Liu, Z., Herbert, T. D., Lawrence, K. T., & Lariviere, J. P. (2009). Greatly expanded tropical warm pool and weakened Hadley circulation in the early Pliocene. *Science, 323*(5922), 1714-1718. doi:10.1126/science.1167625

Brigham-Grette, J., Melles, M., Minyuk, P., Andreev, A., Tarasov, P., DeConto, R., . . . Herzschuh, U. (2013). Pliocene Warmth, Polar Amplification, and Stepped Pleistocene Cooling Recorded in NE Arctic Russia. *Science, 340*(6139), 1421-1427. doi:10.1126/science.1233137

Brown, E., Colling, A., Park, D., Phillips, J., Rothery, D., & Wright, J. (2001). *Ocean circulation* (2 ed.): Butterworth-Heinemann

Bush, M. B., & Weng, C. (2007). Introducing a new (freeware) tool for palynology. *Journal of Biogeography, 34*(3), 377-380. doi:10.1111/j.1365-2699.2006.01645.x

Cai, M. T., Fang, X. M., Wu, F. L., Miao, Y. F., & Appel, E. (2012). Pliocene-Pleistocene stepwise drying of Central Asia: Evidence from paleomagnetism and sporopollen record of the deep borehole SG-3 in the western Qaidam Basin, NE Tibetan Plateau. *Global and Planetary Change, 94-95*, 72-81. doi:10.1016/j.gloplacha.2012.07.002

Chandan, D., & Peltier, W. R. (2017). Regional and global climate for the mid-Pliocene using the University of Toronto version of CCSM4 and PlioMIP2 boundary conditions. *Climate of the Past, 13*(7), 919-942. doi:10.5194/cp-13-919-2017

Coltorti, M., & Ollier, C. D. (2000). Geomorphic and tectonic evolution of the Ecuadorian Andes. *Geomorphology, 32*(1-2), 1-19. doi:Doi 10.1016/S0169-555x(99)00036-7

Contoux, C., Ramstein, G., & Jost, A. (2012). Modelling the mid-Pliocene Warm Period climate with the IPSL coupled model and its atmospheric component LMDZ5A. *Geoscientific Model Development, 5*(3), 903-917. doi:10.5194/gmd-5-903-2012

Demske, D., Mohr, B., & Oberhansli, H. (2002). Late Pliocene vegetation and climate of the Lake Baikal region, southern East Siberia, reconstructed from palynological data. *Palaeogeography Palaeoclimatology Palaeoecology, 184*(1-2), 107-129. doi:10.1016/S0031-0182(02)00251-1

Dowsett, H., Barron, J., & Poore, R. (1996). Middle Pliocene sea surface temperatures: a global reconstruction. *Marine Micropaleontology, 27*, 13-25.

Dowsett, H., Dolan, A., Rowley, D., Moucha, R., Forte, A. M., Mitrovica, J. X., . . . Haywood, A. (2016). The PRISM4 (mid-Piacenzian) paleoenvironmental reconstruction. *Climate of the Past, 12*(7), 1519-1538. doi:10.5194/cp-12-1519-2016

Dupont, L. M. (2006). Late Pliocene vegetation and climate in Namibia (southern Africa) derived from palynology of ODP Site 1082. *Geochemistry Geophysics Geosystems, 7*(5), 1-15. doi:10.1029/2005gc001208

Etourneau, J., Schneider, R., Blanz, T., & Martinez, P. (2010). Intensification of the Walker and Hadley atmospheric circulations during the Pliocene–Pleistocene climate transition. *Earth and Planetary Science Letters, 297*(1-2), 103-110. doi:10.1016/j.epsl.2010.06.010

Faegri, K., & Iversen, J. (1989). *Textbook of Pollen Analysis* (4 ed.). Chichester: John Wiley & Sons.

Fedorov, A. V., Burls, N. J., Lawrence, K. T., & Peterson, L. C. (2015). Tightly linked zonal and meridional sea surface temperature gradients over the past five million years. *Nature Geoscience, 8*(12), 975-983. doi:10.1038/Ngeo2577

Flantua, S., Hooghiemstra, H., Van Boxel, J. H., Cabrera, M., González-Carranza, Z., & González-Arango, C. (2014). Connectivity dynamics since the last glacial maximum in the northern Andes: a pollen-driven framework to assess potential migration. In W. D. Stevens, O. M. Montiel, & P. H. Raven (Eds.), *Paleobotany and Biogeography: A Festschrift for Alan Graham in His 80th Year*. St. Louis: Missouri Botanical Garden Press.

Ford, H. L., Ravelo, A. C., Dekens, P. S., LaRiviere, J., & Wara, M. W. (2015). The evolution of the equatorial thermocline and the early Pliocene El Padre mean state. *Geophysical Research Letters, 42*, 4878-4887.

Gentry, A. H. (1982). Neotropical Floristic Diversity - Phytogeographical Connections between Central and South-America, Pleistocene Climatic Fluctuations, or an Accident of the Andean Orogeny. *Annals of the Missouri Botanical Garden, 69*(3), 557-593. doi:10.2307/2399084

Gentry, A. H. (1986). Species richness and floristic composition of Chocó region plant communities. *Caldasia, 15*, 71-91.

González, C., Urrego, L. E., & Martínez, J. I. (2006). Late Quaternary vegetation and climate change in the Panama Basin: Palynological evidence from marine cores ODP 677B and TR 163-38. *Palaeogeography, Palaeoclimatology, Palaeoecology, 234*(1), 62-80. doi:10.1016/j.palaeo.2005.10.019

Gregory-Wodzicki, K. M. (2000). Uplift history of the Central and Northern Andes: A review. *Geological Society of America Bulletin, 112*(7), 1091-1105. doi:10.1130/0016-7606(2000)112<1091:uhotca>2.0.co;2

Grimm, E. (1991). Tilia and Tiliagraph. Springfield: Illinois State Museum.

Grimmer, F., Dupont, L., Lamy, F., Jung, G., Gonzalez, C., & Wefer, G. (2018). Early Pliocene vegetation and hydrology changes in western equatorial South America. *Climate of the Past, 14*(11), 1739-1754. doi:10.5194/cp-14-1739-2018

Hagemans, K., Tóth, C.-D., Ormaza, M., Gosling, W. D., Urrego, D. H., León-Yánez, S., . . . Donders, T. H. (2019). Modern pollen-vegetation relationships along a steep temperature

gradient in the Tropical Andes of Ecuador. *Quaternary Research*, 1-13. doi:10.1017/qua.2019.4

Haywood, A. M., Dowsett, H. J., & Dolan, A. M. (2016). Integrating geological archives and climate models for the mid-Pliocene warm period. *Nature Communications, 7*. doi:10.1038/ncomms10646

Herbert, J. (2005). *Systematics and Biogeography of Myricaceae*. University of St Andrews, St Andrews.

Hooghiemstra, H. (1984). *Vegetational and Climatic History of the High Plain of Bogotá, Colombia: A Continuous Record of the Last 3.5 Million Years* (Vol. 79). Vaduz: A.R. Gantner Verlag K.G.

Hooghiemstra, H. (1989). Quaternary and Upper-Pliocene Glaciations and Forest Development in the Tropical Andes - Evidence from a Long High-Resolution Pollen Record from the Sedimentary Basin of Bogotá, Colombia. *Palaeogeography Palaeoclimatology Palaeoecology, 72*(1-2), 11-26. doi:10.1016/0031-0182(89)90129-6

Hooghiemstra, H., & Ran, E. T. H. (1994). Late Pliocene-Pleistocene high resolution pollen sequence of Colombia: An overview of climatic change.

Hooghiemstra, H., Wijninga, V. M., & Cleef, A. M. (2006). The Paleobotanical Record of Colombia: Implications for Biogeography and Biodiversity. *Annals of the Missouri Botanical Garden, 93*(2), 297-325. doi:10.3417/0026-6493(2006)93[297:tproci]2.0.co;2

Hoorn, C., Bogotá-A., G. R., Romero-Baez, M., Lammertsma, E. I., Flantua, S., Dantas, E. L., . . . Chemale Jr, F. (2017). The Amazon at sea: Onset and stages of the Amazon River from a marine record, with special reference to Neogene plant turnover in the drainage basin. *Global and Planetary Change, 153*, 51-65.

Hurtado, C., Roddaz, M., Ventura Santos, R., Baby, P., Antoine, P.-O., & Dantas, E. L. (2018). Late Cretaceous-early Paleocene drainage shift of Amazonian rivers driven by Equatorial Atlantic Ocean opening and Andean uplift as deduced from the provenance of northern Peruvian sedimentary rocks (Huallaga basin). *Gondwana Research*. doi:10.1016/j.gr.2018.05.012

Kamae, Y., Ueda, H., & Kitoh, A. (2011). Hadley and Walker Circulations in the Mid-Pliocene Warm Period Simulated by an Atmospheric General Circulation Model. *Journal of the Meteorological Society of Japan, 89*(5), 475-493. doi:10.2151/jmsj.2011-505

Kessler, M. (2002). The "Polylepis problem": Where do we stand? *Ecotropica, 8*, 97-110.

Kessler, W. S. (2006). The circulation of the eastern tropical Pacific: A review. *Progress in Oceanography, 69*(2-4), 181-217. doi:10.1016/j.pocean.2006.03.009

Lawrence, K. T., Liu, Z., & Herbert, T. D. (2006). Evolution of the eastern tropical Pacific through Plio-Pleistocene glaciation. *Science, 312*(5770), 79-83. doi:10.1126/science.1120395

Lisiecki, L. E., & Raymo, M. E. (2005). A Pliocene-Pleistocene stack of 57 globally distributed benthic δ18O records. *Paleoceanography, 20*(1), 1-17. doi:10.1029/2004pa001071

Lozano, P., Bussmann, R. W., & Küppers, M. (2007). A checklist of pioneer plant regeneration on natural and anthropogenic landslides on the eastern side of Podocarpus National Park-Southern Ecuador. *Redesma, 1*(2), 1-15.

Maher, L. J. (1972). Nomograms for computing 0.95 confidence limits of pollen data. *Review of Palaeobotany and Palynology, 13*, 85-93.

Maher, L. J. (1981). Statistics for Microfossil Concentration Measurements Employing Samples Spiked with Marker Grains. *Review of Palaeobotany and Palynology, 32*(2-3), 153-191. doi:10.1016/0034-6667(81)90002-6

Marchant, R., Almeida, L., Behling, H., Berrio, J. C., Bush, M., Cleef, A., . . . Salgado-Labouriau, M. (2002). Distribution and ecology of parent taxa of pollen lodged within the Latin American Pollen Database. *Review of Palaeobotany and Palynology, 121*, 1-75.

Mix, A., Tiedemann, R., & Blum, P. (2003). *Proceedings of the Ocean Drilling Program*. Retrieved from

Mora, A., Parra, M., Strecker, M. R., Sobel, E. R., Hooghiemstra, H., Torres, V., & Jaramillo, J. V. (2008). Climatic forcing of asymmetric orogenic evolution in the Eastern Cordillera of Colombia. *GSA Bulletin, 120*(7/8), 930-949.

Mudelsee, M., & Raymo, M. E. (2005). Slow dynamics of the Northern Hemisphere glaciation. *Paleoceanography, 20*(4). doi:10.1029/2005pa001153

Murillo, M. T., & Bless, M. J. M. (1974). Spores of recent Colombian Pteridophyta. I. Trilete Spores. *Review of Palaeobotany and Palynology, 18*, 223-269.

Murillo, M. T., & Bless, M. J. M. (1978). Spores of recent Colombian Pteridophyta. II. Monolete Spores. *Review of Palaeobotany and Palynology, 25*, 319-365.

Niemann, H., Brunschön, C., & Behling, H. (2010). Vegetation/modern pollen rain relationship along an altitudinal transect between 1920 and 3185 m a.s.l. in the Podocarpus National Park region, southeastern Ecuadorian Andes. *Review of Palaeobotany and Palynology, 159*(1-2), 69-80. doi:10.1016/j.revpalbo.2009.11.001

O'Dea, A., Lessios, A. H., Coates, A. G., Eytan, R. I., Restrepo-Moreno, S. A., Cione, A. L., . . . Jackson, J. B. C. (2016). Formation of the Isthmus of Panama. *Science Advances, 2*, 1-11.

Panitz, S., Salzmann, U., Risebrobakken, B., De Schepper, S., & Pound, M. J. (2016). Climate variability and long-term expansion of peatlands in Arctic Norway during the late Pliocene (ODP Site 642, Norwegian Sea). *Climate of the Past, 12*(4), 1043-1060. doi:10.5194/cp-12-1043-2016

Pazmiño Manrique, N. A. (2005). *Sediment distribution and depositional processes on the Carnegie Ridge.* (Master of Science), Texas A&M University.

Perez-Angel, L. C., & Molnar, P. (2017). Sea Surface Temperatures in the Eastern Equatorial Pacific and Surface Temperatures in the Eastern Cordillera of Colombia During El Niño: Implications for Pliocene Conditions. *Paleoceanography, 32*(11), 1309-1314. doi:10.1002/2017pa003182

Pourrut, P. (1995). *El agua en el Ecuador: clima, precipitaciones, escorrentía*. Quito: Colegio de Geógrafos del Ecuador: Corporación Editora Nacional.

Prescott, C. L., Dolan, A. M., Haywood, A. M., Hunter, S. J., & Tindall, J. C. (2018). Regional climate and vegetation response to orbital forcing within the mid-Pliocene Warm Period: A study using HadCM3. *Global and Planetary Change, 161*, 231-243. doi:10.1016/j.gloplacha.2017.12.015

Prescott, C. L., Haywood, A. M., Dolan, A. M., Hunter, S. J., Pope, J. O., & Pickering, S. J. (2014). Assessing orbitally-forced interglacial climate variability during the mid-Pliocene Warm Period. *Earth and Planetary Science Letters, 400*, 261-271. doi:10.1016/j.epsl.2014.05.030

Rickaby, R. E., & Halloran, P. (2005). Cool La Niña During the Warmth of the Pliocene? *Science, 307*(5717), 1948-1952. doi:10.1126/science.1104666

Rincón-Martínez, D. (2013). *Eastern Pacific background state and tropical South American climate history during the last 3 million years.* Universität Bremen, Bremen.

Rincón-Martínez, D., Lamy, F., Contreras, S., Leduc, G., Bard, E., Saukel, C., . . . Tiedemann, R. (2010). More humid interglacials in Ecuador during the past 500 kyr linked to latitudinal shifts of the equatorial front and the Intertropical Convergence Zone in the eastern tropical Pacific. *Paleoceanography, 25*. doi:10.1029/2009pa001868

Roubik, D. W., & Moreno P., J. E. (1991). *Pollen and spores of Barro Colorado Island [Panama]* (Vol. 36). St. Louis, MO: Missouri Botanical Garden.

Sklenár, P., Dusková, E., & Balslev, H. (2011). Tropical and Temperate: Evolutionary History of Páramo Flora. *Botanical Review, 77*(2), 71-108. doi:10.1007/s12229-010-9061-9

Spikings, R. A., Winkler, W., Hughes, R. A., & Handler, R. (2005). Thermochronology of allochthonous terranes in Ecuador: Unravelling the accretionary and post-accretionary history of the Northern Andes. *Tectonophysics, 399*(1-4), 195-220. doi:10.1016/j.tecto.2004.12.023

Steph, S., Tiedemann, R., Prange, M., Groeneveld, J., Schulz, M., Timmermann, A., . . . Haug, G. H. (2010). Early Pliocene increase in thermohaline overturning: A precondition for the development of the modern equatorial Pacific cold tongue. *Paleoceanography, 25*(2). doi:10.1029/2008pa001645

Stockmarr, J. (1971). Tablets with spores used in absolute pollen analysis. *Pollen et Spores, XIII*(4), 615-621.

Tiedemann, R., Sturm, A., Steph, S., Lund, S. P., & Stoner, J. S. (2007). Astronomically calibrated timescales from 6 to 2.5 Ma and benthic isotope stratigraphies, sites 1236, 1237, 1239, and 1241. *Proceedings of the Ocean Drilling Program, Scientific Results, 202*. doi:10.2973/odp.proc.sr.202.210.2007

U.S. Army Corps of Engineers. (1998). Water Resources Assessment of Ecuador. Retrieved from https://www.sam.usace.army.mil/Portals/46/docs/military/engineering/docs/WRA/Ecuador/Ecuador%20WRA%20English.pdf

U.S. Geological Survey's Center for Earth Resources Observation and Science (EROS). (1996). Global 30 Arc-Second Elevation (GTOPO30).

Vallé, F., Dupont, L. M., Leroy, S. A. G., Schefuss, E., & Wefer, G. (2014). Pliocene environmental change in West Africa and the onset of strong NE trade winds (ODP Sites 659 and 658). *Palaeogeography Palaeoclimatology Palaeoecology, 414*, 403-414. doi:10.1016/j.palaeo.2014.09.023

Van der Hammen, T. (1985). The Plio-Pleistocene record of the tropical Andes. *Journal of the Geological Society, 142*, 483-489. doi:10.1144/gsjgs.142.3.0483

Van der Hammen, T., & Hooghiemstra, H. (1997). Chronostratigraphy and Correlation of the Pliocene and Quaternary of Colombia. *Quaternary International, 40*, 81-91.

Van der Hammen, T., Werner, J. H., & van Dommelen, H. (1973). Palynological record of the upheaval of the Northern Andes: a study of the Pliocene and Lower Quaternary of the Colombian early evolution of its high-Andean biota. *Review of Palaeobotany and Palynology, 16*, 1-122.

Vuille, M., Bradley, R. S., & Keimig, F. (2000). Climate variability in the Andes of Ecuador and its relation to tropical Pacific and Atlantic Sea surface temperature anomalies. *Journal of Climate, 13*, 2520-2535.

Wara, M. W., Ravelo, A. C., & Delaney, M. L. (2005). Permanent El Niño-like conditions during the Pliocene warm period. *Science, 309*(5735), 758-761. doi:10.1126/science.1112596

Wijninga, V. M. (1996). A Pliocene *Podocarpus* forest mire from the area of the high plain of Bogotá (Cordillera Oriental, Colombia). *Review of Palaeobotany and Palynology, 92*, 157-205.

Wijninga, V. M., & Kuhry, P. (1990). A Pliocene Flora from the Subachoque Valley (Cordillera Oriental, Colombia). *Review of Palaeobotany and Palynology, 62*(3-4), 249-290.

World Wildlife Fund (WWF). Retrieved from https://www.worldwildlife.org/ecoregions/

Wu, F. L., Fang, X. M., Ma, Y. Z., Herrmann, M., Mosbrugger, V., An, Z. S., & Miao, Y. F. (2007). Plio-Quaternary stepwise drying of Asia: Evidence from a 3-Ma pollen record from the Chinese Loess Plateau. *Earth and Planetary Science Letters, 257*(1-2), 160-169. doi:10.1016/j.epsl.2007.02.029

6 Synthesis

The aim of the thesis was to investigate vegetation and climate change in western equatorial South America during the Pliocene by means of palynological analysis of marine sediments. The unique spatio-temporal setting offered the possibility to reconstruct the vegetation history under the influences of climatic factors (such as ITCZ shifts, 'permanent El Niño') and tectonic factors (such as the closure of the Central American Seaway, uplift of the Northern Andes). Since long vegetation records from this time and area are sparse, the aim of this study was to approach several open questions related to the development of the vegetation between 4.7 and 2.7 Ma: (1) How was the vegetation influenced by Andean uplift and what are the implications for the development of the páramo? (2) Which inferences about the regional climate can be drawn from the pollen record? (3) Is the onset of global cooling around 3.3 Ma also reflected in the vegetation of the study area? But first I discuss the caveats of the study.

6.1 Limitations/Challenges of the study

The spatiotemporal setting of the study is characterized by various topographic/tectonic processes and climatic effects which influence each other in a complex way. The main variables considered here are the closure of the CAS, the uplift of the Northern Andes, ENSO and the ITCZ. Poor constraints and disagreement on the timing of both, Andean uplift and CAS closure make it difficult to interpret vegetation changes within this dynamic environment. For instance, Andean uplift causes small to large-scale reorganizations of climate patterns, but in turn, climate also exerts a strong influence on topography. Due to the complex interplay of the mentioned variables, it is not straightforward to attribute certain climatic changes to one particular cause., such as an ITCZ shift or amplified frequency or intensity of ENSO.

An integral part of this marine record is its age model, which provides the basis for comparison with other records and allows to temporally link changes in the vegetation to other events. Since the age model of ODP Site 1239 is based on correlation with the orbitally tuned age model of ODP Site 1241, it includes a systematic error of a few thousand years. This error is based on the assumption that a temporal lag exists between a change of the orbital parameters and the associated climate response. Additionally, the stratigraphic correlation of Site 1241 and Hole 1239A reveals some gaps at core breaks (Tiedemann et al. 2007). Due to (unknown) changes in the sedimentation rate, the linear interpolation between age-depth control points includes some uncertainty. To allow for uncertainties in the age model of a few thousand years, mainly long-term trends over several 10k to 100k years are considered in the interpretation and single data points are attached little importance.

Another aspect is the limitation of pollen identification, as many pollen types can be identified only at genus or family level. However, different species of the same genus may occupy very different ecological niches and/or climatic zones. This lowers the predictive capacity of the method (Twiddle 2012). In this study, this problem was scaled down by making climatic inferences predominantly about vegetation belts rather than single taxa.

Finally, it must be considered that the applicability of paleorecords to predict future climate change is limited, since past warm climates were caused by other forcings (Fischer et al. 2018).

6.2 How was the vegetation influenced by Andean uplift and what are the implications for the development of the paramo?

The presented palynological record represents the Pliocene vegetation of western equatorial South America from the coastal lowlands to the high Andean páramos of the western Andean Cordillera (results are discussed in Chapters 4.5, 4.6, 5.5 and 5.6). Representatives from five ecological groups or vegetation belts are found: lowland rainforest, lower montane forest, upper montane forest, páramo, and broad range taxa. Over the analysed interval between 4.7 Ma and 2.7 Ma, the lowland rainforest pollen makes up 2% (range from 0 to 6%) of the pollen sum on average, the lower montane forest pollen represents 9% (range from 4 to 20%), the upper montane forest pollen 33% (range from 16 to 56%), and the páramo pollen 3% (range from 0 to 8%). The Podocarpaceae share is 24% on average (min: 7%, max: 47%). Faegri (1966) noticed that tropical lowland forests might not produce unique pollen spectra, since the very few characteristic taxa that are anemophilous might cover up the main signal of the >90% zoophilous taxa. Additionally, many taxa can only be determined to the family level. This might explain the fairly small share of lowland rainforest pollen in the record of ODP Site 1239.

During the early Pliocene (Chapter 4), the study area was covered by forests with exception of the open páramo vegetation which was already present. The continuously low pollen percentage of dry indicators (Amaranthaceae) suggests the near-absence of dry vegetation and supports the interpretation of a stable, humid climate. This is in agreement with global climate models indicating warmer and wetter conditions for the Pliocene and an expansion of tropical forests (Salzmann et al. 2011). In the early Pliocene interval of our record (4.7-4.2 Ma), the vegetation belts show parallel rather than opposing trends. This indicates that humidity rather than temperature was the main driver of vegetation change at that time.

During the Piacenzian, specifically between 3.3 and 3.0 Ma, both the sedimentation rate and the pollen concentration notably increase at ODP Site 1239 (see Chapter 5.6.1). This points towards a shift in the amount of transported pollen. Additionally, the vegetation is now richer in taxa that are good pollen producers. After pollen transport and erosion have decreased again (~3.1 Ma), pioneer

plants like *Elaphoglossum* and members from the Poaceae, Asteraceae and Ericaceae families expand and possibly occupy free open habitats. From 2.75 Ma on, montane forest trees (*Hedyosmum*, Podocarpaceae) expand again.

Concerning question (1), the páramo of the Western Andean Cordillera had a steady floristic composition with a neotropical signature (*Jamesonia*/*Eriosorus*, *Huperzia*, and *Polylepis*/*Acaena*) in the early Pliocene (4.7-4.2 Ma). When using the development of páramo vegetation as an indicator for Andean uplift, the taxa grouped as "páramo" should preferably be limited to this vegetation type. Although the taxa in this group have occurrences beyond the páramo, they grow predominantly at and above the upper forest line. Thus, this record is considered to be suitable to broadly infer stages of Andean uplift. After 3.75 Ma, new taxa immigrated to the area from distant floristic realms. *Sisyrinchium* (Iridaceae) was originally native to temperate and cool climate zones of both hemispheres, whereas *Orthrosanthus* (Iridaceae) came from southern temperate areas (Sklenár, Dusková, and Balslev 2011). This temporal development suggests that the páramo was first colonized by neotropical taxa from close localities. These taxa subsequently adapted to the new climatic conditions. Only later, taxa from more distant floristic realms settled there (see Chapter 5.6.2 for full discussion).

6.3 Which inferences about the regional climate can be drawn from the pollen record?

Concerning question (2), the pollen record shows possible influences of ITCZ shifts, the easterly trade winds and ENSO dynamics (mean state). Changes in humidity, inferred from the group of 'humid indicators' and the Fe/K ratio of the sediment, are interpreted to be caused by latitudinal shifts of the ITCZ. Between 4.7 and 4.42 Ma, the pollen record shows an expansion of the lowland rainforest, high relative abundances of humid indicators and a high Fe/K ratio, pointing towards a southward displacement of the ITCZ. This interval was followed by a less humid phase (4.42-4.26 Ma) when humid indicators, lowland rainforest pollen, lower montane forest pollen and the Fe/K ratio decreased. At that time, the ITCZ might have had a more northern position. An increase of Amaranthaceae pollen after 3.1 Ma indicates an enlargement of the coastal desert, whereas humidity was still abundant in the montane forest (see also Chapter 5.6.4).

An intensification of the easterly trade winds is proposed to be responsible for an increased eolian transport of Podocarpaceae pollen at 4.63 Ma and between 4.4 and 4.25 Ma. An increased trade wind strength after 4.4 Ma would have coincided with a shift of the location of maximum opal accumulation rates in the eastern equatorial Pacific (Farrell et al. 1995). Furthermore, the thermocline shoaled between 4.8 and 4.0 Ma (Steph, Tiedemann, Groeneveld, et al. 2006), which may have been caused by stronger trade winds as shown by dynamic modeling (Zhang et al. 2012).

An influence of El Niño-related variations on the coastal and montane vegetation appears in the pollen record between 4.7 and 4.55 Ma and around 4.2 Ma, when pollen percentages of the respective vegetation belts strongly fluctuate. Since they do not show a pattern indicating extensive altitudinal shifts, these dynamic changes suggest that moisture availability might have been the main factor driving vegetation changes in the early Pliocene. In the Piacenzian, the climate was stable and warm until 3.5 Ma, when shifts of the upper forest line point to temperature fluctuations towards cooler conditions (see also Chapter 5.6.2).

6.4 Is the onset of global cooling around 3.3 Ma also reflected in the vegetation of the study area?

Concerning question (3), the start of the major climate transition from the warm Pliocene to the cooler Pleistocene with its glacial-interglacial oscillations is indicated globally by different events, such as the first occurrence of ice rafted debris from the Greenland ice sheet at 3.3 Ma (Flesche Kleiven et al. 2002), cooling temperatures in the Northern Hemisphere shown by vegetation records from northern Norway (Panitz et al. 2016), Central Asia (Demske, Mohr, and Oberhansli 2002) and northern Siberia (Andreev et al. 2014; Brigham-Grette et al. 2013), and a growing ice volume as reflected by global benthic oxygen isotopes (Lisiecki and Raymo 2005). In our pollen record from tropical South America, first indication of cooling is shown by shifts of the upper forest line after 3.5 Ma, when the abundance of upper montane forest pollen decreases. Around 3.3 Ma, the forest line may have remained at a lower position, indicating cooler conditions. The SST at ODP site 846 (EEP) decreased at the same time (Lawrence, Liu, and Herbert 2006). While the abundance of upper montane forest decreased, the abundance of páramo vegetation and some associated taxa (Asteraceae Tubuliflorae, Poaceae, Ericaceae) increased. This trend continues until 2.75 Ma, with páramo pollen showing maximum abundances during the glacial stages MG4, M2 and KM2. Thus, the cooling trend in the study area starts before the M2 glacial, which is the first prominent glacial peak of the LR04 stack (~3.3 Ma; Lisiecki and Raymo 2005).

The shifting extent of the vegetation belts during glacial-interglacial climatic oscillations shows that páramo pollen has glacial maxima whereas lowland rainforest pollen shows minima during glacials. Thus, the expansion and contraction reflecting the response of the vegetation to glacial-interglacial climatic variability apparently affects all vegetation belts. After 3.1 Ma, an increase of Amaranthaceae pollen suggests an expansion of the coastal desert. This coastal drying trend would have predated other global climatic shifts associated with the intensification of the Northern Hemisphere glaciation, e.g. the strengthening of the NE trade winds around 2.7 Ma (Vallé et al. 2014; Yang and Ding 2010; Naafs et al. 2012) and the aridification of Central Asia after 2.6 Ma (Cai et al. 2012; Wu et al. 2007).

The environmental changes in western equatorial South America occurred contemporaneously with the first event of ice-rafted debris and cooling climate in the Northern Hemisphere, signaling that this development could be a precursor of the intensification of the Northern Hemisphere glaciation.

6.5 Hypothesis testing

The research questions discussed above are the basis for the investigation of the three hypotheses which may now be revisited.

1) The ITCZ shifted southwards after the surface water exchange between the Pacific and Atlantic Ocean through the CAS became restricted between 4.7 and 4.2 Ma, resulting in increased precipitation in Ecuador.

Hydrological changes were recorded by two complementary proxies: the indicators of humid conditions, a group consisting of pollen and spores that need permanently humid conditions, and the elemental ratio of Fe/K in the sediment, a tracer of fluvial input. Within the regarded interval, the observed hydrological changes in both records, pollen and Fe/K, are generally rather small. Between 4.55 and 4.42 Ma, increasing humidity in the record (expressed through high relative abundances of indicators of humid conditions and lowland rainforest pollen and a high Fe/K ratio) points towards a southward shift of the ITCZ. This interval was followed by a less humid phase between 4.42 and 4.26 Ma, recorded by decreasing pollen percentages of humid indicators, lowland rainforest, lower montane forest, and a lower Fe/K ratio. During this phase, the ITCZ might have shifted slightly northward. Eolian deposition patterns from the EEP indicate a mean southward shift of the ITCZ between 6 and 4 Ma (Hovan 1995). The overall stable and permanently humid conditions rather support a southerly position of the ITCZ in the early Pliocene, despite a short less humid phase. Another main factor that could have influenced humidity in the study region, uplift induced orographic precipitation change, can be excluded since according to our reconstruction of páramo vegetation, the Andes had already reached high elevations by the early Pliocene.

2) The Walker circulation (WC) strengthened before the intensification of the Northern Hemisphere glaciations (iNHG), between 3.6 and 3.1 Ma, resulting in further changes in vegetation and hydrology of Ecuador.

Model simulations yield contrasting results regarding the strength of the WC during the Pliocene (MPWP) and the mechanism behind it. Yan et al. (2021) emphasize that not only the intensity of the WC changes over time, but also its width and its longitudinal position. In the Pliocene, the Pacific WC shifted eastwards and weakened, which is linked to the closure of the tropical seaways

(Indonesian and Panamanian; Yan et al. 2021). Different model simulations carried out with the same boundary and forcing conditions disagree regarding changes of the WC and the mean climate state of the Pacific. CESM1.2 and CESM2 show a weakened WC and an El-Niño like mean state of the tropical Pacific during the MPWP compared to preindustrial. On the contrary, CCSM4 shows a strengthened WC and a tropical Pacific mean climate state similar to preindustrial (Feng et al. 2020).

In the present-day setting, a strengthening of the WC with strong trade winds, low sea surface temperatures and a shallow thermocline in the EEP would cause aridity in the lowlands of southwestern Ecuador and northern Peru, comparable to La Niña conditions (Waylen and Poveda 2002). Our pollen record indicates a development towards drier coastal conditions in southern Ecuador starting from ~3.1 Ma. This shift is recorded by an increasing abundance of Amaranthaceae pollen. Climate reconstructions indicate steadily decreasing SSTs in the EEP (ODP Sites 1239 and 846; Etourneau et al. 2010; Lawrence, Liu, and Herbert 2006), an enlarged zonal SST gradient in the tropical Pacific between 3.6 and 3.1 Ma (Fedorov et al. 2013) and a shoaling thermocline in the eastern Pacific after 3.5 Ma (Ronge, Nurnberg, and Tiedemann 2020; Cannariato and Ravelo 1997). Taken together, this would be in accordance with a strengthened WC at ~3.1 Ma. However, since this inference is based on a single pollen type, it must be treated with caution. It is not considered to be robust enough to draw definite conclusions about the strength of the WC.

3) Assuming a similar uplift history of both, the Eastern and Western Cordillera of the Northern Andes, the páramos of both Cordilleras also developed under temporally similar conditions, after ~3 Ma.

The pollen record from ODP Site 1239 shows a continuous existence of páramo vegetation since 6 Ma (late Miocene). During the warm Pliocene, the upper montane forest presumably extended to altitudes at least as high as today. Despite this probable upslope migration of the upper montane forest belt, the páramo was still represented in the pollen record, implying that the Western Cordillera of the Ecuadorian Andes had already reached substantial elevations by that time. Furthermore, the pollen record would not have such a large montane signature if the Andes had reached less than half of their modern elevation by the early Pliocene (Coltorti and Ollier 2000). The upper montane forest makes up up to 60% of the pollen sum, showing that montane habitats were already existent. Taken together, these findings suggest an earlier development of the páramo ecosystem compared to the area of the high plain of Bogotá (Eastern Cordillera, Colombia), where evidence of páramo vegetation is not found until the late Pliocene (Hooghiemstra, Wijninga, and Cleef 2006; Van der Hammen, Werner, and van Dommelen 1973). Thus, our paleobotanical data

indicates that the development of páramo vegetation in the Western Andean Cordillera preceded this development in the Eastern Cordillera by around 3 Ma. These results go well together with current paleoaltimetry research, suggesting that the formation of the Northern Andes was highly diachronous (Boschman 2021 and references therein).

In the Central Andean Plateau, the earliest evidence for a Puna-like ecosystem is from Pliocene times (Martinez et al. 2020). Palynomorphs from the páramo were found in sediments of the Amazon Fan since 5.4 Ma (Hoorn et al. 2017). Since the westernmost source of the Amazon is in Peru, this signal is possibly related to the uplift of the Central Andes. The earliest evidence for páramo vegetation in the northern Andes is now from the late Miocene. Although the emergence of the páramo ecosystem dates back into the Miocene, its diversification took place mainly during Pleistocene times (Madriñán, Cortes, and Richardson 2013).

6.6 Outlook

More studies investigating the timing of Andean uplift, especially of the Northern Andean Western Cordillera, are required in order to better constrain paleoaltitudes. More reliable uplift estimates could help with the interpretation of paleovegetation and -climate records. Uplift estimates incorporated in climate models could also yield more accurate modelling results. On the other hand, extending the pollen record of ODP Site 1239 further back into the Miocene could elucidate the beginnings of the development of the high montane ecosystem. Although this method would not yield precise paleoaltitudes, it could be one further step in constraining the uplift history of the Western Cordillera.

In order to disentangle the effects of Andean uplift, CAS closure, El Niño and ITCZ shifts on the vegetation and climate of northwestern South America, more marine and terrestrial records from different proxies are needed, for instance, analysis of stable carbon isotopes of plant waxes to determine the ratio of C3 and C4 plants in the vegetation. This could complement the pollen record and indicate changes in precipitation, temperature and pCO_2 (as shown by Boom et al. 2001 for the Colombian páramo).

6.7 References

Anderson, V. J., J. E. Saylor, T. M. Shanahan, and B. K. Horton. 2015. 'Paleoelevation records from lipid biomarkers: Application to the tropical Andes', *Geological Society of America Bulletin*, 127: 1604-16.

Andreev, A. A., P. E. Tarasov, V. Wennrich, E. Raschke, U. Herzschuh, N. R. Nowaczyk, J. Brigham-Grette, and M. Melles. 2014. 'Late Pliocene and Early Pleistocene vegetation history of northeastern Russian Arctic inferred from the Lake El'gygytgyn pollen record', *Climate of the Past*, 10: 1017-39.

Andriessen, P. A. M., K. F. Helmens, H. Hooghiemstra, P. A. Riezebos, and T. Van der Hammen. 1993. 'Absolute Chronology of the Pliocene-Quaternary Sediment Sequence of the Bogotá Area, Colombia', *Quaternary Science Reviews*, 12: 483-501.

Balslev, H. 1988. 'Distribution Patterns of Ecuadorean Plant-Species', *Taxon*, 37: 567-77.

Barnes, J. B., T. A. Ehlers, N. Insel, N. McQuarrie, and C. J. Poulsen. 2012. 'Linking orography, climate, and exhumation across the central Andes', *Geology*, 40: 1135-38.

Bartoli, G., M. Sarnthein, M. Weinelt, H. Erlenkeuser, D. Garbe-Schönberg, and D. W. Lea. 2005. 'Final closure of Panama and the onset of northern hemisphere glaciation', *Earth and Planetary Science Letters*, 237: 33-44.

Behling, H., H. Hooghiemstra, and A. J. Negret. 1998. 'Holocene history of the Choco Rain Forest from Laguna Piusbi, Southern Pacific Lowlands of Colombia', *Quaternary Research*, 50: 300-08.

Bendix, A. , and J. Bendix. 2006. 'Heavy rainfall episodes in Ecuador during El Nino events and associated regional atmospheric circulation and SST patterns', *Advances in Geosciences*, 6: 43-49.

Bendix, J., and W. Lauer. 1992. 'Die Niederschlagsjahreszeiten in Ecuador und ihre klimadynamische Interpretation', *Erdkunde*, 46: 118-34.

Billups, K., A. C. Ravelo, J. C. Zachos, and R.D. Norris. 1999. 'Link between oceanic heat transport, thermohaline circulation, and the Intertropical Convergence Zone in the early Pliocene Atlantic', *Geology*, 24: 319-22.

Boom, A., G. Mora, A. M. Cleef, and H. Hooghiemstra. 2001. 'High altitude C-4 grasslands in the northern Andes: relicts from glacial conditions?', *Review of Palaeobotany and Palynology*, 115: 147-60.

Boschman, L. M. 2021. 'Andean mountain building since the Late Cretaceous: A paleoelevation reconstruction', *Earth-Science Reviews*, 220.

Brierley, C. M., A. V. Fedorov, Z. Liu, T. D. Herbert, K. T. Lawrence, and J. P. Lariviere. 2009. 'Greatly expanded tropical warm pool and weakened Hadley circulation in the early Pliocene', *Science*, 323: 1714-8.

Brigham-Grette, J., M. Melles, P. Minyuk, A. Andreev, P. Tarasov, R. DeConto, S. Koenig, N. Nowaczyk, V. Wennrich, P. Rosen, E. Haltia, T. Cook, C. Gebhardt, C. Meyer-Jacob, J. Snyder, and U. Herzschuh. 2013. 'Pliocene Warmth, Polar Amplification, and Stepped Pleistocene Cooling Recorded in NE Arctic Russia', *Science*, 340: 1421-27.

Brown, E., A. Colling, D. Park, J. Phillips, D. Rothery, and J. Wright. 2001. *Ocean circulation* (Butterworth-Heinemann Milton Keynes).

Bush, Mark B., and Chengyu Weng. 2007. 'Introducing a new (freeware) tool for palynology', *Journal of Biogeography*, 34: 377-80.

Cai, M. T., X. M. Fang, F. L. Wu, Y. F. Miao, and E. Appel. 2012. 'Pliocene-Pleistocene stepwise drying of Central Asia: Evidence from paleomagnetism and sporopollen record of the deep borehole SG-3 in the western Qaidam Basin, NE Tibetan Plateau', *Global and Planetary Change*, 94-95: 72-81.

Cannariato, K. G., and A. C. Ravelo. 1997. 'Pliocene-Pleistocene evolution of eastern tropical Pacific surface water circulation and thermocline depth', *Paleoceanography*, 12: 805-20.

Chandan, D., and W. R. Peltier. 2017. 'Regional and global climate for the mid-Pliocene using the University of Toronto version of CCSM4 and PlioMIP2 boundary conditions', *Climate of the Past*, 13: 919-42.

Colinvaux, P., P. E. De Oliveira, and J. E. Moreno Patino. 1999. *Amazon Pollen Manual and Atlas* (Harwood Academic Publishers: Amsterdam).

Coltorti, M., and C. D. Ollier. 2000. 'Geomorphic and tectonic evolution of the Ecuadorian Andes', *Geomorphology*, 32: 1-19.

Contoux, C., G. Ramstein, and A. Jost. 2012. 'Modelling the mid-Pliocene Warm Period climate with the IPSL coupled model and its atmospheric component LMDZ5A', *Geoscientific Model Development*, 5: 903-17.

Corredor, F. 2003. 'Eastward extent of the Late Eocene-Early Oligocene onset of deformation across the northern Andes: constraints from the northern portion of the Eastern Cordillera fold belt, Colombia', *Journal of South American Earth Sciences*, 16: 445-57.

CPC Merged Analysis of Precipitation. Accessed February 2008. https://www.esrl.noaa.gov/psd/data/gridded/data.ncep.reanalysis.derived.html.

Demske, D., B. Mohr, and H. Oberhansli. 2002. 'Late Pliocene vegetation and climate of the Lake Baikal region, southern East Siberia, reconstructed from palynological data', *Palaeogeography Palaeoclimatology Palaeoecology*, 184: 107-29.

Dowsett, H., J. Barron, and R. Poore. 1996. 'Middle Pliocene sea surface temperatures: a global reconstruction', *Marine Micropaleontology*, 27: 13-25.

Dowsett, H., A. Dolan, D. Rowley, R. Moucha, A. M. Forte, J. X. Mitrovica, M. Pound, U. Salzmann, M. Robinson, M. Chandler, K. Foley, and A. Haywood. 2016. 'The PRISM4 (mid-Piacenzian) paleoenvironmental reconstruction', *Climate of the Past*, 12: 1519-38.

Dupont, L. M. 2006. 'Late Pliocene vegetation and climate in Namibia (southern Africa) derived from palynology of ODP Site 1082', *Geochemistry Geophysics Geosystems*, 7: 1-15.

ETOPO1. Accessed June 2018. https://maps.ngdc.noaa.gov/viewers/wcs-client/.

Etourneau, J., R. Schneider, T. Blanz, and P. Martinez. 2010. 'Intensification of the Walker and Hadley atmospheric circulations during the Pliocene–Pleistocene climate transition', *Earth and Planetary Science Letters*, 297: 103-10.

Faegri, K. 1966. 'Some problems of representativity in pollen analysis', *The Palaeobotanist*, 1: 135-40.

Faegri, K., and J. Iversen. 1989. *Textbook of Pollen Analysis* (John Wiley & Sons: Chichester).

Farrell, J.W., I. Raffi, T.R. Janecek, D.W. Murray, M. Levitan, K.A. Dadey, K.-C. Emeis, M. Lyle, J. A. Flores, and S. Hovan. 1995. 'Late Neogene Sedimentation Patterns in the eastern equatorial Pacific Ocean', *Proceedings of the Ocean Drilling Program, Scientific Results*, 138: 717-56.

Fedorov, A. V., C. M. Brierley, K. T. Lawrence, Z. Liu, P. S. Dekens, and A. C. Ravelo. 2013. 'Patterns and mechanisms of early Pliocene warmth', *Nature*, 496: 43-9.

Fedorov, A. V., N. J. Burls, K. T. Lawrence, and L. C. Peterson. 2015. 'Tightly linked zonal and meridional sea surface temperature gradients over the past five million years', *Nature Geoscience*, 8: 975-83.

Fedorov, A. V., P. S. Dekens, M. McCarthy, A. C. Ravelo, P. B. deMenocal, M. Barreiro, R. C. Pacanowski, and S. G. Philander. 2006. 'The Pliocene paradox (mechanisms for a permanent El Niño)', *Science*, 312: 1485-9.

Feng, R., B. L. Otto-Bliesner, E. C. Brady, and N. Rosenbloom. 2020. 'Increased Climate Response and Earth System Sensitivity From CCSM4 to CESM2 in Mid-Pliocene Simulations', *Journal of Advances in Modeling Earth Systems*, 12: 1-17.

Feng, R., and C. J. Poulsen. 2014. 'Andean elevation control on tropical Pacific climate and ENSO', *Paleoceanography*, 29: 795–809.

Fischer, H., K. J. Meissner, A. C. Mix, N. J. Abram, J. Austermann, V. Brovkin, E. Capron, D. Colombaroli, A. L. Daniau, K. A. Dyez, T. Felis, S. A. Finkelstein, S. L. Jaccard, E. L. McClymont, A. Rovere, J. Sutter, E. W. Wolff, S. Affolter, P. Bakker, J. A. Ballesteros-Canovas, C. Barbante, T. Caley, A. E. Carlson, O. Churakova, G. Cortese, B. F. Cumming, B. A. S. Davis, A. de Vernal, J. Emile-Geay, S. C. Fritz, P. Gierz, J. Gottschalk, M. D. Holloway, F. Joos, M. Kucera, M. F. Loutre, D. J. Lunt, K. Marcisz, J. R. Marlon, P. Martinez, V. Masson-Delmotte, C. Nehrbass-Ahles, B. L. Otto-Bliesner, C. C. Raible, B. Risebrobakken, M. F. S. Goni, J. S. Arrigo, M. Sarnthein, J. Sjolte, T. F. Stocker, P. A. V. Alvarez, W. Tinner, P. J. Valdes, H. Vogel, H. Wanner, Q. Yan, Z. C. Yu, M. Ziegler, and L. P. Zhou. 2018. 'Palaeoclimate constraints on the impact of 2 degrees C anthropogenic warming and beyond', *Nature Geoscience*, 11: 615-15.

Flantua, S., H. Hooghiemstra, J.H. Van Boxel, M. Cabrera, Z. González-Carranza, and C. González-Arango. 2014. 'Connectivity dynamics since the last glacial maximum in the northern Andes: a pollen-driven framework to assess potential migration.' in W. D. Stevens, O. M. Montiel and P. H. Raven (eds.), *Paleobotany and Biogeography: A Festschrift for Alan Graham in His 80th Year* (Missouri Botanical Garden Press: St. Louis).

Flesche Kleiven, H., E. Jansen, T. Fronval, and T. M. Smith. 2002. 'Intensification of Northern Hemisphere glaciations in the circum Atlantic region (3.5-2.4 Ma) - ice-rafted detritus evidence', *Palaeogeography Palaeoclimatology Palaeoecology*, 184: 213-23.

Flohn, H. 1981. 'A hemispheric circulation asymmetry during Late Tertiary', *Geologische Rundschau*, 70: 725-36.

Ford, H. L., A. C. Ravelo, P. S. Dekens, J. LaRiviere, and M. W. Wara. 2015. 'The evolution of the equatorial thermocline and the early Pliocene El Padre mean state', *Geophysical Research Letters*, 42: 4878-87.

Garzione, C. N., G. D. Hoke, J. C. Libarkin, S. Withers, B. MacFadden, J. Eiler, P. Ghosh, and A. Mulch. 2008. 'Rise of the Andes', *Science*, 320: 1304-7.

Gentry, A. H. 1982. 'Neotropical Floristic Diversity - Phytogeographical Connections between Central and South-America, Pleistocene Climatic Fluctuations, or an Accident of the Andean Orogeny', *Annals of the Missouri Botanical Garden*, 69: 557-93.

———. 1986. 'Species richness and floristic composition of Chocó region plant communities', *Caldasia*, 15: 71-91.

González, C., L. E. Urrego, and J. I. Martínez. 2006. 'Late Quaternary vegetation and climate change in the Panama Basin: Palynological evidence from marine cores ODP 677B and TR 163-38', *Palaeogeography, Palaeoclimatology, Palaeoecology*, 234: 62-80.

Govin, A., U. Holzwarth, D. Heslop, L. Ford Keeling, M. Zabel, S. Mulitza, J. A. Collins, and C. M. Chiessi. 2012. 'Distribution of major elements in Atlantic surface sediments (36°N-49°S): Imprint of terrigenous input and continental weathering', *Geochemistry, Geophysics, Geosystems*, 13: 1-23.

Gregory-Wodzicki, K. M. 2000. 'Uplift history of the Central and Northern Andes: A review', *Geological Society of America Bulletin*, 112: 1091-105.

Grimm, EC. 1991. "Tilia and Tiliagraph." In. Springfield: Illinois State Museum.

Grimmer, F., L. Dupont, F. Lamy, G. Jung, C. Gonzalez, and G. Wefer. 2018. 'Early Pliocene vegetation and hydrology changes in western equatorial South America', *Climate of the Past*, 14: 1739-54.

Groeneveld, J., E. C. Hathorne, S. Steinke, H. DeBey, A. Mackensen, and R. Tiedemann. 2014. 'Glacial induced closure of the Panamanian Gateway during Marine Isotope Stages (MIS) 95–100', *Earth and Planetary Science Letters*, 404: 296-306.

Hagemans, K., C.-D. Tóth, M. Ormaza, W. D. Gosling, D. H. Urrego, S. León-Yánez, F. Wagner-Cremer, and T. H. Donders. 2019. 'Modern pollen-vegetation relationships along a steep temperature gradient in the Tropical Andes of Ecuador', *Quaternary Research*: 1-13.

Haug, G. H., and R. Tiedemann. 1998. 'Effect of the formation of the Isthmus of Panama on Atlantic Ocean thermohaline circulation', *Nature*, 393: 673-76.

Haug, G. H., R. Tiedemann, R. Zahn, and A. C. Ravelo. 2001. 'Role of Panama uplift on oceanic freshwater balance', *Geology*, 29: 207-10.

Haywood, A. M., H. J. Dowsett, and A. M. Dolan. 2016. 'Integrating geological archives and climate models for the mid-Pliocene warm period', *Nature Communications*, 7:10646: 1-14.

Herbert, J. 2005. 'Systematics and Biogeography of Myricaceae', University of St Andrews.

Hooghiemstra, H. 1984. *Vegetational and Climatic History of the High Plain of Bogotá, Colombia: A Continuous Record of the Last 3.5 Million Years* (A.R. Gantner Verlag K.G.: Vaduz).

———. 1989. 'Quaternary and Upper-Pliocene Glaciations and Forest Development in the Tropical Andes - Evidence from a Long High-Resolution Pollen Record from the Sedimentary Basin of Bogotá, Colombia', *Palaeogeography Palaeoclimatology Palaeoecology*, 72: 11-26.

Hooghiemstra, H., and E. Th. H. Ran. 1994a. 'Late Pliocene-Pleistocene high resolution pollen sequence of Colombia: An overview of climatic change', *Quaternary International*, 21: 63-80.

Hooghiemstra, H., V. M. Wijninga, and A. M. Cleef. 2006. 'The Paleobotanical Record of Colombia: Implications for Biogeography and Biodiversity', *Annals of the Missouri Botanical Garden*, 93: 297-325.

Hoorn, C., G.R. Bogotá-A., M. Romero-Baez, E.I. Lammertsma, S. Flantua, E.L. Dantas, R. Dino, D.A. do Carmo, and F. Chemale Jr. 2017. 'The Amazon at sea: Onset and stages of the Amazon River from a marine record, with special reference to Neogene plant turnover in the drainage basin', *Global and Planetary Change*, 153: 51-65.

Hoorn, C., and S. Flantua. 2015. 'An early start for the Panama land bridge', *Science*, 348: 186-87.

Hoorn, C., J. Guerrero, G.A. Sarmiento, and M.A. Lorente. 1995. 'Andean tectonics as a cause for changing drainage patterns in Miocene northern South America', *Geology*, 23: 237-40.

Hoorn, C., F. P. Wesselingh, H. ter Steege, M. A. Bermudez, A. Mora, J. Sevink, I. Sanmartin, A. Sanchez-Meseguer, C. L. Anderson, J. P. Figueiredo, C. Jaramillo, D. Riff, F. R. Negri, H. Hooghiemstra, J. Lundberg, T. Stadler, T. Sarkinen, and A. Antonelli. 2010. 'Amazonia through time: Andean uplift, climate change, landscape evolution, and biodiversity', *Science*, 330: 927-31.

Hovan, S. A. . 1995. 'Late Cenozoic atmospheric circulation intensity and climatic history recorded by Eolian deposition in the Eastern Equatorial Pacific Ocean, Leg 138', *Proceedings of the Ocean Drilling Program, Scientific Results*, 138: 615-25.

Hurtado, C., M. Roddaz, R. Ventura Santos, P. Baby, P.-O. Antoine, and E.L. Dantas. 2018. 'Late Cretaceous-early Paleocene drainage shift of Amazonian rivers driven by Equatorial Atlantic Ocean opening and Andean uplift as deduced from the provenance of northern Peruvian sedimentary rocks (Huallaga basin)', *Gondwana Research*, 63: 152-68.

Jørgensen, P. M., and S. León-Yánez. 1999. *Catalogue of the vascular plants of Ecuador = Catálogo de las plantas vasculares del Ecuador* (Missouri Botanical Garden Press: St. Louis, Missouri).

Kaandorp, R. J. G., F. P. Wesselingh, and H. B. Vonhof. 2006. 'Ecological implications from geochemical records of Miocene Western Amazonian bivalves', *Journal of South American Earth Sciences*, 21: 54-74.

Kamae, Y., H. Ueda, and A. Kitoh. 2011. 'Hadley and Walker Circulations in the Mid-Pliocene Warm Period Simulated by an Atmospheric General Circulation Model', *Journal of the Meteorological Society of Japan*, 89: 475-93.

Kessler, M. 2002. 'The "Polylepis problem": Where do we stand?', *Ecotropica*, 8: 97-110.

Kessler, W. S. 2006. 'The circulation of the eastern tropical Pacific: A review', *Progress in Oceanography*, 69: 181-217.

Lawrence, K. T., Z. Liu, and T. D. Herbert. 2006. 'Evolution of the eastern tropical Pacific through Plio-Pleistocene glaciation', *Science*, 312: 79-83.

Li, G., and S. P. Xie. 2014. 'Tropical Biases in CMIP5 Multimodel Ensemble: The Excessive Equatorial Pacific Cold Tongue and Double ITCZ Problems', *Journal of Climate*, 27: 1765-80.

Lisiecki, L. E., and M. E. Raymo. 2005. 'A Pliocene-Pleistocene stack of 57 globally distributed benthic $\delta^{18}O$ records', *Paleoceanography*, 20: 1-17.

Lozano, P., R. W. Bussmann, and M. Küppers. 2007. 'A checklist of pioneer plant regeneration on natural and anthropogenic landslides on the eastern side of Podocarpus National Park-Southern Ecuador', *Redesma*, 1: 1-15.

Luteyn, J. L. 1999. *Páramos* (Memoirs of The New York Botanical Garden).

Madriñán, S., A. J. Cortes, and J. E. Richardson. 2013. 'Páramo is the world's fastest evolving and coolest biodiversity hotspot', *Frontiers in Genetics*, 4: 1-7.

Maher, L. J. 1972. 'Nomograms for computing 0.95 confidence limits of pollen data', *Review of Palaeobotany and Palynology*, 13: 85-93.

———. 1981. 'Statistics for Microfossil Concentration Measurements Employing Samples Spiked with Marker Grains', *Review of Palaeobotany and Palynology*, 32: 153-91.

Marchant, R., L. Almeida, H. Behling, J. C. Berrio, M. Bush, A. Cleef, J. Duivenvoorden, M. Kappelle, P. De Oliveira, A. Teixeira de Oliveira-Filho, S. Lozano-Garcia, H. Hooghiemstra, M.-P. Ledru, B. Ludlow-Wiechers, V. Markgraf, V. Mancini, M. Paez, A. Prieto, O. Rangel, and M. Salgado-Labouriau. 2002. 'Distribution and ecology of parent taxa of pollen lodged within the Latin American Pollen Database', *Review of Palaeobotany and Palynology*, 121: 1-75.

Marchant, R., H. Behling, J. C. Berrio, A. Cleef, J. Duuivenvoorden, H. Hooghiemstra, P. Kuhry, B. Melief, B. Van Geel, T. Van der Hammen, G. Van Reenen, and M. Wille. 2001. 'Mid- to Late-Holocene pollen-based biome reconstructions for Colombia', *Quaternary Science Reviews*, 20: 1289-308.

Martinez, C., C. Jaramillo, A. Correa-Metrio, W. Crepet, J. E. Moreno, A. Aliaga, F. Moreno, M. Ibanez-Mejia, and M. B. Bush. 2020. 'Neogene precipitation, vegetation, and elevation history of the Central Andean Plateau', *Science Advances*, 6: 1-9.

Milliman, J. D., and K. L. Farnsworth. 2011. *River discharge to the coastal ocean: a global synthesis* (Cambridge University Press: Cambridge; New York).

Montes, C., A. Cardona, C. Jaramillo, A. Pardo, J.C. Silva, V. Valencia, C. Ayala, L.C. Pérez-Angel, L.A. Rondriguez-Parra, V. Ramirez, and H. Nino. 2015. 'Middle Miocene closure of the Central American Seaway', *Paleoceanography*, 348: 226-29.

Mora-Páez, Héctor, David J. Mencin, Peter Molnar, Hans Diederix, Leonardo Cardona-Piedrahita, Juan-Ramón Peláez-Gaviria, and Yuli Corchuelo-Cuervo. 2016. 'GPS velocities and the construction of the Eastern Cordillera of the Colombian Andes', *Geophysical Research Letters*, 43: 8407-16.

Mora, A., M. Parra, M.R. Strecker, E.R. Sobel, H. Hooghiemstra, V. Torres, and J.V. Jaramillo. 2008. 'Climatic forcing of asymmetric orogenic evolution in the Eastern Cordillera of Colombia', *GSA Bulletin*, 120: 930-49.

Mudelsee, M., and M. E. Raymo. 2005. 'Slow dynamics of the Northern Hemisphere glaciation', *Paleoceanography*, 20: 1-14.

Mulitza, S., M. Prange, J. B. Stuut, M. Zabel, T. von Dobeneck, A. C. Itambi, J. Nizou, M. Schulz, and G. Wefer. 2008. 'Sahel megadroughts triggered by glacial slowdowns of Atlantic meridional overturning', *Paleoceanography*, 23: 1-11.

Murillo, M. T., and M. J. M. Bless. 1974. 'Spores of recent Colombian Pteridophyta. I. Trilete Spores', *Review of Palaeobotany and Palynology*, 18: 223-69.

———. 1978. 'Spores of recent Colombian Pteridophyta. II. Monolete Spores', *Review of Palaeobotany and Palynology*, 25: 319-65.

Naafs, B. D. A., J. Hefter, G. Acton, G. H. Haug, A. Martinez-Garcia, R. Pancost, and R. Stein. 2012. 'Strengthening of North American dust sources during the late Pliocene (2.7 Ma)', *Earth and Planetary Science Letters*, 317: 8-19.

NCEP reanalysis data provided by the NOAA/OAR/ESRL PSD, Boulder, Colorado, USA,. Accessed January 2010. http://www.esrl.noaa.gov/psd/data/gridded/data.ncep.reanalysis.derived.html

Niemann, H., C. Brunschön, and H. Behling. 2010. 'Vegetation/modern pollen rain relationship along an altitudinal transect between 1920 and 3185 m a.s.l. in the Podocarpus National Park region, southeastern Ecuadorian Andes', *Review of Palaeobotany and Palynology*, 159: 69-80.

NODC (Levitus) World Ocean Atlas. 1994. Accessed March 2010. http://www.esrl.noaa.gov/psd/data/gridded/data.nodc.woa94.html.

O'Dea, A. , A.H. Lessios, A.G. Coates, R.I. Eytan, S.A. Restrepo-Moreno, A.L. Cione, L.S. Collins, A. de Queiroz, D.W. Farris, R.D. Norris, R.F. Stallard, M.O. Woodburne, O. Aguilera, M.-P. Aubry, W.A. Berggren, A.F. Budd, M.A. Cozzuol, S.E. Coppard, H. Duque-Caro, S. Finnegan, G.M. Gasparini, E.L. Grossman, K.G. Johnson, L.D. Keigwin, N. Knowlton, E.G. Leigh, J.S. Leonard-Pingel, P.B. Marko, N.D. Pyenson, P.G. Rachello-Dolmen, E. Soibelzon, L. Soibelzon, J.A. Todd, G.J. Vermeij, and J.B.C. Jackson. 2016. 'Formation of the Isthmus of Panama', *Science Advances*, 2: 1-11.

Pak, H., and J. R. Zaneveld. 1974. 'Equatorial Front in the Eastern Pacific Ocean', *Journal of Physical Oceanography*, 4: 570-78.

Panitz, S., U. Salzmann, B. Risebrobakken, S. De Schepper, and M. J. Pound. 2016. 'Climate variability and long-term expansion of peatlands in Arctic Norway during the late Pliocene (ODP Site 642, Norwegian Sea)', *Climate of the Past*, 12: 1043-60.

Pazmiño Manrique, N. A. 2005. 'Sediment distribution and depositional processes on the Carnegie Ridge', Texas A&M University.

Perez-Angel, L. C., and P. Molnar. 2017. 'Sea Surface Temperatures in the Eastern Equatorial Pacific and Surface Temperatures in the Eastern Cordillera of Colombia During El Niño: Implications for Pliocene Conditions', *Paleoceanography*, 32: 1309-14.

Pettke, T., A. N. Halliday, and D. K. Rea. 2002. 'Cenozoic evolution of Asian climate and sources of Pacific seawater Pb and Nd derived from eolian dust of sediment core LL44-GPC3', *Paleoceanography*, 17: 1-13.

Pisias, N. 1995. 'Paleoceanography of the eastern equatorial Pacific during the Neogene: Synthesis of Leg 138 drilling results', *Proceedings of the Ocean Drilling Program, Scientific Results*, 138: 5-21.

Pourrut, P. 1995. *El agua en el Ecuador: clima, precipitaciones, escorrentía* (Colegio de Geógrafos del Ecuador: Corporación Editora Nacional: Quito).

Prescott, C. L., A. M. Dolan, A. M. Haywood, S. J. Hunter, and J. C. Tindall. 2018. 'Regional climate and vegetation response to orbital forcing within the mid-Pliocene Warm Period: A study using HadCM3', *Global and Planetary Change*, 161: 231-43.

Prescott, C. L., A. M. Haywood, A. M. Dolan, S. J. Hunter, J. O. Pope, and S. J. Pickering. 2014. 'Assessing orbitally-forced interglacial climate variability during the mid-Pliocene Warm Period', *Earth and Planetary Science Letters*, 400: 261-71.

Ravelo, A. C., D. H. Andreasen, M. W. Lyle, A. O. Lyle, and M. W. Wara. 2004. 'Regional climate shifts caused by gradual global cooling in the Pliocene epoch', *Nature*, 429: 263-67.

Regal, P. J. . 1982. 'Pollination by Wind and Animals: Ecology of Geographic Patterns', *Annual Review of Ecology and Systematics*, 13: 497-524.

Richter, T. O., S. van der Gaast, B. Koster, A. Vaars, R. Gieles, H. C. de Stigter, H. de Haas, and T. C. E. van Weering. 2006. 'The Avaatech XRF Core Scanner: Technical description and applications to NE Atlantic sediments.' in R. G. Rothwell (ed.), *New Techniques in Sediment Core Analysis* (Geological Society, London, Special Publications).

Rickaby, R. E., and P. Halloran. 2005. 'Cool La Niña During the Warmth of the Pliocene?', *Science*, 307: 1948-52.

Rincón-Martínez, D. 2013. 'Eastern Pacific background state and tropical South American climate history during the last 3 million years', Universität Bremen.

Rincón-Martínez, D., F. Lamy, S. Contreras, G. Leduc, E. Bard, C. Saukel, T. Blanz, A. Mackensen, and R. Tiedemann. 2010. 'More humid interglacials in Ecuador during the past 500 kyr linked to latitudinal shifts of the equatorial front and the Intertropical Convergence Zone in the eastern tropical Pacific', *Paleoceanography*, 25: 1-15.

Rodbell, D. T., G. O. Seltzer, D. M. Anderson, M. B. Abbott, D. B. Enfield, and J. H. Newman. 1999. 'An ~15,000-year record of El Nino-driven alluviation in southwestern Ecuador', *Science*, 283: 516-20.

Ronge, T. A., D. Nurnberg, and R. Tiedemann. 2020. 'Plio-Pleistocene Variability of the East Pacific Thermocline and Atmospheric Systems', *Paleoceanography and Paleoclimatology*, 35.

Roubik, D. W., and J. E. Moreno P. 1991. *Pollen and spores of Barro Colorado Island [Panama]* (Missouri Botanical Garden: St. Louis, MO).

Salzmann, U., M. Williams, A. M. Haywood, A. L. A. Johnson, S. Kender, and J. Zalasiewicz. 2011. 'Climate and environment of a Pliocene warm world', *Palaeogeography, Palaeoclimatology, Palaeoecology*, 309: 1-8.

Sánchez-Baracaldo, P. 2004. 'Phylogenetics and biogeography of the neotropical fern genera Jamesonia and Eriosorus (Pteridaceae)', *American Journal of Botany*, 91: 274-84.

Schneider, T., T. Bischoff, and G. H. Haug. 2014. 'Migrations and dynamics of the intertropical convergence zone', *Nature*, 513: 45-53.

Seilles, B., M. F. S. Goni, M. P. Ledru, D. H. Urrego, P. Martinez, V. Hanquiez, and R. Schneider. 2016. 'Holocene land-sea climatic links on the equatorial Pacific coast (Bay of Guayaquil, Ecuador)', *The Holocene*, 26: 567-77.

Shipboard Scientific Party. 2003. "Site 1239." In *Proceedings of the Ocean Drilling Program, Initial Reports*, edited by A.C. Mix, R. Tiedemann and P. Blum, 1-93. College Station, Texas: Ocean Drilling Program.

Sklenár, P., E. Dusková, and H. Balslev. 2011. 'Tropical and Temperate: Evolutionary History of Páramo Flora', *Botanical Review*, 77: 71-108.

Sklenár, P., and P. M. Jorgensen. 1999. 'Distribution patterns of Páramo Plants in Ecuador', *Journal of Biogeography*, 26: 681-91.

Spikings, R. A., W. Winkler, R. A. Hughes, and R. Handler. 2005. 'Thermochronology of allochthonous terranes in Ecuador: Unravelling the accretionary and post-accretionary history of the Northern Andes', *Tectonophysics*, 399: 195-220.

Steph, S. 2005. 'Pliocene stratigraphy and the impact of Panama uplift on changes in Caribbean and tropical east Pacific upper ocean stratification', Christian-Albrechts-Universität Kiel.

Steph, S., R. Tiedemann, J. Groeneveld, A. Sturm, and D. Nürnberg. 2006. 'Pliocene Changes in Tropical East Pacific Upper Ocean Stratification: Response to Tropical Gateways?', *Proceedings of the Ocean Drilling Program, Scientific Results*, 202.

Steph, S., R. Tiedemann, M. Prange, J. Groeneveld, D. Nurnberg, L. Reuning, M. Schulz, and G. H. Haug. 2006. 'Changes in Caribbean surface hydrography during the Pliocene shoaling of the Central American Seaway', *Paleoceanography*, 21: 1-25.

Steph, S., R. Tiedemann, M. Prange, J. Groeneveld, M. Schulz, A. Timmermann, D. Nürnberg, C. Rühlemann, C. Saukel, and G. H. Haug. 2010. 'Early Pliocene increase in thermohaline overturning: A precondition for the development of the modern equatorial Pacific cold tongue', *Paleoceanography*, 25.

Stockmarr, J. 1971. 'Tablets with spores used in absolute pollen analysis', *Pollen et Spores*, XIII: 615-21.

Takahashi, K., and D. S. Battisti. 2007. 'Processes Controlling the Mean Tropical Pacific Precipitation Pattern. Part I: The Andes and the Eastern Pacific ITCZ', *Journal of Climate*, 20: 3434-51.

Tiedemann, R, A. Sturm, S. Steph, S.P. Lund, and J.S. Stoner. 2007. 'Astronomically calibrated timescales from 6 to 2.5 Ma and benthic isotope stratigraphies, sites 1236, 1237, 1239, and 1241', *Proceedings of the Ocean Drilling Program, Scientific Results*, 202.

Tjallingii, R., U. Röhl, M. Kölling, and T. Bickert. 2007. 'Influence of the water content on X-ray fluorescence core-scanning measurements in soft marine sediments', *Geochemistry, Geophysics, Geosystems*, 8.

Twiddle, C. L. 2012. 'Pollen Analysis: Not Just a Qualitative Tool.' in S.J. Cook, L.E. Clarke and J.M. Nield (eds.), *Geomorphological Techniques (Online Edition)* (British Society for Geomorphology: London).

Twilley, R.R., W. Cárdenas, V.H. Rivera-Monroy, J. Espinoza, R. Suescum, M.M. Armijos, and L. Solórzano. 2001. 'The Gulf of Guayaquil and the Guayas River Estuary, Ecuador.' in U. Seeliger and B. Kjerfve (eds.), *Coastal Marine Ecosystems of Latin America* (Springer: Heidelberg).

U.S. Army Corps of Engineers. 1998. 'Water Resources Assessment of Ecuador', Accessed 27 May 2020. https://www.sam.usace.army.mil/Portals/46/docs/military/engineering/docs/WRA/Ecuador/Ecuador%20WRA%20English.pdf.

U.S. Geological Survey's Center for Earth Resources Observation and Science (EROS). 1996. 'Global 30 Arc-Second Elevation (GTOPO30)'.

Vallé, F., L. M. Dupont, S. A. G. Leroy, E. Schefuss, and G. Wefer. 2014. 'Pliocene environmental change in West Africa and the onset of strong NE trade winds (ODP Sites 659 and 658)', *Palaeogeography Palaeoclimatology Palaeoecology*, 414: 403-14.

Van der Hammen, T. 1974b. 'The Pleistocene Changes of Vegetation and Climate in Tropical South America', *Journal of Biogeography*, 1: 3-26.

———. 1985. 'The Plio-Pleistocene record of the tropical Andes', *Journal of the Geological Society*, 142: 483-89.

Van der Hammen, T., and H. Hooghiemstra. 1997. 'Chronostratigraphy and Correlation of the Pliocene and Quaternary of Colombia', *Quaternary International*, 40: 81-91.

Van der Hammen, T., J. H. Werner, and H. van Dommelen. 1973. 'Palynological record of the upheaval of the Northern Andes: a study of the Pliocene and Lower Quaternary of the Colombian early evolution of its high-Andean biota', *Review of Palaeobotany and Palynology*, 16: 1-122.

Vuille, M., R.S. Bradley, and F. Keimig. 2000. 'Climate variability in the Andes of Ecuador and its relation to tropical Pacific and Atlantic Sea surface temperature anomalies', *Journal of Climate*, 13: 2520-35.

Wara, M. W., A. C. Ravelo, and M. L. Delaney. 2005. 'Permanent El Niño-like conditions during the Pliocene warm period', *Science*, 309: 758-61.

Waylen, P., and G. Poveda. 2002. 'El Niño-Southern Oscillation and aspects of western South American hydro-climatology', *Hydrological Processes*, 16: 1247-60.

Wijninga, V. M. 1996b. 'A Pliocene *Podocarpus* forest mire from the area of the high plain of Bogotá (Cordillera Oriental, Colombia)', *Review of Palaeobotany and Palynology*, 92: 157-205.

Wijninga, V. M., and P. Kuhry. 1990. 'A Pliocene Flora from the Subachoque Valley (Cordillera Oriental, Colombia)', *Review of Palaeobotany and Palynology*, 62: 249-90.

World Wildlife Fund (WWF). Accessed October 2017. https://www.worldwildlife.org/ecoregions/

Wu, F. L., X. M. Fang, Y. Z. Ma, M. Herrmann, V. Mosbrugger, Z. S. An, and Y. F. Miao. 2007. 'Plio-Quaternary stepwise drying of Asia: Evidence from a 3-Ma pollen record from the Chinese Loess Plateau', *Earth and Planetary Science Letters*, 257: 160-69.

Yan, Q., R. Korty, Z. S. Zhang, C. Brierley, X. Y. Li, and H. J. Wang. 2021. 'Large shift of the Pacific Walker Circulation across the Cenozoic', *National Science Review*, 8: 1-9.

Yang, S., and Z. Ding. 2010. 'Drastic climatic shift at ~2.8 Ma as recorded in eolian deposits of China and its implications for redefining the Pliocene-Pleistocene boundary', *Quaternary International*, 219: 37-44.

Zhang, X., M. Prange, S. Steph, M. Butzin, U. Krebs, D. J. Lunt, K. H. Nisancioglu, W. Park, A. Schmittner, B. Schneider, and M. Schulz. 2012. 'Changes in equatorial Pacific thermocline

depth in response to Panamanian seaway closure: Insights from a multi-model study', *Earth and Planetary Science Letters*, 317-318: 76-84.

Zhang, Y. G., M. Pagani, and Z. Liu. 2014. 'A 12-million-year temperature history of the tropical Pacific Ocean', *Science*, 344: 84-7.

7 Acknowledgments

First, I would like to thank Prof. Gerold Wefer for giving me the chance to work on this project under his supervision and for his valuable guidance throughout my studies.
I am grateful to Hermann Behling for being second examiner. Also for his help with pollen identification and for inviting me to Göttingen to study the reference collection of pollen from Ecuador.
My deepest gratitude is expressed to Lydie Dupont, who introduced me to the wonderful world of palynology. Her expertise was invaluable and her replies extremely fast, even after her retirement. Thank you, Lydie, for your continuous and excellent support over all the years!
I would like to thank my other two Thesis Committee members, Gerlinde Jung and Frank Lamy. Gerlinde for her help especially with understanding and interpreting climate models, and Frank as an expert on eastern Pacific paleoclimate and ODP Site 1239.
I am very thankful to Catalina Gonzalez Arango who helped me with the pollen identification and invited me to Bogotá for a research stay, which turned out to be the best time of my PhD. Colombia is an amazing and beautiful country and the people are the kindest and most hospitable I've ever met. Muchas gracias to Catalinas working group at the Universidad de los Andes (especially Valentina, Juanita, Aura and Catalina) for making this time unforgettable!
Thanks to Ralf Tiedemann, Frank Lamy and James Collins for explaining their work on ODP Site 1239 to me.
I thank my office mates and fellow PhD students Katja, Nicole, Xueqin, Christoph, Yanming, and Vera for their company and nice lunch breaks together. Special thanks go to Xueqin, who was there during all the years, for exchanging ideas, solving problems, and finally going through a lot of moving to different offices and containers together.
I thank GLOMAR for providing financial support to attend various conferences, courses and to realize a research stay abroad. The variety of courses offered by GLOMAR gave me the opportunity to develop my hard and soft skills.
I am extremely grateful to my friend Maroula for suffering together along the way and for motivating me to finish this.
Finally, I thank my family for their endless patience and support throughout all the years, and especially my parents without whom I wouldn't be where I am now. The sweetest thanks goes to my son Willem for making me smile every single day.

8 Appendix

Supplement of

Early Pliocene vegetation and hydrology changes in western equatorial South America

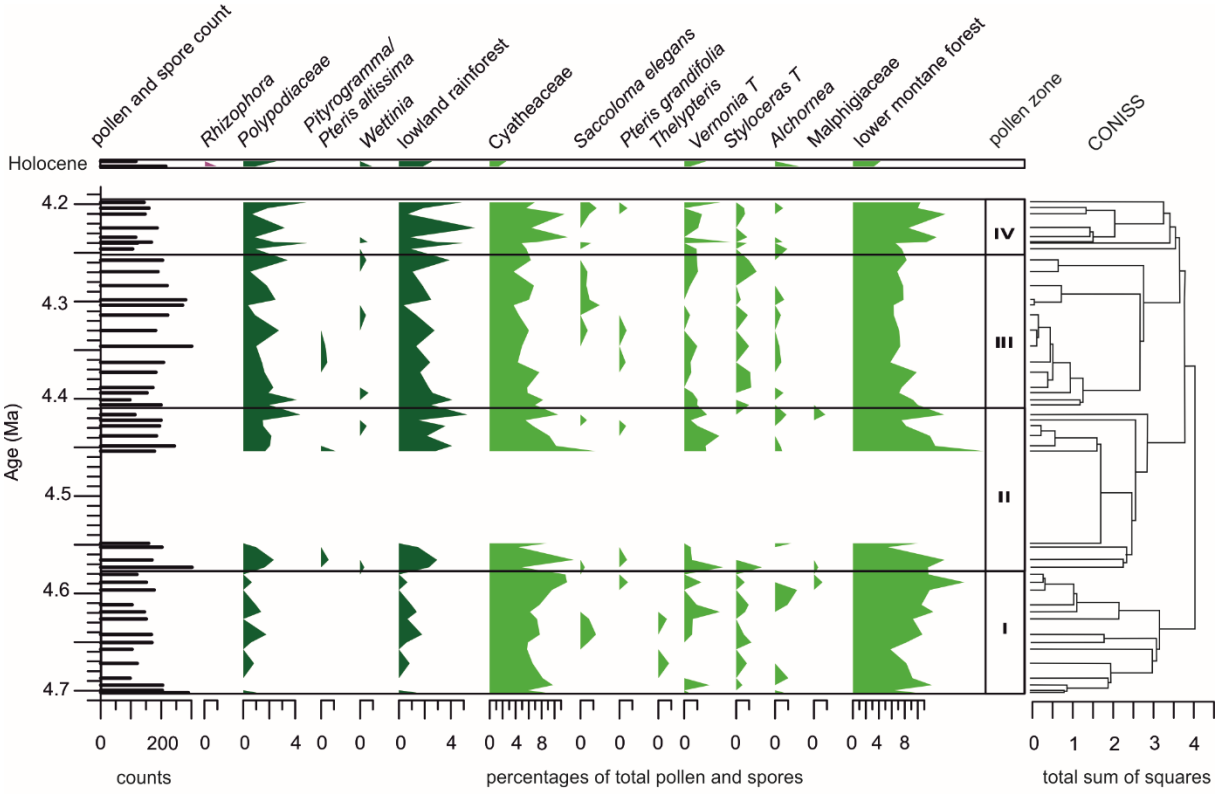

Figure S1. Pollen percentage diagram against age (Tiedemann et al., 2007), with total counts, percentages of single taxa and groups, pollen zones, CONISS clusters based on the curves of single pollen taxa. On top two samples from the Holocene. Minor ticks denote 1%, major ticks 2%, unless stated differently. This panel shows pollen and spore taxa from mangrove, lowland rainforest and lower montane forest. Panels on the next page show the pollen percentages for taxa from the upper montane forest, páramo, and broad range taxa.

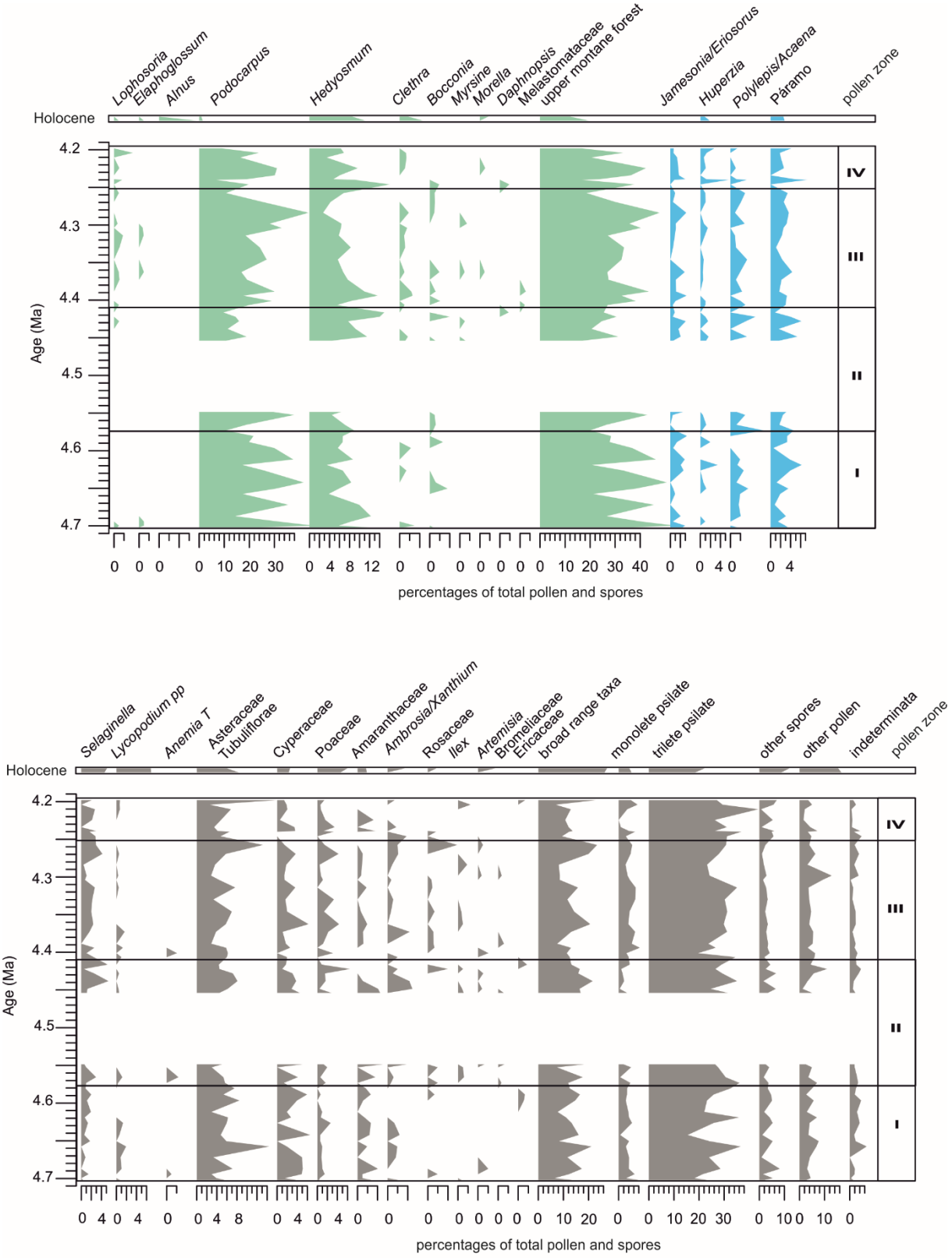

Figure S1 (continued)

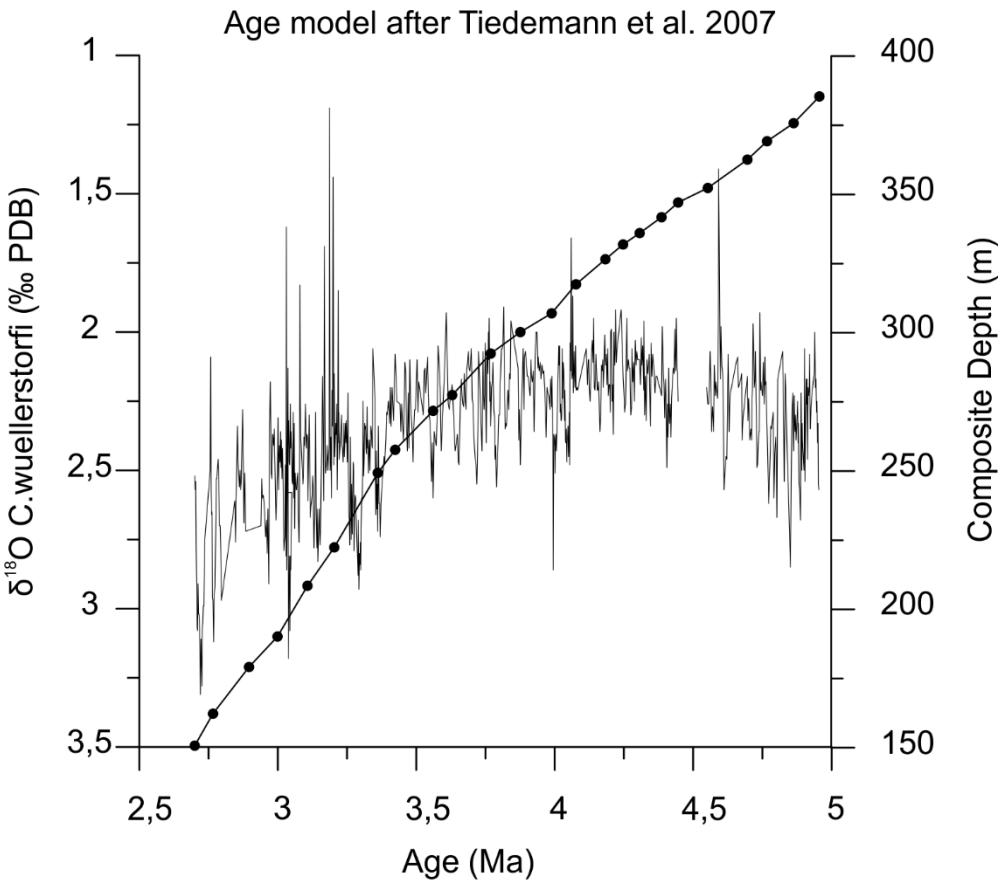

Figure S2: Composite depth (right axis) and stable oxygen isotopes of benthic foraminifers (left axis) on the age model after Tiedemann et al. (2007). (PDB: Pee Dee Belemnite)